Biology Master's Theses   Department of Biology

8-2009

The Role of the MRX Complex and the Non-homologous End Joining DNA Repair Pathway in Mitochondrial Genome Stability and Repair

Garry L. Coles
The College at Brockport

The Role of the MRX Complex and the Non-homologous
End Joining DNA Repair Pathway in Mitochondrial Genome
Stability and Repair

A thesis submitted to the Department of Biological Sciences at The College at Brockport,
State University of New York

By Mr. Garry L. Coles

Date Submitted: August 4, 2009
Date Approved: August 12, 2009

THESIS DEFENSE

Garry Coles

APPROVED	NOT APPROVED	MASTER'S DEGREE ADVISORY COMMITTEE

APPROVED   **NOT APPROVED**   **MASTER'S DEGREE ADVISORY COMMITTEE**

X   _Rey a Lii_   8/12/09

                                         Major Advisor   Date

X   _Stuart Mulate_   8/12/09

                                           Committee Member   Date

✓   _Laurie B. Cook_   8/12/09

                                           Committee Member   Date

_GR_

Chairman, Graduate Committee   _Rey A. Lii_

                                           Chairman, Dept. of Biological Sciences

Acknowledgements

I am extremely thankful to have been given the opportunity to work in the biomedical sciences. I would like to thank everyone that has assisted me throughout my education here at The College at Brockport. I would like to thank my mother, Bonnie Coles who has supported me with endless devotion for these last 26 years. I would also like to thank my thesis advisor and mentor, Dr. Rey Sia. Working for Dr. Rey Sia was one of the most rewarding experiences I have ever had.

Dedication

This work is dedicated to my mother, Bonnie. I would like my mother to know that her strength and wisdom are truly inspirational.

Table of Contents

Abstract:

Mitochondria are required for cellular respiration, which is essential in the production of ATP. Mitochondrial genome maintenance is necessary for the continued function of the mitochondrion. Deletions within the mitochondrial DNA (mtDNA) have been shown to be associated with a variety of human neuromuscular and age-related diseases. In this study we investigated the role of the MRX complex and the non-homologous end joining (NHEJ) DNA repair pathway in mitochondrial genome stability and repair. Specifically, we investigated the role of the MRX complex and the NHEJ pathway in the occurrence of spontaneous mitochondrial direct repeat-mediated deletions, nuclear direct repeat-mediated deletions, mitochondrial point mutations, nuclear point mutations, and spontaneous respiration loss using fluctuation analysis in the budding yeast, *Saccharomyces cerevisiae*. In this study, we have demonstrated that spontaneous mitochondrial direct repeat-mediated deletions are reduced 75 fold ($p<0.001$), and spontaneous mitochondrial point mutations are reduced 13 fold ($p=0.013$) in the absence of the MRX complex and the NHEJ pathway. While in the absence of the MRX complex and the NHEJ pathway, spontaneous respiration loss increased 3.54 fold ($p<0.003$) suggesting that this pathway is required for mitochondrial genome stability. In addition to investigating these DNA repair pathways, which are known to regulate nuclear genome stability, we localized the NHEJ factor Ku70p to the mitochondria using cellular fractionation and western blot analysis. This localization data in combination with the wealth of genetic data presented in this study support our hypothesis that the MRX complex and the NHEJ DNA repair pathway act in concert to stabilize the integrity of the mitochondrial genome.

Background & Significance

The Mitochondrion and Cellular Respiration

The mitochondrion is the site of cellular respiration and is essential for eukaryotic cell viability. The mitochondrion is a double membrane-bound organelle of approximately 1-3 μm in size. This organelle houses the chemical reactions involved in the synthesis of adenosine tri-phosphate (ATP), the primary biological molecule used in the storage and transfer of energy. ATP synthesis is accomplished in 4 essential steps, 3 of which occur within the mitochondrion. The first step in ATP synthesis is glycolysis, or the oxidation of glucose to pyruvate, which occurs within the cytosol of a eukaryotic cell, and is then transported through Porin, a multi-pass mitochondrial protein channel, where it is further oxidized into acetyl coenzyme A. Acetyl coenzyme A then enters into step 2, the tricarboxylic acid cycle (TCA). The TCA cycle oxidizes carbon atoms into CO_2 and temporarily stores or conserves this energy as reduced coenzyme molecules. The 3rd step involved in ATP synthesis is the electron transport chain. The electron transport chain involves the transfer of electrons from the reduced coenzymes to oxygen. This transfer of electrons is the source of energy that drives the active transport of protons across the inner membrane of the mitochondria, thereby generating the electrochemical proton gradient necessary for the final stage of ATP synthesis, oxidative phosphorylation. Oxidative phosphorylation uses the energy of the electrochemical proton gradient to drive ATP synthesis (Becker at el., 2006). Figure 1 below describes the structure and several key components of the mitochondrion within the eukaryotic cell.
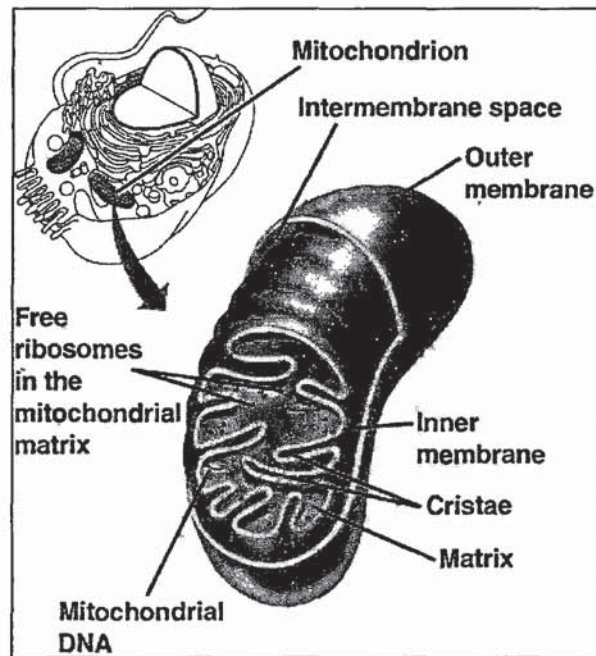
Figure 1. Diagram of mitochondrial structure. Applied from kvhs.nbed.nb.ca/-gallant/biology/mitochondrion.jpg

Additional Cytological Roles of the Mitochondrion

The mitochondrion possesses many cytological roles within the eukaryotic cell in addition to ATP synthesis. Phospholipid synthesis, fatty acid desaturation, and fatty acid elongation occur between the inner and outer mitochondrial membranes. Metabolite transport occurs within the inner membrane of the mitochondrion, while mitochondrial DNA (mtDNA) replication, mtDNA transcription, and mtDNA translation occur within the mitochondrial matrix (Becker et al. 2006).

In higher eukaryotes the mitochondrial membrane is also involved in the activation and regulation of apoptotic signal transduction pathways. Upon the sensing of DNA damage or the removal of specific trophic factors, pro-apoptotic proteins accumulate upon the outer

membrane of the mitochondria. These pro-apoptotic proteins destabilize mitochondrial membrane proteins such as Bcl-2, leading to the breakdown of the membrane, and the release of the Cyctochrome C. The release of Cyctochrome C triggers the caspase cascade leading to the activation of apoptosis and controlled cell death (Becker et al. 2006).

The mitochondrion and the endoplasmic reticulum have been shown to be involved in the storage of free calcium within the cell. Free calcium is taken up into the matrix of the mitochondrion via a calcium uniporter, and is released back into the cytosol using sodium-calcium channels. The storage and release of calcium ions in the cell plays an important role in regulating membrane potential as well as signal transduction and cellular proliferation. The mitochondrion has also been shown to be involved in the synthesis of heme as well as steroids in higher eukaryotes. (Becker et al. 2006).

The Mitochondrial Genome

Unlike other organelles, mitochondria possess their own genome housed within the mitochondrial matrix. The existence of mitochondrial DNA (mtDNA) was discovered in 1963 when Margit and Sylvan Nass discovered a DNAase sensitive molecule within the mitochondria. Initially these authors described the mitochondrial genome as an intra-mitochondrial DNA fiber, but due to advances in molecular and biochemical techniques, considerably more is known to date about the mitochondrial genome. These technological advances have lead to an extensive increase in our understanding of the structure of mtDNA, mtDNA nucleoid structure and remodeling, the components of the mitochondrial genome, mtDNA inheritance patterns, mtDNA replication, mitochondrial genome repair, and mitochondrial related diseases.

Mitochondrial Genome Structure

Our understanding of the structure of the mitochondrial genome has increased considerably since the 1963 discovery of intra-mitochondrial DNA fibers. In 1998 and 2001 the mitochondrial genomes of *Saccharomyces cerevisiae* and *Homo sapiens* were mapped. Today it is known that the structure of the mitochondrial genome of both yeast and man is a double-stranded circular DNA molecule, and similar to that of bacterial genomes, the mitochondrial genome lacks introns. The human mitochondrial genome is 16,569 nucleotides in length and possesses 37 genes as well as an origin of replication (ORI). Twenty-eight of these genes are located on the heavy strand, while the other 9 genes are located on the light strand (ncbi.nlm.nih.gov). The respective terms and "heavy" and "light" strand are applied due to differences in their molecular weights which vary according to nucleotide composition. The mitochondrial genome of *Saccharomyces cerevisiae* is approximately 78,000 nucleotides in length, and it possesses several polypeptide-encoding genes required for respiration, as well as the structural RNAs required for their synthesis. Refer to Figure 2 below for a comparison between the mitochondrial genomes of *Saccharomyces cerevisiae* and *Homo sapiens*.
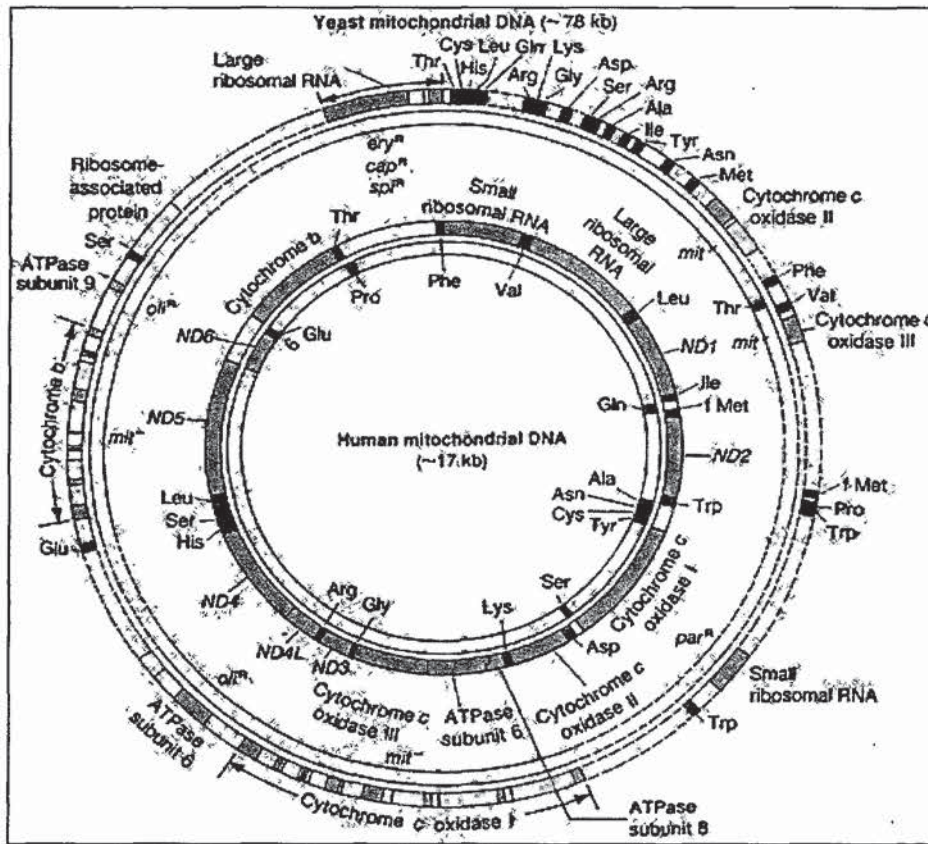
Figure 2. A comparative map of the mitochondrial genomes of *Saccharomyces cerevisiae* and *Homo sapiens*. Applied from: www.clinsci.org

Mitochondrial DNA Nucleoid Structure and Remodeling

The organization of nuclear DNA and nucleosome remodeling has been extensively studied due to its involvement in the regulation of gene expression. Genomic DNA exists primarily as DNA molecules condensed tightly around an octamer of histones making up chromatin. Chromatin is further compacted into nucleosomes which must be remodeled to regulated gene expression, DNA replication, recombination, repair, and chromosomal segregation during cell division (Ehrenhofer-Murray, 2004).

The mitochondrial genome is organized as compact structures associated with numerous protein factors known as mtDNA nucleoids. MtDNA nucleoids are made up of approximately 2 - 5 copies of the mitochondrial genome wrapped around a series of protein

co-factors which reside within the inner membrane of the mitochondrion (Grimes et el. 1974). When comparing chromatin and mtDNA nucleoid remodeling, it is clear that significantly less in understood about mtDNA nucleoid remodeling. Unlike chromatin, mtDNA nucleoids do not possess histones. In contrast, mtDNA nucleoids are packaged with high-mobility group

(HMG)-like proteins which act as chaperone and scaffolding proteins (Ehrenhofer-Murray, 2004). Examples of members of the HMG-like group of proteins are Abf2p in yeast, and Tfamp in mammals (Cheng et al., 2005). Abf2p and Tfamp are known to bind mtDNA in a sequence inspecific manner, and promote resistance to reactive oxygen species (ROS) induced damage (O'Rourke et al., 2002). Using chromatin immuno-precipitation experiments it has been demonstrated that mtDNA nucleoids have been shown to undergo remodeling upon glucose and amino-acid starvation (Ehrenhofer-Murray, 2004), yet the exact mechanisms responsible for mtDNA nucleoid remodeling has yet to be discovered.

Components of the Mitochondrial Genome

As previously mentioned, the mitochondrion possesses numerous functions. The vast majority of the genes required for mitochondrial function are encoded and transcribed within the nucleus, translated within the cytosol, and then targeted to the mitochondria via targeting sequences. Proteins which are targeted to the mitochondria are thought to be captured and chaperoned by the yeast cHSP70p (cytosolic heat shock 70 protein) and MSF (the mitochondrial stimulation factor) where they are guided through the TOM and TIM protein complexes, which are located on the outer and inner mitochondrial membranes (Pfanner and Meijer, 1997). The remaining genes required for mitochondrial function are located in the mitochondrial genome within the matrix along with the molecular machinery required for there transcription and translation.

The human mitochondrial genome encodes 37 genes in total. Of these 37 human genes, 13 encode proteins (polypeptides), while the remaining 24 encode structural RNAs. Of those structural RNAs 2 are ribosomal RNAs, while 20 are transfer RNAs (Alexeyev et al. 2004). Refer to Table 1 below for a complete list of the 37 genes within the human mitochondrial genome.

While there are no introns in mtDNA, the human mitochondrial genome is only 68% coding. The remaining 32% of mtDNA encodes the mtDNA origin of replication in addition to the regulatory sequences. In yeast only 35% of the mitochondrial genome is coding, while the other 65% of mtDNA is comprised of conserved regulatory regions and at least 7 origins of replication (De Zamaroczy, and Bernardi 1986). Interestingly there is also a highly conserved mitochondrial coding bias in that GC content makes up only 44% of human mtDNA (Alexeyev et al. 2004).

mtDNA Gene Name	Category	Function
MT-ND1	polypeptide	Components of NADH dehydrogenase
MT-ND2	polypeptide	Requred for respiratory complex 1
MT-ND3	polypeptide	
MT-ND4	polypeptide	
MT-ND5	polypeptide	
MT-ND6	polypeptide	
MT-CYB	polypeptide	Coenzyme Q: cytochrome c reductase / Cytochrome b Required for respiratory complex 3
MT-CO1	polypeptide	Component of cytochrome c oxidase
MT-CO2	polypeptide	Required for respiratory complex 4
MT-CO3	polypeptide	
MT-AP6	polypeptide	Component of ATP synthase
MT-AP8	polypeptide	
MT-RNR1	structural RNA	12s rRNA
MT-RNR2	structural RNA	16s rRNA
MT-TA	structural RNA	Alanine tRNA
MT-TR	structural RNA	Arginine tRNA
MT-TN	structural RNA	Asparagine tRNA
MT-TD	structural RNA	Aspartic acid tRNA
MT-TC	structural RNA	Cysteine tRNA
MT-TE	structural RNA	Glutamic acid tRNA
MT-TQ	structural RNA	Glutamine tRNA
MT-TG	structural RNA	Glycine tRNA
MT-TH	structural RNA	Histidine tRNA
MT-TI	structural RNA	Isoleucine tRNA
MT-TL1	structural RNA	Component of Leucine tRNA
MT-TL2	structural RNA	Component of Leucine tRNA
MT-TK	structural RNA	Lysine tRNA
MT-TM	structural RNA	Methionine tRNA
MT-TF	structural RNA	Phenylalanine tRNA
MT-TP	structural RNA	Proline tRNA
MT-TS1	structural RNA	Component of Serine tRNA
MT-TS2	structural RNA	Component of Serine tRNA
MT-TT	structural RNA	Threonine tRNA
MT-TW	structural RNA	Tryptophan tRNA
MT-TY	structural RNA	Tyrosine tRNA
MT-TV	structural RNA	Valine tRNA

Table 1. Genes encoded by the human mitochondrial genome.

Sources of Mitochondrial Genome Instability

Similar to that of nuclear DNA, mitochondrial DNA is subject to mutation. There are numerous sources of mutagens ranging from exogenous to endogenous, some of which are manmade while others are naturally occurring. Chemicals such as ethidium bromide are known to intercalate into double stranded DNA, whereas UV light and ionizing radiation have been shown to cause DNA damage via the formation of pyrimidine dimers (Griffiths et al. 2002).

The sources for genomic instability that are discussed in this study are the occurrence of spontaneous point mutations, microsatellite instability and polymerase slippage, and direct repeat-mediated deletions. Point mutations at the molecular level range from transitions and transversions to indel mutations. These mutations can result in single base pair substitutions and can disrupt either the coding or regulatory sequence of DNA resulting in numerous types of mutations (Griffiths et al. 2002). Microsatellites are a series of repeating nucleotides that may be the source of polymerase slippage which allows for the expansion of di-nucleotide repeats into minisatellites, or larger repeating DNA sequences (Griffiths et al. 2002, Schoffner et al. 1989). Direct repeat-mediated deletions are the final source of genomic instability that will be discussed in this study. Direct repeat-mediated deletions (DRMDs), can be defined as a series of directly repeating nucleotides flanking a region of DNA which spontaneously undergo a recombination event at the sites of direct repeats. During these recombination events the excised section of genetic material between these direct repeats is lost (Schoffner et al. 1989). Refer to Figure 3 below for an example of a mitochondrial direct repeat-mediate deletion.

A highly-characterized example of a mtDNA direct repeat-mediated deletion is the 4,977 base pair deletion known to accumulate in aging individuals suffering from Kearns-Sayre syndrome. This deletion has been shown to reduce the functional activity of respiratory complex 1 and may occur in up to 50% of mtDNA molecules isolated from patients suffering from this syndrome (Schoffner et al. 1989). Figure 3 below is a simulated example of how the mtDNA DRMDs which have been documented in patients suffering from Kearns-Sayre syndrome may occur.

Direct Repeat Mediated Deletions within the Mitochondrial Genome

Before a spontaneous direct repeat-mediated deletion the *NADH dehydrogenase* gene is intact

| ATACGCGATA | *NADH dehydrogenase* | ATACGCGATA |

| ATACGCGATA |

After a direct repeat mediated deletion event *NADH dehydrogenase* has been excised and can no longer be expressed
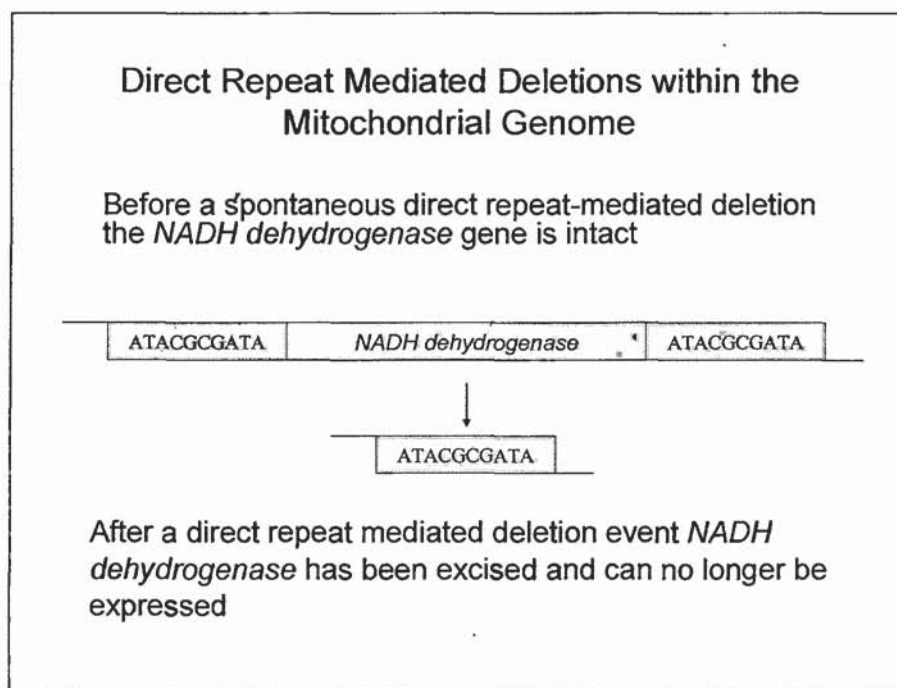
Figure 3. A simulated mitochondrial direct repeat-mediated deletion. The loss of the *NADH dehydrogenase* gene along with other members of respiratory complex 1 have been shown to occur as a result of mitochondrial direct repeat-mediated deletions in patients suffering from Kearns-Sayre syndrome (Schoffner et al. 1989).

In addition to human direct repeat-mediated deltions, the budding yeast *Saccharomyces cerevisiae* has also been shown to spontaneously acquire large deletions within their mitochondrial DNA and are referred to as *rho-*. Due to their nature as facultative anaerobic organisms, yeast cells possess the ability to produce energy through the fermentation pathway after they have acquired these deletions and lost mitochondrial function (Dujon

1981). A substantial portion of the mitochondrial DNA deletions that occur within *rho-* cells are known to occur as a result of direct repeat-mediated deletion events (Dujon 1981).

Mitochondrial DNA Inheritance Patterns

The inheritance of nuclear DNA from mother to daughter cells is well-characterized and occurs during mitosis and meiosis. The distribution of nuclear DNA is regarded as equitable, or even, in that each cell receives an equal number of DNA molecules. While in contrast, the inheritance of mitochondrial DNA is not yet as widely characterized. Mitochondrial DNA is thought to be inherited in a stochastic manner due to the increased copy number and uneven distribution throughout the cytosol of mother and daughter cells after the cell divides (Barr et al. 2005). The inheritance pattern of mtDNA varies considerable from yeast to man. Heteroplasmy, or the presence of more than type or variation between mitochondrial DNA molecules, is rare in later stages of cell division prior to sexual reproduction in fungi where, in contrast, heteroplasmy is more common in animals prior to sexual reproduction (Barr et al., 2005).

In mammals there is a strict system that ensures that the inheritance of mtDNA is from maternal sources alone. Upon fertilization, but prior to meiosis-1, paternally inherited mtDNA is labeled with ubiquitin for degradation (Sutovsky et al. 1999). Paternal mtDNA degradation ensures that materially inherited mtDNA is the only source of mtDNA for embryogenesis. There are similarities between the occurrence of mitochondrial DNA heteroplasmy in both yeast and humans. Two examples of potential sources of heteroplasmy in yeast are infidelity in the replication of mitochondrial genome and meiosis based recombination. Recombination between mtDNA molecules has been well documented in

yeast (MacAlpine et. at. 1998), while significantly less is known about the occurrence of recombination events between mtDNA molecules in higher eukaryotes.

Human heteroplasmy has been well documented in aging individuals, with 50 to 4977bp deletions in patients suffering from Kearns-Sayre syndrome, and gastric adenocarcinomas. These accumulating deletions or mtDNA heteroplasmy may arise due to mitochondrial D-loop mutations, direct repeat-mediated deletions, polymerase slippage and replication errors, microsatellite instability, and the occurrence of spontaneous point mutations (Schoffner et al. 1989, Zeviani at al. 1989, and Burgart et al. 1995).

Mitochondrial Genome Replication and Transcription

The regulation of mitochondrial genome replication is controlled by the systematic expression and coordination of the mitochondrial DNA polymerase. In humans mtDNA replication is thought to be coupled to mtDNA transcription because the production of primers is required for replication during transcription (Krishnan et al. 2008). Both the human mtDNA polymerase Pol gammap, and the yeast mtDNA polymerase Mip1p are encoded within the nucleus. In humans there are at least three mtDNA transcription factors, TFAM, TFB1M, and TFB2M which initiate the transcription process. These transcription factors bind one of the three mitochondrial promoters, H1 (heavy strand 1), H2 (heavy strand 2), and L (light strand promoter). The H1 promoter allows for the transcription of the entire heavy chain on the mtDNA molecule, the L promoter transcribes the light chain, while the H2 promoter allows for the transcription of the 12S and 16S rRNA molecules. The primers are required for the binding of the mtDNA polymerase and is accomplished by processing the light strand mtDNA RNAse MRP enzyme (mitochondrial RNA Processing) (Becker at el., 2006).

Once the RNA primers have been laid, mtDNA bi-directional replication is initiated in yeast, birds, and mammals (Giuseppe et al. 1984, Reyes et al. 2005). Mitochondrial genome replication is thought to occur through 3 potential mechanisms (Krishnan et al. 2008). Figure 4 below was originally published by Krishnan et al. in 2008, describes the three potential mechanisms for mtDNA replication. The first mechanism for mtDNA replication described by these authors is asynchronous mtDNA replication (letters a - c of Figure 4). The asynchronous method of mtDNA replication begins at the D-loop at O_H by displacing the light strand from the heavy strand. The light strand exists as a single stranded DNA until synthesis of the heavy strand exposes O_L (letter a in Figure 4). Replication of the light strand begins in the alternate direction until both the heavy and light strands have been completely replicated (letters b - c of Figure 4).

The second proposed mechanism for mtDNA replication described by Krishnan et al. in 2008 is synchronous or coupled mtDNA replication (letter d of Figure 4). In this model replication initiates from OriZ and occurs bi-directionally via coupled leading and lagging strand synthesis.

The final proposed mechanism for mtDNA replication possesses RNA intermediates and is referred to as RITOLS, or Ribonucleotide Incorporation Throughout the Lagging Strand model (letter e – f of Figure 4). The RITOLS model of mtDNA replication begins in the noncoding region at O_H. In this model the light strand is initially displaced from the heavy strand. This model functions similar to that of the asynchronous model of replication, but RNA intermediates are produced (seen here as dashed lines) on the light strand. These RNA intermediates are then converted to DNA thereby completing the faithful replication of mtDNA (Krishnan et al. 2008).
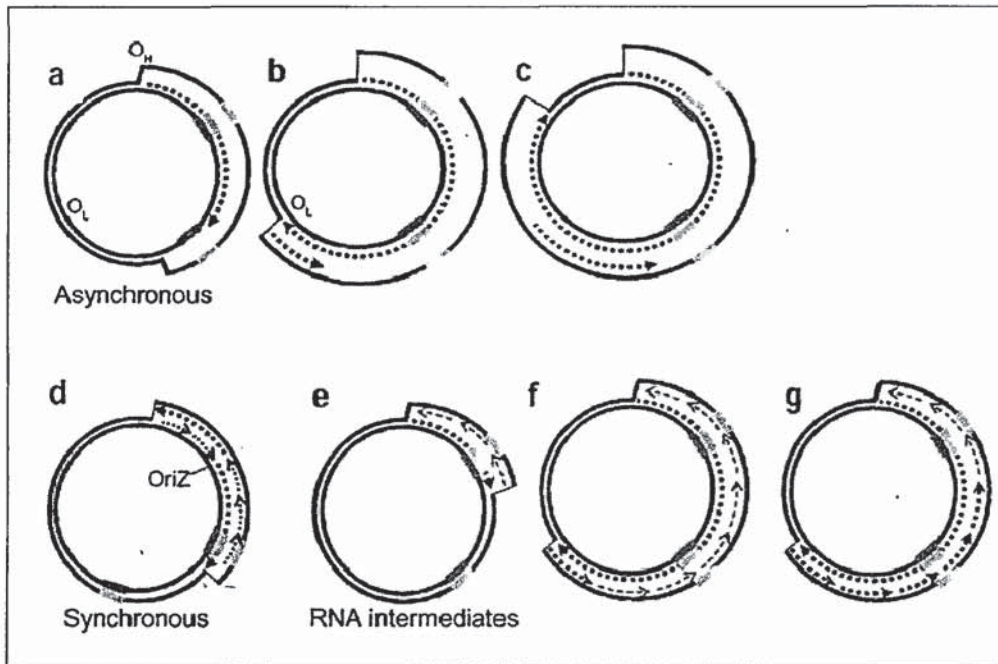
Figure 4. The Proposed Mechanisms for Mitochondrial Genome Replication.
Published by Krishnan et al. 2008. *Nature Genetics* 40, 275 – 279.

Mitochondrial DNA Repair Pathways

The DNA molecule is constantly being bombarded with numerous damaging agents. Ultraviolet light, ionizing radiation, and reactive oxygen species have all been shown to lead to DNA damage. In the event that DNA damage is left unrepaired it may lead to replication fork blocks and collapse, which may lead to mutation and even cell death. The mtDNA polymerase MIP1p possesses 3' – 5' exonuclease activity (Foury et al. 1992), but this singular function is not sufficient to promote genomic stability. Mitochondrial DNA is especially susceptible to DNA damage due to its close proximity to the synthesis of reactive oxygen

species within the mitochondria itself. Similar to that of nuclear DNA (nDNA), the cell has evolved specific repair pathways to preserve the integrity of mtDNA. To date there are at least 6 distinct pathways that have been shown to repair damaged nDNA, 4 of which have also been shown to repair mtDNA (Larsen et al. 2005). Refer to Figure 5 below for a comparison of nuclear DNA and mitochondrial DNA repair pathways published by Larsen et al. in 2005.
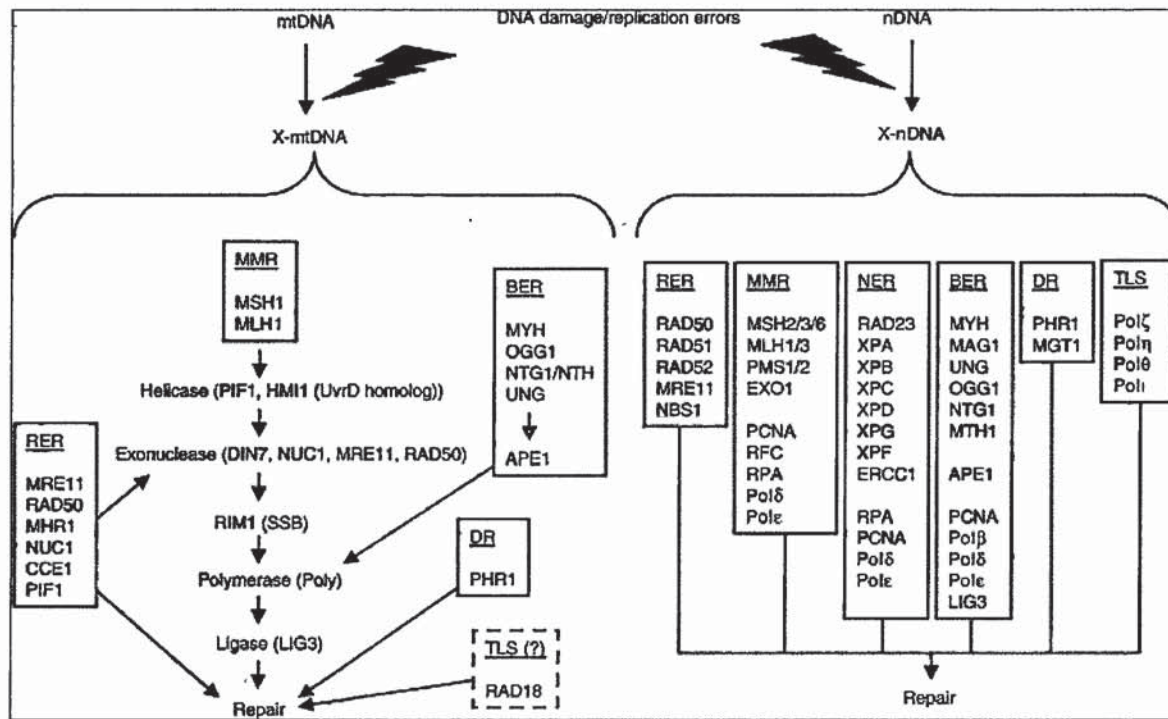
Figure 5. A comparison of nuclear and mitochondrial DNA repair pathways. Larsen et al. 2005. *Mitochondrion,* **5, Issue 2, 89-108.**

In this review of nuclear and mitochondrial DNA repair pathways published in 2005 by Larsen et al., these authors stated that that the primary mtDNA repair pathways are mismatch repair (MMR), base excision repair (BER), direct reversal (DR), and recombinational repair (RER). In both yeast and humans the mismatch repair pathway relies

upon the combination of the gene products of *MSH2* and *MSH6* to generate MutSα, while the products of *MSH2* and *MSH3* combine to from MutSβ. These complexes recognize single basepair mismatches and insertion deletion loops in a newly synthesized DNA molecule, and allow for their removal. Mismatch repair is believed to increase the fidelity of the replication of DNA 1000-fold (Larsen et al. 2005). Base excision repair employs the use of a DNA glycosylase that recognizes a smaller subset of base changes and allows for their removal. Base excision repair is known to repair reactive oxygen induced damage, therefore it should come at no surprise that the BER pathway functions in the mitochondria. The nucleotide excision repair (NER) pathway is involved in removing pyrimidine dimers and bulky DNA adducts that alter the double helix structure of the DNA molecule (Larsen et al. 2005). Recombinational repair (RER) employs the use of either the homologous recombination pathway, or the MRX complex and the non-homologous end joining pathway to repair a specific type of DNA damage known as a DNA double strand break (DSB). Unlike non-homologous end joining, homologous recombination relies upon the use of a homologous DNA sequence (from a homologous chromosome) for the re-synthesis of a damaged strand of DNA (Larsen et al. 2005). The final mtDNA repair pathway described by Larsen et al. in Figure 4 is direct reversal (DR). Direct reversal is one of the most efficient DNA damage repair pathways because it immediately repairs a damaged nucleotide without its removal upon the cells recognition of DNA damage. Direct reversal is known to occur in bacteria and yeast, but is not present in higher eukaryotes.

Mitochondrial Related Diseases and mtDNA Deletions

In recent years the importance of mitochondrial genome maintenance has come into the spotlight of the biomedical sciences due to its role in the onset of disease and aging.

With the advent of the polymerase chain reaction (PCR) in 1983, it became possible to amplify regions of DNA in order to detect mutations and naturally occurring polymorphisms. In 1990 PCR was used to amplify specific regions of the mitochondrial genome isolated from the heart muscle, and brain tissues of stillborn infants and aging individuals by Cortopassi et al. These scientists discovered that a portion of the tissue samples taken from aging individuals possessed specific mtDNA deletions, which were not present in samples taken from the same tissue types of stillborn infants. These authors went on to postulate that these deletions may have occurred during the aging process because they were not present in fetal or juvenile tissue samples (Cortopassi et al. 1990). In 2003 Chromyn and Attardi published a study which suggested that the occurrence of these age-related mtDNA deletions may possess additional medical relevance due to the possibility that these deletions may lead to an increased chance of the development of disease. They theorized that certain age related mtDNA deletions could impair the rate of mitochondrial-dependent apoptosis by possible altering the production of reactive oxygen species and thereby altering the homeostatic redox state of the cell. They suggested that this fluctuation in redox state could potentially reduce the functional activity of apoptosis, and increase the chances of disease onset in aging individuals (Chomyn and Attardi 2003).

To date, mitochondrial DNA deletions have been shown to be present in patients suffering from an incredible array of diseases ranging from diabetes and deafness, cardiomyopathy, CPEO, Kearns Sayre's disease, as well as the occurrence of sudden death (Solano et al.,2001). Any alteration in the structure or sequence of mtDNA has the potential to lead to human diseases. Thus it becomes increasingly obvious that any source of genomic instability can be a potential source of human disease. Several examples of mtDNA-related

human diseases are listed in Table 2 below.

Human disease	Affected gene	Source of mutation
Diabetes and deafness	tRNA (leu)	Point mutation
Cardiomypatny	tRNA (leu)	Point mutation
Sudden Death	tRNA (leu)	Point mutation
CPEO	tRNA (Asn)	Point mutation
Pearson	tRNA (glu)	Point mutation
Heptocellular carcinoma	ND5, COX-1	Microsattelite instability
Kearns-Sayre's	ND2 - ND5	Direct repeat-mediated deletion

Table 2. A comparison between mtDNA deletions and human disease. Adapted from Solano A, Playán A, López-Pérez MJ, Montoya J. Enfermedades genéticas del mitocondrial humano. Salud Publica Mex 2001; 43: 151-161, Tong Wu 2005, and Schoffner et al. 1989.

Saccharomyces cerevisiae

Saccharomyces cerevisiae, is a single celled eukaryotic fungi often referred to as the budding yeast, brewers yeast, or bakers yeast. It possesses both haploid (n) and diploid stages (2n) in its life cycle, allowing for cell division by both mitosis and meiosis. When environmental conditions are favorable *Saccharomyces cerevisiae* reproduces through mitosis, but when conditions become less favorable a diploid cell undergoes meiosis producing 4 haploid spores, 2 of which are mating type **a** and 2 are mating type α. These alternate mating types represent simple sexual differentiation, and when mated produce a diploid organism that can either divide through mitosis, or can sporulate once again generating 4 haploid cells after meiosis. One of the incredibly unique features of *Saccharomyces cerevisiae* is that all of the products of meiosis are contained within an ascus and generate a tetrad. Tetrads can be

dissected and the resulting spores can be sub-cultured, allowing for samples of each spore to be harvested and genotyped. Once the genotype of each of each of these spores is determined, yeast cells of opposite mating types can be mated to generate genotypes of interest. Refer to Figure 6 below for a diagram of the life cycle of *Saccharomyces cerevisiae*.
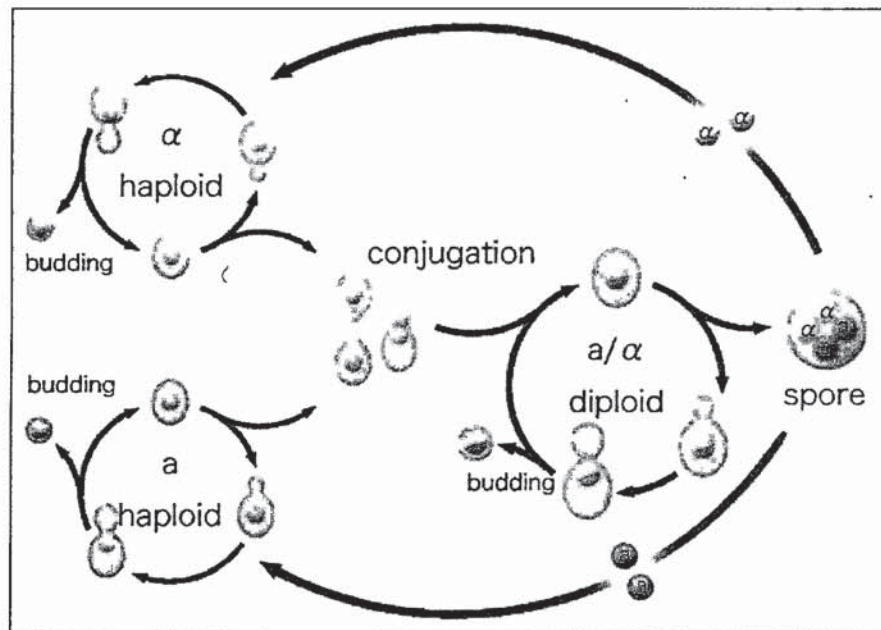
Figure 6. The life cycle of the budding yeast, *Saccharomyces cerevisiae*. Adapted from http://www.padre.kutno.pl/index.php?vin=Saccharomyces_cerevisiae

Saccharomyces cerevisiae also possesses the ability to spontaneously switch mating types. The regulation of mating type is determined by a single allele (**a** or α) at a locus known as the *MAT* locus (Haber 1998). Mating type switching is accomplished after the *H0-endonuclease* gene expresses HO-endonuclease, which is then targeted to the *MAT* locus. HO-endonuclease digests double stranded DNA at the HO-endonuclease restriction site at the *MAT* locus on chromosome 3 (Haber 1998). In the event that a yeast cell of the **a** mating

type undergoes HO-endonuclease digestion at the *MAT* locus, then exonucleases are shuttled to this site where they then degrade both ends of the double strand break and the remaining *MAT* locus. Following exonuclease digestion, and non-homologous end joining at the sites of the double strand DNA break, *HML* (hidden *MAT* left) or *HMR* (Hiden *MAT* Right) alleles are brought into frame. *HML* and *HMR* genes are silenced previous to HO-endonuclease digestion, but after HO-endonuclease digestion they are brought into frame allowing for their expression, and the completion of mating type switching (Haber 1998).

Saccharomyces cerevisiae as a Model Organism

Saccharomyces cerevisiae has become one of the most widely studied model organisms in the fields of genetics and molecular biology because it possesses numerous inherent properties that have become increasingly valuable in a model system. In 1996 *Saccharomyces cerevisiae* became the first eukaryote to have its complete genome sequenced via an international collaboration of scientists from the United States, Canada, the United Kingdom, Germany, France, Switzerland, Belgium, and Japan. From this work it was discovered that the *Saccharomyces cerevisiae* genome contained 12,068 kilobases, which made up at least 5,885 protein coding genes. In addition to these 5,885 protein coding genes, 140 ribosomal RNA genes, 40 small nuclear RNA genes, and 275 transfer RNA genes were discovered. In total over 6,000 potential open reading frames were discovered on 16 linear chromosomes, 25% of these encode genes which are thought to be conserved from yeast to humans (Goffeau et al. 1996).

With the wealth of genetic information that became available after the sequencing of the yeast genome in 1996, the use of *Saccharomyces cerevisiae* as a model eukaryotic organism expanded incredibly. *Saccharomyces cerevisiae* possesses several key traits that have become

incredible valuable in a model organism. *Saccharomyces cerevisiae* possesses a doubling time of 90 - 180 minutes depending upon the carbon source and nutrient availability of the media it is cultured in. This remarkably short doubling time increases the rate at which experiments can be performed compared to that of higher eukaryotic model systems. In the fields of genetics and molecular biology gene disruption is one of the most valuable tools used to elucidate the function of a gene of interest. Therefore the ability to culture *Saccharomyces cerevisiae* as a haploid organism increases the ease of the targeted disruption of nearly all of the non-essential genes with in its genome. *Saccharomyces cerevisiae* possesses a higher rate of homologous recombination than many other eukaryotes. Scientists have used this phenomenon to their advantage by using homologous recombination in unison with knockout cassettes to disrupt genes of interest. By July of 2002, 96% of the 6000 open reading frames had been disrupted using this method of site-directed mutagenesis to assist in the determination of the function of each of these genes (Giaever et el, 2002). All of the current information regarding the yeast genome, individual genes and their protein products are available for bioinformatic analysis at the *Saccharomyces* genome database (SGD) at yeastgenome.org.

Saccharomyces cerevisiae also possesses valuable traits that allow for researchers to use this model organism as a system to investigate several highly specialized areas of science. As previously described *Saccharomyces cerevisiae* possesses a homoplasmic mitochondrial genome. A eukaryotic model organism which possesses this trait it is an extremely valuable tool in investigating the genes or pathways involved in the regulation and maintenance of cellular respiration, and mitochondrial genome repair. As a facultative anaerobe, *Saccharomyces cerevisiae* can produce ATP through fermentation or cellular respiration. Therefore if one

wanted to investigate the genes or metabolic pathways involved in cellular respiration, *Saccharomyces cerevisiae* is one of the only model systems that would allow for the manipulation or disruption of these genes and still be viable. A homoplasmic mitochondrial genome is also extremely valuable when investigating mitochondrial genome stability and repair. This feature allows for the creation of transformed yeast cells that possess uniform recombinant mtDNA. Cells that possess uniform mtDNA are of great value to researchers attempting to incorporate reporter constructs, perform metabolic engineering, and when studying heteroplasmy.

The Non-homologous End Joining DNA Repair Pathway

When reviewing Figure 5, we see that recombinational repair is a key mechanism involved in maintaining the stability of both the nuclear and mitochondrial genomes. There are currently two types of recombinational repair of damaged DNA. The first is homologous recombination. Homologous recombination relies upon the use of or interaction of DNA sequences with a high degree or near perfect sequence homology. The second type of recombinational repair is non-homologous end joining (NHEJ). Non-homologous end joining refers to recombination between sequences of DNA with little or no DNA sequence homology. Recombinational repair is essential for meiosis, DNA double strand break repair, and eukaryotic cell viability (Krough and Symington, 2004). In this study we are investigating the role of the non-homologous end joining DNA repair pathway in maintaining the integrity of the mitochondrial genome of *Saccharomyces cerevisiae*.

Non-homologous end joining is one of the most prevalent double strand break (DSB) repair pathways in higher eukaryotes (Jeggo 1998). The term non-homologous end joining was initially coined in 1996 by JK Moore and JE Haber due to the NHEJ pathway's

28

ability to repair HO-endonuclease induced DNA double strand breaks. The role non-homologous end joining plays in the processing of DNA double strand breaks is conserved throughout evolution and is important from maintaining genomic stability in both yeast and human. The NHEJ pathway is required for site-specific VDJ recombination which is necessary for T-cells to recognize antigens in the adaptive immune response in higher eukaryotes (Becker et al. 2006). This pathway is also involved in the occurrence of single strand annealing, the repair of collapsed or blocked replication forks, and *MAT* locus heterozygosity (SGD).

The non-homologous end joining DNA repair pathway functions through 2 multi protein complexes known as the KU and MRX complexes, which function in combination with 3 co-factors, Dnl4p, Lif1p, and Nej1p . The KU complex is often referred to as the "KU telomeric complex" because it has been shown to function in telomere maintenance and repair as well as NHEJ (SGD). The KU complex is composed of a heterodimer of Ku70p and Ku80p. Ku70p and Ku80p were initially identified by Feldmann and Winnacker in 1993 as a HDF-70, and HDF-80 (high affinity DNA binding factor) due to their respective molecular weights, and the ability to bind DNA in a sequence in-specific manner (Feldman and Winnacker, 1993). Ku70p and Ku80p both possess DNA and protein binding domains which allows for the formation of the Ku70p-Ku80p dimer (KU complex), and the binding to DNA at sites of double strand breaks (SGD). Ku70p and Ku80p have been shown to localize to regions surrounding the nucleus in yeast, but upon the sensing of DNA double strand breaks, the KU complex is targeted to these sites for interaction with the MRX complex and the completion of non-homologous end joining (Krough and Symington, 2004).

The second multi-protein complex involved in non-homologous end joining is the MRX complex. Outside of NHEJ, the MRX complex is involved in the generation of the 3' overhang necessary for strand invasion prior to homologous recombination during meiosis and double strand break repair, as well as the degradation of bulky adducts from DNA at the sites of DNA double strand breaks (SGD). The MRX complex is a pentamer, which is composed of 2 molecules of Rad50p, 2 molecules of Mre11p, and 1 molecule of Xrs2p generating a stociometric ratio of 2:2:1. *RAD50, MRE11,* and *XRS2* were identified in 1974 in a genetic screen by Game and Mortimer due to their sensitivity to x-rays and ionizing radiation (Game and Mortimer, 1974). Rad50p is a 152 kDa protein which possesses both DNA and protein binding domains involved in the structural maintenance of telomeres and chromosomes (SGD). Mre11p is a 77 kDa protein which possesses 5'-3' exonuclease activity that has been shown to possess the ability to degrade bulky protein/DNA adducts at the site of DNA double strand breaks (SGD). The the MRX complex is formed when a dimer of Mre11p binds the base of a Rad50p dimer, creating a heterotetramer, which allows for the binding of Xrs2p. Xrs2p is a 96 kDa protein which is known to be involved in telomere maintenance and cell cycle checkpoint signaling at the G1-S interface. Xrs2p possesses DNA and protein binding domains which allows for a monomer of Xrs2p to bind to the Mre11-Rad50p heterotetramer leading to formation of the MRX complex (SGD).

As previously described, the NHEJ pathway relies upon 3 protein co-factors to repair DNA double strand breaks. The co-factors are Dnl4p, Lif1p, and Nej1p. Dnl4p is a 180 kDA ATP dependent DNA ligase. It was initially identified in 1997 due to its ability to re-circularize linearized plasmids by Schar et al. Lif1p was discovered in 1998 as a 48 kDa protein that interacts in a complex with Dnl4p to mediate non-homologous end joining in

yeast (Hermann et al. 1998). Nej1p (also known as Lif2p) is a 39 kDa protein involved in nuclear localization and targeting of Lif1p to sites of DNA double strand breaks within the nucleus (Valencia et al. 2001).

In 2004, in the *Annual Review of Genetics,* Berit Krogh and Lorraine Symington published a review article titled "Recombination Proteins in Yeast" which described in detail the non-homologous end joining DNA repair pathway. In this publication they included a model for the repair of nuclear DNA double strand breaks by the NHEJ pathway in *Saccharomyces cerevisiae.* This model for the repair of nuclear DNA double strand breaks is displayed in Figure 7 below. In this model the initiating event is a DNA double strand break. Upon the cell's recognition of the DNA double strand break, 2 copies of the KU complex are recruited from their position neighboring chromosomal telomeres to the sites of the DNA double strand break. Once the KU complex has located the double strand break, each complex stabilizes and tethers one side of the DNA DSB. With both KU complexes in place, 2 copies of the MRX complex are recruited to the DSB. Each copy of the MRX complex (with the exonuclease function of Mre11p) then processes both ends of the DSB prior to ligation. In the event that the DSB possesses compatible ends, the break is directly ligated together. If the DSB does not possess compatible ends the MRX complexes will generate them with the loss of minimal nucleotides. Once both ends have been positioned and processed for ligation, Lif1p (with the assistance of Nej1p) activates and targets Dnl4p to the site of the DNA double strand break. Dnl4p then ligates the gap while the KU and MRX complexes disassociate from the site of DNA double strand break (Krough and Symington, 2004). The NHEJ pathway is sometimes referred to as an "error prone DNA repair pathway" because of the potential for loss of genetic material. The

processing and mediation of DNA double strand breaks by the NHEJ pathway as described by Krogh and Symington is described in Figure 7 below.
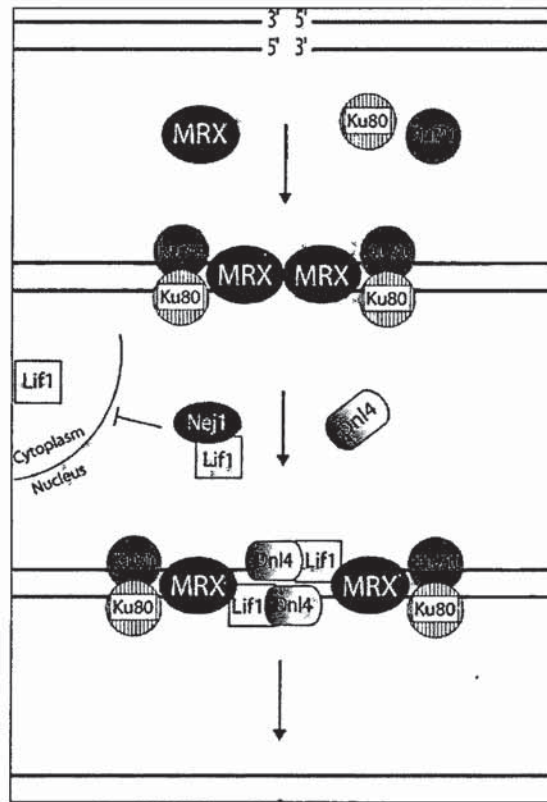
Figure 7. The Non-homologous end joining nuclear DNA double strand break repair model. Krogh and Symington. (2004). Recombination proteins in Yeast. *Annual Review of Genetics.* 2004. 38:233–71.

The Non-homologous End Joining DNA Repair Pathway is Conserved throughout Evolution

The non-homologous end joining DNA repair pathway is present in some form in nearly all eukaryotes ranging from yeast, to mice, to humans. In yeast homologous recombination is the most prevalent form of recombination-induced repair of DNA double strand breaks. While in higher eukaryotes, including humans, non-homologous end joining is the most prevalent form of recombination induced repair of DNA double strand breaks

(Jeggo PA, 1998). Table 3 below lists all of the *Saccharomyces cerevisiae* NHEJ members and protein cofactors, and their *Homo sapiens* homologs.

Saccharomyces cerevisiae NHEJ Members	*Homo sapiens* NHEJ Members
Ku70p	Ku70p
Ku80p	Ku80p
?	DNA protein kinases
Rad50p	Rad50p
Mre11p	Mre11p
Xrs2p	Nbs1p
Dnl4p	LigIVp
Lif1p	Xrcc4p
Nej1p	?

Table 3. Yeast non-homologous end joining members and key cofactors, and there human homologs.

Specific Aims

While much is known regarding the role of the non-homologous end joining DNA repair pathway in its ability to repair nuclear DNA DSBs, their has been little work done to elucidate the role of this pathway in ameliorating mtDNA DSBs. For this reason we perofmed this study. Working under the guidance of Dr. Rey Sia in collaboration with our colleagues Dr. Elaine Sia and Lidza Kalifia from the University of Rochester, the focus of our research is to identify factors that regulate the structure, organization, and repair of the mitochondrial genome in *Saccharomyces cerevisiae*. Currently, the immediate focus of the research in our lab centers around the role of the MRX complex and non-homologous end joining in mitochondrial genome stability and repair. Deletions within the mitochondrial genome lead to respiration loss and cell death in higher eukaryotes. Therefore the use of the facultative anaerobic model organism, *Saccharomyces cerevisiae* has become an incredibly powerful tool when investigating the maintenance of the mitochondrial genome. Due to the

high rate of the conservation of nuclear DNA repair pathways among eukaryotes, it is our hope that the insights we make into the mtDNA repair mechanisms in yeast, may lead to insights into human mtDNA repair. This study has 2 Specific Aims:

Aim I. Determine the role of the MRX complex and the non-homologous end joining DNA repair pathway in the occurrence of spontaneous mitochondrial and nuclear direct repeat-mediated deletions, the occurrence of mitochondrial and nuclear point mutations, as well as the occurrence of spontaneous respiration loss in the model organism *Saccharomyces cerevisiae*. Advancements in the molecular, genetic, and pharmacological tools available for use with *Saccharomyces cerevisiae* allowed us to quantify the roles of the MRX complex and NHEJ in the previously described aspects known to govern genomic stability. To quantify the roles of the MRX complex and non-homologous end joining in these aspects governing genomic stability, knock out strains were generated for *RAD50*, *XRS2*, *MRE11*, *KU70*, and *KU80*. A *KU70-KU80* double mutant, a *RAD50-MRE11-XRS2* triple mutant, a *RAD50-KU70-KU80* triple mutant, and a *RAD50-MRE11-XRS2-KU70-KU80* mutant strain were generated to further determine the roles of the MRX and KU complexes, as well as the entire NHEJ pathway in maintaining genomic stability. All of the strains in this NHEJ knock out library were mated with alternate strains which possessed nuclear and mitochondrial reporter constructs which allowed for the detection and quantification of direct repeat-mediated deletions using genetic assays and fluctuation analysis. The occurrence of spontaneous respiration loss was documented and quantified using a genetic assay that relies upon the use of specialized media (YPG with 0.2% dextrose) that allows for the determination and quantification of yeast cells which have lost

mitochondrial function and the ability to respire. The role of the MRX complex and the NHEJ pathway in the occurrence of spontaneous nuclear and mitochondrial point mutations was quantified using resistance to the pharmacological agents canavanine and erythromycin.

Aim II. Localize the non-homologous end joining factor Ku70p to the mitochondria using cellular fractionation and western blot analysis. Individual components of the cell can be isolated and purified using differential centrifugation. This process relies upon the different sedimentation coefficients, or sedimentation rates of the major components of the cell. By performing a differential centrifugation protocol originally devised by Glick and Pon in 1995 we were able to successfully isolate mitochondria from *Saccharomyces cerevisiae*. Mitochondria were further purified using discontinuous Nycodenz gradients and ultracentrifugation. Once mitochondria had been isolated and purified from yeast cells, western blot analysis was performed to monitor for the presence of the NHEJ factor Ku70p. The successful isolation and purification of mitochondria from lysed cells was verified by probing mitochondrial fractions for the presence of Cox2p and Histone H4p respectively. *COX2* is encoded, transcribed, translated, and localized within the mitochondria. Therefore a significant enrichment in the presence of Cox2p per unit weight of total protein over a whole cell lysate control can verify the successful isolation of mitochondrial fractions from cell lysates. Histone H4p is known to be localized only within the nucleus, therefore the presence or absence of Histone H4p within isolated mitochondrial fractions can confirm if mitochondria have been purified from nuclear contaminates. Upon the verification of successful purification of mitochondrial fractions using western blot analysis, probing for the presence of NHEJ factor Ku70p can then determine whether non-homologous end joining

factors can be localized to the mitochondria of *Saccharomyces cerevisiae*. A *KU70:HA* epitope strain was created and employed in this localization experiment. The use of the *KU70:HA* epitope strain and an anti-HA antibody reduces the presence and detection of non-specific signal, thereby ensuring with greater accuracy the validity of this localization experiment. Once the presence of Ku70:HAp had been verified in purified mitochondrial fractions sequential proteinase K treatments were performed to further localize the presence of Ku70:HAp within the mitochondria.

Tools used in the Investigation of the Role of the MRX Complex and NHEJ in Mitochondrial Genome Stability and Repair

The Direct Repeat-Mediated Deletion Assays

The use of reporter genes when investigating genetic and molecular events within the cell is becoming increasingly popular. In this study mitochondrial and nuclear reporters were employed to determine the rate of direct repeat-mediated deletions as described by Phadnis et al. in 2005. Both the nuclear and mitochondrial direct repeat-mediated deletion reporters have been transformed in yeast cells allowing for both the nuclear and mitochondrial DRMD assays to be performed simultaneously. For the ease of description the assays are described separately below. The rate of nuclear and mitochondrial direct repeat-mediated deletions per cell division was then calculated using fluctuation analysis and the method of the median (Lea and Coulson et al., 1949).

The Mitochondrial Direct Repeat-Mediated Deletion Reporter

In the mitochondrial direct repeat-mediated deletion assay the nuclear *ARG8^m* gene has been translocated from its wild-type nuclear locus to the mitochondrial genome within

36

the reading frame of the *COX2* gene to monitor for the occurrence of spontaneous direct repeat-mediated deletions. The nuclear *ARG8* gene is a required component of the arginine biosynthetic pathway and is thus required for growth on media lacking arginine. The structure of *ARG8ᵐ* mitochondrial direct repeat-mediated deletion reporter can be seen in Figure 8 below. The *ARG8ᵐ* mitochondrial reporter contains a single ATG start codon upstream of 96 base pairs of homology to the n-terminus of the *COX2* gene which have been introduced or fused in frame upstream of the *ARG8ᵐ* gene. Directly downstream of *ARG8ᵐ* gene is the full length *COX2* gene which encodes cytochrome c oxidase subunit 2. Cox2p is involved in the final stage of the electron transfer chain required to generate the electrochemical gradient needed to synthesize ATP. Cells which possess the *ARG8ᵐ* reporter do not possess *COX2* function and are respiration deficient, are ARG +, and will not grow in the presence of glycerol. A precise direct repeat recombination event directly downstream of the ATG start codon will bring the *COX2* gene back into frame, restore the function of *COX2*, and allow yeast cells to survive in the presence of glycerol as the sole carbon source.

Mitochondrial Direct Repeat Reporter

- Inactive *COX2*
- Respiration deficient
- Arg$^+$

- Active *COX2*
- Respiration proficient
- Arg$^-$

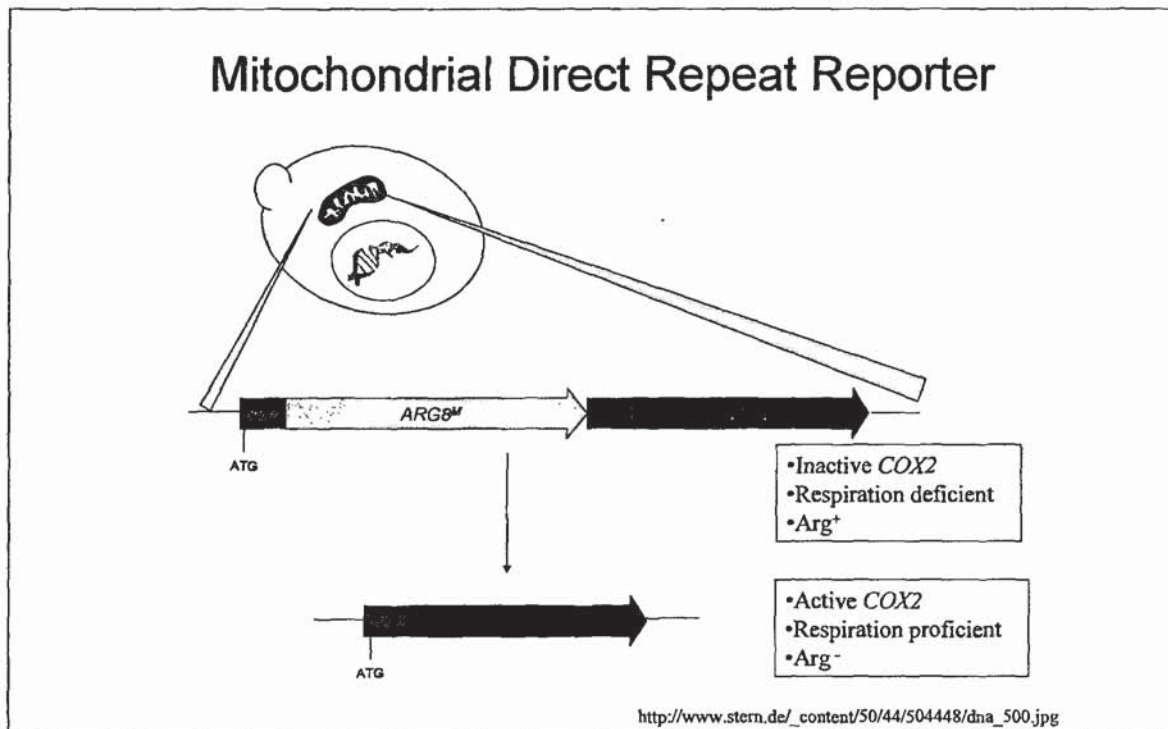http://www.stern.de/_content/50/44/504448/dna_500.jpg

Figure 8. The mitochondrial direct repeat-mediated deletion reporter. This reporter contains the *ARG8* gene flanked by 96 base pairs of homology of the N-terminus of *COX2* gene. Disruption of the reading frame of *COX2* gene by the *ARG8^m* gene leads to respiration deficient cells and prevents growth on media containing glycerol. After a precise spontaneous recombination event at this locus the *ARG8^m* gene is excised restoring the reading frame of the *COX2* gene generating respiration proficient cells. Cells which possess direct repeat-mediated deletion events at this locus are selected for on YPG media.

The Nuclear Direct Repeat Mediated Deletion Reporter

In the nuclear direct repeat-mediated deletion assay the nuclear *URA3* gene has been translocated from its wild-type nuclear locus to interrupt the coding sequence of the *TRP1* gene to monitor for the occurrence of spontaneous nuclear direct repeat-mediated deletions. The nuclear *TRP1* gene is a required component of the tryptophan biosynthetic pathway and is thus required for growth on media lacking tryptophan. The structure of *URA3* nuclear direct repeat-mediated deletion reporter can be seen in Figure 9 below. The *URA3* reporter consists of 96 base pairs of homology to the n-terminus of the *TRP1* gene

flanking the *URA3* gene with a single ATG start codon. Cells which possess the *URA3*

reporter will not possess *TRP1* function and are TRP1-, and thus will not grow in the

absence of tryptophan. Upon a precise direct repeat recombination event at this locus cells

will be able to restore the function of *TRP1*, and will survive in the absence of tryptophan in

the growth media.
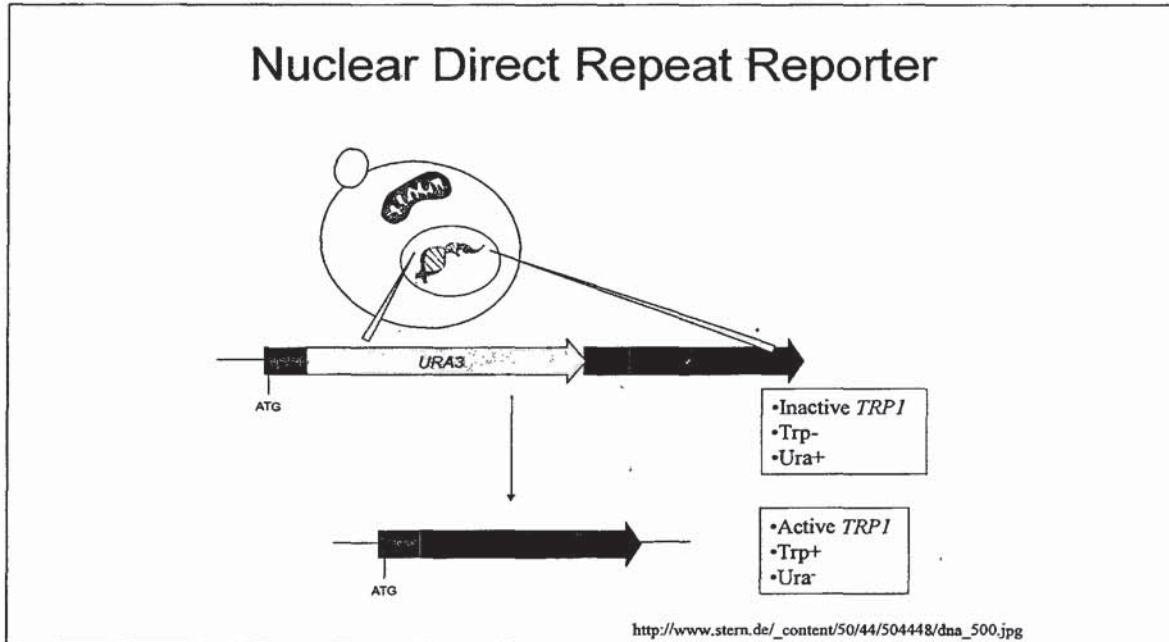
Figure 9. The nuclear direct repeat-mediated deletion reporter. This reporter
contains the *URA3* gene flanked by 96 base pairs of homology of the N-terminus of
TRP1 gene. Disruption of the reading frame of *TRP1* gene by the *URA3* gene leads
to *TRP1* deficient cells and prevents growth on media lacking tryptophan. After a
precise spontanoues recombination event at this locus the *URA3* gene is excised
restoring the reading frame of the TRP1 gene generating tryptophan proficient cells.
Cells which possess direct repeat-mediated deletion events at this locus are selected
for on media lacking tryptophan.

The Nuclear Point Mutation Assay

The nuclear point mutation assay relies upon the acute toxicity of canavanine to

yeast cells. Canavanine (CAN) is a molecular mimic to arginine and when it is transported

into the cell it is incorporated into a growing polypeptide chain (in place of arginine) resulting in cell death. Canavanine is taken up from the environment by yeast cells via the membrane bound arginine permease, encoded by the *CAN1* gene. Point mutations within the *CAN1* gene lead to canavanine resistance by preventing canavanine from being transported into the cell (Fantes and Creanor, 1984). The rate of nuclear point mutations per cell division was calculated using fluctuation analysis and the method of the median (Lea and Coulson et al., 1949).

The Mitochondrial Point Mutation Assay

The mitochondrial point mutation assay relies upon the acute toxicity of erythromycin to yeast cells. Erythromycin (ERY) mimics a charged tRNA and when entering the P site in a mitochondrial ribosome, preventing translation leading to cell death. Point mutations in 21S rRNA gene will prevent erythromycin from entering the yeast mitochondrial ribosome leading to erythromycin resistance. Review Figure 10 below to further elaborate on the mechanism responsible for the toxicity of erythromycin to yeast cells. Erythromycin resistance and the mitochondrial point mutation assay were used initially by Francoise Foury and Sylvie Vanderstraeten in 1992. These authors used ERY resistance to study the 3'-5' exonuclease activity of the *MIP1* gene (the yeast mitochondrial polymerase).

There are at least two specific point mutations in the 21S rRNA gene that have been documented which lead to erythromycin resistance and cell viability when cultured on YG plus 0.4% erythromycin (Sor and Fukuhara, 1982). A copy of the restriction map for the yeast mitochondrial 21S rRNA gene listing the sites which lead to erythromycin resistance is posted in the Appendix following this study. The rate of mitochondrial point mutations per

40

cell division was calculated using fluctuation analysis and the method of the median (Lea and

Coulson et al., 1949).
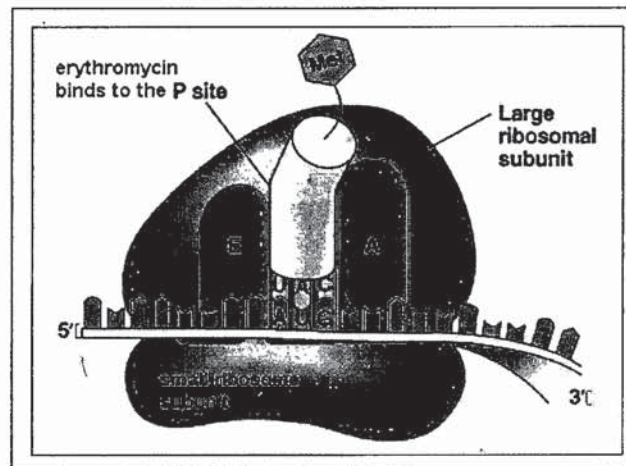
Figure 10. Mechanism for the acute toxicity of erythromycin. Erythromycin resistance is used as a tool to investigate the occurrence of spontaneous point mutations in the mitochondrial genome. Erythromycin mimics a charged tRNA and when entering the P site in a mitochondrial ribosome, it prevents translation leading to cell death. Image adapted from http://fig.cox.miami.edu/~cmallery/150/cells/ribosome.jpg

The Spontaneous Respiration Loss Assay

The spontaneous respiration loss assay is used to assess the role of specific proteins

and pathways in maintaining mitochondrial function. As previously described *Saccharomyces*

cerevisiae is a facultative anaerobe and can produce ATP using both fermentation and cellular

respiration depending upon the carbon source provided in the growth media. Yeast cells can

survive with large mtDNA deletions (*rho-*) when cultured on a fermentable carbon source

such as YPD (yeast extract, peptone, and dextrose). Yeast cells that are *rho-* are unable to

survive with these deletions when cultured on a growth media with the sole carbon source of

glycerol as in YPG (yeast extract, peptone, and glycerol). These metabolic restrictions are the

basis for the peteite phenotype seen in the spontaneous respiration loss assay seen in Figure

41

11 below. Yeast cells are initially cultured on YPG to select for respiration proficient cells. They are then cultured in YPD media which removes the nutritional requirement for mitochondrial function and cellular respiration thereby allowing for the occurrence of spontaneous respiration loss. Cells are then plated on YPG plus 0.2% dextrose which possess glycerol as the primary carbon source but is supplemented with dextrose. Yeast cells which have lost ability to respire (rho-) will grow in the presence of dextrose but when they have exhausted the supply of his carbon source will arrest because they are unable to utilize the remaining glycerol due to the impairment of mitochondrial function. Yeast cells whose growth has arrested possess the petite phenotype, and appear as colonies which are significantly reduced in size. Yeast cells which still possess mitochondrial function (rho+) will continue to grow after they have exhausted the dextrose in the growth media by utilizing the remaining glycerol via cellular respiration. Rho+ yeast cells possess the grand phenotype when they are plated on this media because they are significantly larger when compared to rho- yeast cells. The frequency of spontaneous respiration loss can then be determined by counting and scoring yeast colonies as either grand (rho+) or petite (rho-), adding the number of grand and petite colonies, and then dividing the total number of colonies by the number of petites. Figure 11 below describes the relationship between the grand and petite phenotypes, rho+ and rho-, and the ability yeast cells with this phenotype to be cultured in the presence of dextrose and glycerol.
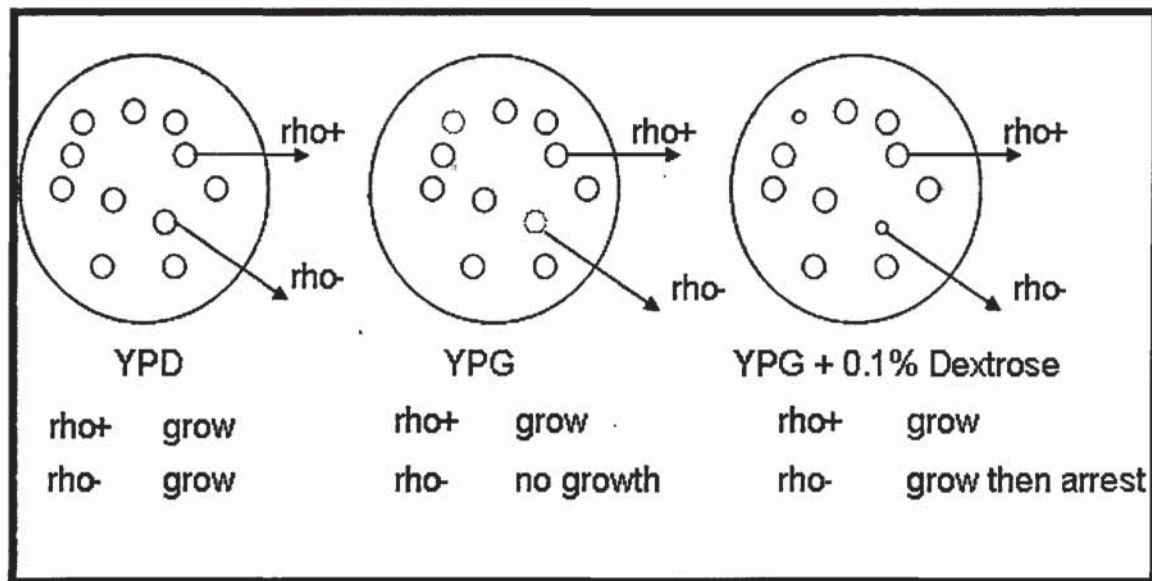
Figure 11. Determining respiration proficiency using the spontanoues respiration loss assay. The frequency of spontaneous respiration loss was calculated by scoring counting the number of petite non-respiring (*rho-*) colonies as well as well as wild-type grande (*rho+*) respiration proficient colonies when cultured on YPG plus 0.2% dextrose.

Hypothesis

Our understanding of the molecular mechanisms responsible for regulating mitochondrial genomic stability is significantly less clear than their nuclear genomic counterpart. The role of the MRX complex and the non-homologous end joining pathway in regulating genomic stability in the nucleus has been well characterized, yet it is unclear exactly what role the MRX complex and NHEJ plays in regulating mitochondrial genome stability and repair. Therefore it is our hypothesis that members of the MRX complex and the NHEJ pathway are present in the mitochondria where they are involved in the regulation of mtDNA stability and repair. Furthermore we hypothesized that the absence of the MRX complex and non-homologous end joining will alter the overall stability of the mitochondrial genome, which will be manifested through a change in the occurrence of spontaneous

mitochondrial direct repeat-mediated deletions, spontaneous mitochondrial point mutations, and the occurrence of spontaneous respiration loss within *Saccharomyces cerevisiae*.

Materials & Methods

Yeast strains:

Saccharomyces cerevisiae strains used in this study were isogenic prior to transformation and are referred to as DFS188. DFS188 possessed the following genotype: *Mata ura3-52 leu2-3, 112 his 3 arg8*. All strains were grown in either rich media or synthetic media lacking the appropriate amino acid to maintain selection of cells of interest. All of the strains used in this study were provided by our collaborators Dr. Elaine Sia and Lidza Kalifa from The University of Rochester. All yeast strains were cultured in an environmental growth chamber at 30 degrees Celsius. Refer to Table 4 for all relevant genotypes.

Yeast media:

Yeast strains were cultured on the following media: YPD, YPG, YPRaff, SD-Trp, SD-Ura-Arg, SD-Arg, YPG plus 0.2% dextrose, YG plus 0.4% erythromycin, or SD-Arg plus 0.006% canavanine. YPD media contains 1% yeast extract, 2% bactopeptone, and 2% dextrose. YPG and YPRaff media are identical to YPD media except that YPG and YPRaff contained 2% glycerol or 2% raffinose as the respective carbon source. YG plus erythromycin media contains 2% yeast extract, 2% glycerol, buffered phosphate solution, and 4 g/l erythromycin. Synthetic (SD) media contained 0.17% yeast nitrogen base minus amino acids, 0.5% ammonium sulfate, 2% dextrose and 0.077% of the appropriate amino acid dropout mix. SD-Arg plus canavanine media was generated in the same manner as previously described but was enhanced with 60 mg/l canavanine.

Table 4: Yeast strains used in this study

Experiment:	Direct Repeat-Mediated Deletion Assay
Strain	Relevent Genotype
Lky196 (wt)	DFS188 Rep96::ARG8m::cox2 Rep96::URA3::trp1
rad50Δ	Lky196 rad50Δ::KanMX
mre11Δ	Lky196 mre11Δ::KanMX
xrs2Δ	Lky196 xrs2Δ::KanMX
ku70Δ	Lky196 ku70Δ::KanMX
ku80Δ	Lky196 ku80Δ::KanMX
ku70Δku80Δ	Lky196 ku70Δ::KanMXku80Δ::KanMX
rad50Δmre11Δxrs2Δ	Lky196 rad50Δ::KanMXmre11Δ::KanMXxrs2Δ::KanMX
rad50Δku70Δku80Δ	Lky196 rad50Δ::KanMXku70Δ::KanMXku80Δ::KanMX
rad50Δmre11Δxrs2Δku70Δku80Δ	Lky196 rad50Δ::KanMXmre11Δ::KanMXxrs2Δ::KanMXku70Δ::KanMXku80Δ::KanMX

Experiment:	Respiration Loss & Erythromycin Resistance Assays
Strain	Relevent Genotype
DFS188 (wt)	Mat a ura3-52 leu2-3, 112 his 3 arg8
rad50Δ	DFS188 rad50Δ::KanMX
mre11Δ	DFS188 mre11Δ::KanMX
xrs2Δ	DFS188 xrs2Δ::KanMX
ku70Δ	DFS188 ku70Δ::KanMX
ku80Δ	DFS188 ku80Δ::KanMX
ku70Δku80Δ	DFS188 ku70Δ::KanMXku80Δ::KanMX
rad50Δmre11Δxrs2Δ	DFS188 rad50Δ::KanMXku70Δ::KanMXku80Δ::KanMX
rad50Δku70Δku80Δ	DFS188 rad50Δ::KanMXku70Δ::KanMXku80Δ::KanMX
rad50Δmre11Δxrs2Δku70Δku80Δ	DFS188 rad50Δ::KanMXmre11Δ::KanMXxrs2Δ::KanMXku70Δ::KanMXku80Δ::KanMX

Experiment:	Canavinine Resistance
Strain	Relevent Genotype
Lky202 (wt)	Mat a ura3-52 leu2-3, 112 his 3 ARG8
rad50Δ	DFS188 rad50Δ::KanMX
mre11Δ	DFS188 mre11Δ::KanMX
xrs2Δ	DFS188 xrs2Δ::KanMX
ku70Δ	DFS188 ku70Δ::KanMX
ku80Δ	DFS188 ku80Δ::KanMX
ku70Δku80Δ	DFS188 ku70Δ::KanMXku80Δ::KanMX
rad50Δmre11Δxrs2Δ	DFS188 rad50Δ::KanMXku70Δ::KanMXku80Δ::KanMX
rad50Δku70Δku80Δ	DFS188 rad50Δ::KanMXku70Δ::KanMXku80Δ::KanMX
rad50Δmre11Δxrs2Δku70Δku80Δ	DFS188 rad50Δ::KanMXmre11Δ::KanMXxrs2Δ::KanMXku70Δ::KanMXku80Δ::KanMX

Experiment:	Western Analysis
Strain	Relevent Genotype
KU70::HA	DFS188 KU70::Citrine::HA

Direct Repeat-Mediated Deletion Assay:

The direct repeat-mediated deletion (DRMD) assay employs the use of the nuclear and mitochondrial DRMD reporter constructs in unison with selective and non-selective media to determine the rate of spontaneous direct repeat-mediated deletion events via fluctuation analysis.

To determine the rate of DRMD per cell division for both the wild type and knockout strains freezer stocks were patched out onto SD minus Ura minus Arg to select for cells that possessed the reporter constructs. These cultures were incubated for two nights at $30°$ C. Inoculum from this plate was taken to streak singles on YPD plates and incubated for 3 over nights at $30°$ C. 20 independent colonies were collected and a serial dilution was generated. Independent colonies were transferred into an Eppendorf tube containing 100 µl of distilled water and vortexed into a homogenous solution ("tube A"). 5 µl of this solution was then transferred into another Eppendorf tube containing 500 µl of distilled water and vortexed into a homogenous solution thereby generating a 10^{-2} dilution ("tube B"). 5 ul of the 10^{-2} dilution was then transferred to another Eppendorf tube containing 500 µl of distilled water and vortexed into a homogenous solution thereby generating a 10^{-4} dilution ("tube C"). 95 µl of the solution from "tube A" was then plated on the SD minus Trp plates. 100 µl of the solution from "tube B" was then plated on the YPG plates. 50 µl of the solution form "tube C" was then plated on the YPD plates. Solutions were uniformly spread across each of the plates by applying 3 mm glass beads to each of the plates and then agitating the plates in a horizontal and vertical manner. The glass beads were then poured off and the plates were incubated at $30°$ C for three over nights. Following the incubation period, plates were removed from the growth chamber and colonies were counted. The rate of nuclear and mitochondrial direct repeat-mediated deletions per cell division was then

calculated using fluctuation analysis and the method of the median (Lea and Coulson et al., 1949). Refer to table 5. Statistical significance was determined using a students two-tailed T-test and by calculating 95% confidence limits for two independent trials.

Nuclear Point Mutation Assay:

The nuclear point mutation assay relies upon the acute toxicity of Canavanine to yeast cells. Canavanine (CAN) is a molecular mimic to arginine and when it is transported into the cell and incorporated into a growing polypeptide chain (in place of arginine) it results in cell death. Canavanine is taken up from the environment via the membrane bound arginine permease, encoded by the *CAN1* gene. Mutations within the *CAN1* gene lead to canavanine resistance.

To determine the rate of nuclear point mutations per cell division freezer stocks of Lky202 and knockout strains were streaked onto SD plates lacking arginine to select for cells that were Arg+. These cultures were incubated for three over nights at 30° C. 15 colonies were then collected and inoculated into 5 ml of liquid SD minus Arg media and incubated overnight at 30° C. This culture was spun down and re-suspended in 1ml of distilled water and a serial dilution was then performed. 50 μl of each of the cultures was transferred to an Eppendorf tube containing 500 μl of distilled water and vortexed into a homogenous solution ("tube A"). 5 μl of this solution was then transferred into another Eppendorf tube containing 500 μl of distilled water and vortexed into a homogenous solution thereby generating a 10^{-3} dilution ("tube B"). 5 ul of the 10^{-3} dilution was then transferred to another Eppendorf tube containing 500 μl of distilled water and vortexed into a homogenous solution thereby generating a 10^{-5} dilution ("tube C"). 100 μl of the solution from the undiluted re-suspended culture was then plated on the SD minus Arg plus Canavanine plates. 50 μl of the solution from "tube C" was then plated on the SD minus Arg plates.

Solutions were spread uniformly across each of the plates by applying 3 mm glass beads and then agitating the plates in a horizontal and vertical manner. The glass beads were then poured off and the plates were incubated at 30° C for 3 over nights. Following the incubation period, plates were removed from the growth chamber and colonies were counted. The rate of spontaneous nuclear point mutations per cell division was then calculated using fluctuation analysis and the method of the median (Lea and Coulson et al., 1949). Refer to table 5. Statistical significance was determined using a students two-tailed T-test and by calculating 95% confidence limits for two independent trials.

Mitochondrial Point Mutation Assay:

The mitochondrial point mutation assay relies upon the acute toxicity of erythromycin to yeast cells. Erythromycin (ERY) mimics a charged tRNA and when entering the P site in a mitochondrial ribosome it haults translation leading to cell death. Point Mutations in the mitochondrial 21S rRNA gene lead to erythromycin resistance and cell viability.

To determine the rate of mitochondrial point mutation per cell division, singles were streaked directly from freezer stocks of DFS188 and knockout strains onto YPG to select for respiration proficient cells and incubated at 30° C for 3 over nights. 20 independent colonies were then inoculated into 5 ml of YPG and incubated for 2 over nights at 30° C. These cultures were spun down and re-suspended in 1 ml of distilled water and a serial dilution was then performed in an identical manner to that of the nuclear point mutation assay. 100 μl of the solution from the undiluted re-suspended culture was then plated on the YG plus 0.4% erythromycin plates. 50 μl of the solution from "tube C" was then plated on the YPG plates. Once again the glass bead method was employed to uniformly distribute the

solution across the plates. The plates were incubated for 7 over nights at 30° C. Following

the incubation period, plates were removed from the growth chamber and colonies were

counted. The rate of spontaneous mitochondrial point mutations per cell division was then

calculated using fluctuation analysis and the method of the median (Lea and Coulson et al.,

1949). Refer to table 5 Statistical significance was determined using a student two-tailed T-

test and by calculating 95% confidence limits for two independent trials.

Spontaneous Respiration Loss Assay:

The spontaneous respiration loss assay was used as a tool to determine the potential

role of gene knockouts in maintaining mitochondrial genome stability (by means of

monitoring mitochondrial dependent oxidative phosphorylation) compared to that of a wild

type control.

To determine the rate of spontaneous respiration loss assay for both the wild type

and knockout strains this assay was performed by patching freezer stocks onto YPG to

select for yeast cells that were respiration proficient. These cultures were incubated at 30° C

for 2 over nights. From this culture singles were streaked onto YPD and incubated at 30° C

for 3 over nights. 10 independent colonies were then collected and then inoculated into 5 ml

of liquid YPD and incubated at 30° C for 1 over night. Cultures were pelleted and re-

suspended in 1 ml of distilled water and a serial dilution was performed. 50 µl of each of

these 10 cultures was then transferred into an Eppendorf tube containing 500 µl of distilled

water and vortexed into a homogenous solution thereby generating a 10^{-1} dilution ("tube

A"). 5 µl of the 10^{-1} dilution was then transferred to another Eppendorf tube containing 500

µl of distilled water and vortexed into a homogenous solution thereby generating a 10^{-3}

dilution ("tube B"). 5 ul of the 10^{-3} dilution was then transferred to another Eppendorf tube

containing 500 μl of distilled water and vortexed into a homogenous solution thereby generating a 10^{-5} dilution ("tube C"). 100 μl of the homogenous solutions from "tube C" was plated on YPG plus 0.2% dextrose plates. Solutions were uniformly spread across each of the plates by applying 3 mm glass beads and agitating the plates in a horizontal and vertical manner. The glass beads were then poured off and the plates were incubated at 30° C for three over nights. Following the incubation period, plates were removed from the growth chamber and colonies were scored and counted. Yeast colonies whose growth had arrested were counted and scored as *rho-* (petite colonies which possess mitochondrial deletions), while colonies whose growth had not arrested were counted and scored as *rho+* (cells which still possessed mitochondrial function). The frequency of spontaneous respiration loss was then determined by adding the number of *rho-* and *rho+* colonies together and then dividing this total number by the number of *rho-* colonies, and then multiplying by 100 to generate a percent. Statistical significance was determined using a student stwo-tailed T-test and by calculating 95% confidence limits for three independent trials.

Calculating the Rate of Mutation:

The method of the median (Lea and Coulson, 1949) was used to determine the rate of mutations per cell division for the direct repeat-mediated deletion assay and the nuclear and mitochondrial point mutation assays. Colonies were counted on the control and experimental plates for all assays and data was recorded using Microsoft Excel. Initially an average number of colonies per plate were generated for all of the values for the control plates. Then the average was multiplied by 0.5 and by 2, yielding ½ and 2 times the average. At this point any plates which possessed more than two times or less than ½ the average number of colonies were removed from the data set and a final average was then calculated.

This final average was then multiplied by the appropriate dilution factor to generate the average number of cells plated (either the total number of cells/colony, or the total number of cells per culture). The rate of mutation was then determined by calculating the number of mutations divided by the total number of cells.

The number of mutations is calculated with the assistance of the chart devised by Lea and Coulson in 1949 (refer to table 5). The median number of colonies was then determined from all of the experimental plates. The median was then multiplied by the appropriate dilution factor to generate the r_0 value. The chart is then used to determine the corresponding r_0/m value for a specific r_0 value. Refer to Table 5 for an example of chart devised by Lea and Coulson in 1949 to generate the rate of mutation. The r_0 value was then divided by the r_0/m value generating m, the rate of mutation. M was then divided by the total number of cells to generate the rate of mutations per cell division.

When an experimental r_0 value is not present on the chart because it falls between two listed r_0 values, it is calculated mathematically. A sample calculation using the hypothetical r_0 value of 2.5 is listed below. Using the chart provided in table 5, we see that an r_0 value of 2.5 falls between an r_0 of 2.3 and 2.7. The lower r_0 value is subtracted from the derived r_0 value of 2.5 to generate 0.2. The difference between the two listed r_0 values of 2.3 and 2.7 is then calculated to yield 0.4 (2.7-2.3). The result of the difference between the derived r_0 value and the lower r_0 value (0.2) is then divided by the difference between the two listed values (0.4), generating 0.5. This quotient is then multiplied by 0.1 yielding 0.05. This number is then added to the r_0/m value directly across from the lower r_0 value used previously (2.3) to generate the new r_0/m of 1.65 (1.6 + 0.05). The experimentally derived r_0 value was then divided by the r_0/m value generating m, the rate of mutation. M was then divided by the total number of cells to generate the rate of mutations per cell division.

Table 5. A representative sample of the chart described by Lea and Coulson (1949) used to determine the rate of mutation per cell division.

	r_0	r_0/m
	1.4	1.3
0.2		
	1.6	1.4
0.3		
	1.9	1.5
0.4		
	2.3	1.6
0.4		
	2.7	1.7
0.5		
	3.2	1.8
0.5		
	3.7	1.9
0.6		
	4.3	2
0.7		
	5	2.1
0.7		
	5.7	2.2

Whole Cell Lysate Preparation:

Whole cell protein lysates (WCL) were generated for use as a control to identify the signal associated with the presence of Ku70p, Histone H4p, and Cox2p in purified mitochondria by western blot analysis. Freezer stocks of the Lky209 and *KU70::HA* strains were patched onto YPG and incubated for 3 over nights at 30° C. Samples of these cultures were inoculated into 50 ml of YPRaff and were cultured at 30° C to mid-log phase. Cultures were spun down and treated with 0.5 ml of the B150 lysis buffer and the Protease Inhibitor Cocktail (Sigma®) at 1:1000. The B150 lysis buffer is composed of 50 mM Tris pH 7.4, 150 mM NaCl, and 0.2% Triton-X 100. 500 micron glass beads were added to an Eppendorf

tube containing the previously described reagents, and the mixture was vortexed for 30 seconds then placed on ice for 30 seconds. This procedure of vortexing for 30 seconds and then placing tubes on ice of 30 seconds was repeated 5 times. The lysate was spun at 13,000 rpm for 1 minute generating an insoluble and soluble fraction. The soluble fraction was then removed and frozen at -80° C. The total protein concentration of the WCL was determined using the Bio-Rad® Protein Assay System in combination with a bovine serum albumin standard.

Mitochondrial Purification Protocol:

In order to localize Ku70p to the mitochondria via western analysis, differential centrifugation and Nycodenz purification were employed to isolate mitochondria from yeast cultures. This protocol is a modified form published by Glick et al. in 1995. Freezer stocks of DFS188 and *KU70::HA* were patched onto YPG and cultured at 30° C for 3 over nights. Samples of these cultures were inoculated into 2 L of YPRaff and grown to mid-log phase. Cultures were spun down at 4000 rpm in a Sorvall centrifuge and washed 1 time with ice cold distilled water. Cultures were transferred to 50 ml conical tubes and spun again in a tabletop Sorvall at 2000 rpm and the distilled water was aspirated off. The pellet was then weighed and re-suspended in Tris-SO$_4$ buffer (pH 9.4) 2 ml/g wet weight. Cultures were rocked for 10 minutes at 30° C. Cultures were spun down at 5000 rpm and washed with MP2 buffer (1.2 M sorbitol, 20 mM KH$_2$PO$_4$ pH 7.4), and pelleted at 5000 rpm. The pellet was re-suspended in MP2 buffer and 3 mg/g zymolyase and rocked for 30 minutes. The culture was pelleted at 5000 rpm, re-suspended in 13.4 ml/g of dounce buffer (10 mM Tris pH 7.4, 1mM EDTA, 0.2% BSA, Protease Inhibitor Cocktail 1:1000, and 0.6% sorbitol) and dounced 20 times in a 40 ml dounce homogenizer. The culture was pelleted at 4000 rpm, and supernatant was removed. The supernatant was spun at 4000 rpm and the supernatant

was transferred to a fresh tube and spun at 12,000 rpm to pellet mitochondria. The pellet was removed, re-suspended in SHE buffer (20 mM HEPES pH 7.4, 0.6 M sorbitol, 1 mM EDTA), and spun at 4000 rpm. The supernatant was spun at 12,000 rpm again to pellet mitochondria. The mitochondrial pellet was re-suspended in 300 µl SHE buffer and the concentration was determined using spectrophometric analysis according to the methods described by Glick et al., 1995. Discontinuous Nycodenz (MP Biomedicals®) gradients were then generated by overlaying 2 ml of 25, 20, 15, 10, and 5 % Nycodenz (in SHE buffer) in ultracentrifuge tubes. The mitochondrial/SHE buffer solution was suspended on top of the 5 % Nycodenz layer, and samples were loaded into ultracentrifuge and spun at 40,000 rpm for 35 minutes at 4° C. 3 - 4 stratified bands were then visible in the Nycodenz gradients and were removed individually with a pipette. Individual bands were then diluted with 25 ml SHE buffer and spun at 12,000 rpm for 10 minutes. Pellets were re-suspended in 250 µl SHE buffer and the concentration was determined once again as previously described by Glick et al.,1995. Aliquots were then frozen at -80° C for proteinase K treatment and Western Blot analysis.

Proteinase K and PMSF Treatment:

In order to verify that Ku70p resides within the mitochondrial membrane, proteinase K and PMSF treatment was applied to purified mitochondria prior to Western Blot analysis. 0.5 mg aliquots of purified mitochondria were thawed and washed 1 time with sorbitol buffer (0.6 M sorbitol, 20 mM HEPES). Purified mitochondria were then re-suspended in 400 µl of sorbitol buffer. 100 µg of purified mitochondria was aliquoted into 5 Eppendorf tubes labeled samples 1 - 5. 5 separate reactions were set up as Table 6 describes below.

Table 6: Purified Mitochondria Proteinase K Reaction Conditions

Stages of Protection from Protease Degradation							
Samples	Stage of Protease Degradation	Sorbitol buffer	20 mM HEPES	20 mM HEPES + 1% octo-glucopyranoside	100 mg/ml BSA	200mM PMSF	Protease 10 mg / ml
1	Intact Mitos	900µl			10µl	10µl	
2	Mitochondria + Protease	900µl			10µl		10µl
3	Mitoplasts (MP)		900µl		10µl	10µl	
4	Mitoplasts + Protease		900µl		10µl		10µl
5	Ruptured MP + protease			900µl			10µl

After all of the individual components of all 5 reactions were assembled, reactions were incubated on ice for 30 minutes and vortexed for 2 seconds every 5 minutes. 10 µl of 100 mM PMSF was added to samples 2, 4, and 5, and vortexed again. Eppendorf tubes 1-4 were spun for 5 minutes at 14,000rpm at 4° C in a micro-centrifuge. Pellets were re-suspended in sorbitol buffer and then transferred to a new tube, and spun again under the same parameters. Pellets 1 - 4 were re-suspended in 250 µl sorbitol buffer and 23 µl of 50 % TCA was added to reactions 1 - 4, and heated to 60° C for 5 minutes to denature proteinase K. Reactions were then placed on ice for 10 minutes. Reactions 1 - 5 were spun for 5 minutes at 14,000 rpm at 4° C and then washed with 500 µl cold acetone, spun again, and then re-suspended in 50 µl 2X modified sample buffer (1mM HEPES, 1mM PMSF). All reactions were then treated with 5X laemmli sample buffer, boiled for 5 minutes, spun down, and analyzed by Western Blot analysis.

Western Blot Analysis:

Ku70p sub-cellular localization was verified in purified mitochondrial via Western Blot analysis. Western Blot analysis was performed by adding 100 μg of total protein from each sample with the appropriate volume of 5X laemmli sample buffer. Samples were boiled for 5 minutes, spun down, and loaded onto a 10% polyacrylamide gel, and run at 150 volts for 1 hour. Gels, nitrocellulose membrane and transfer pads were incubated in semi-dry transfer buffer (0.58%Tris base, 0.29% glycine, 0.039% SDS, 20% methanol) for 15 minutes. Protein was transferred to pure nitrocellulose membranes via a semi-dry transfer apparatus for 1 hour at 15 volts. Membranes were blocked in 5% milk in TBS-T (0.88% NaCl, 0.02% KCl, 0.3% ultra pure Tris, 0.05% Tween-20) for 1 hour.

Blots were probed with either anti-HA probe (Santa Cruz Biotechnologies®) at 1:500 to detect the presence of Ku70p:HA, anti-Histone H4 (Abcam®) at 1:1000 to verify the purification of mitochondria from nuclei, and anti-Cox2 (Invitrogen®) to verify the presence of mitochondria at 1:1000 in 5% milk in TBS-T overnight. The blots were washed 3 times in TBS-T for 10 minutes each, and then secondary goat anti-rabbit-HRP or goat anti-mouse-HRP antibodies (purchased from Bio-Rad®) were applied at 1:2000 and incubated for 1 hour at room temperature. The blots were washed again, and 3 ml of the combined Western Lighting Chemiluminescent Substrate Kit (PerkinElmer®) was added to each blot and incubated for 1 minute. Signal was detected by exposing X-OMAT AR film (Kodak®) to blots for 1 - 5 minutes. The blots were then stripped and reprobed for alternate proteins.

The blots were initially washed 3 times in TBS-T, and stripped by incubating blots in 20 ml of stripping buffer (66.8% distilled water, 12.5% pH 6.8, 2% SDS, 0.7% Beta-mercaptoethanol) at 65° C for 30 minutes. Blots were re-blocked, re-probed, and signal was detected as previously described.

Results

Specific Aim I:

The first specific goal of my research was to determine the role of the individual members, as well as the entire MRX complex and the non-homologous end joining DNA repair pathway in the occurrence of mitochondrial and nuclear direct repeat-mediated deletions, mitochondrial and nuclear point mutations, as well as the occurrence of spontaneous respiration loss. To accomplish this goal a set of *Saccharomyces cerevisiae* knock out strains was generated by our collaborators Lidza Kalfia and Dr. Elaine Sia from the University of Rochester and provided to us for use in 5 genetic assays that allowed us to quantify the role each of these genes on these factors involved in regulating genomic stability. Knock out strains for each of the individual members of the MRX complex and the NHEJ pathway (*RAD50, MRE11, XRS2, KU70,* and *KU80*) were subjected to these 5 assays to elucidate the individual role of each of theses genes in the occurrence of direct repeat-mediated deletions, the occurrence of point mutations, as well as the occurrence of spontaneous respiration loss. A KU70-*KU80* double mutant, a *RAD50-MRE11-XRS2* triple mutant, a *RAD50-KU70-KU80* triple mutant, and a *RAD50-MRE11-XRS2-KU70- KU80* mutant were also generated and subjected to these 5 assays to investigate the epistatic interactions of these genes.

Non-homologous end joining plays a role in the occurrence of mitochondrial and nuclear direct-repeat mediated deletions.

Direct repeat-mediated deletions (DRMD) have been shown to lead to mitochondrial genomic instability and large scale deletions events (Zevian et al. 1989,

Burgart et al. 1995). Therefore the direct repeat-mediated deletion assay was performed to determine the role of the NHEJ pathway on the occurrence of DRMDs. The nuclear and mitochondrial direct repeat mediated deletion assays were performed simultaneously, but are discussed separately below.

Mitochondrial Direct Repeat-Mediated Deletions:

The use of the *ARG8* mitochondrial direct repeat-mediated deletion reporter allowed for the quantification of the role of the NHEJ pathway in mitochondrial DRMDs. Direct repeat-mediated deletions at this locus restored the coding sequence of the *COX2* gene and rescued the function of oxidative phosphorylation. The restoration of oxidative phosphorylation allowed for growth on YPG, and allowed for the detection and determination of the rate of spontaneous mitochondrial direct repeat-mediated deletions per cell division. The rate of mitochondrial direct repeat mediated deletions per cell division for all strains in our MRX and NHEJ knock out library are complied in Table 7 listed below.

Yeast Strain	Average rate of mitochondrial direct repeat-mediated deletions / cell divison	Fold change	P value
wild-type	0.000156	1	
rad50-Δ	2.01E-05	-7.75	0.00014
mre11-Δ	1.56E-05	-10	0.00275
xrs2-Δ	3.21E-05	-4.84	0.00595
ku70-Δ	0.000458	2.9	0.00001
ku80-Δ	0.000144	1.07	0.62445
ku70-Δ ku80-Δ	0.000556	3.57	<0.0001
rad50-Δ mre11-Δ xrs2-Δ	3.62E-05	-4.29	0.00149
rad50-Δ ku70-Δ ku80-Δ	1.43E-06	-108.48	0.00003
rad50-Δ mre11-Δ xrs2-Δ ku70-Δ ku80-Δ	2.07E-06	-75.24	0.00027

Table 7. The role of MRX complex and NHEJ members in the occurrence of mitochondrial direct-repeat medated deletions. The average rate of mitochondrial direct repeat-mediated deletions was calculated using fluctuation analysis and the method of the median (Lea and Coulson et al., 1949). Fold change compared to the wild-type control is reported as positive unless otherwise noted. P values were determined using a student's two-tailed t-test. Statistical significance was determined by calculating 95% confidence limits for two independent trials.

As we compare the wild-type rate of mitochondrial direct repeat mediated deletions per cell division to each of the mutants in our MRX complex and NHEJ knockout library, we see that all of the individual genes, with the exception of *KU80* (p=0.62), have a statistically significant impact on the role of mitochondrial DRMDs (p=0.0001 – 0.006). Mitochondrial DRMDs are reduced 4 – 10 fold in the absence of *RAD50, MRE11, XRS2*, as well as the entire MRX complex (as seen in the *RAD50-MRE11-XRS2* triple mutant). While in contrast the rate of mitochondrial DRMD increased approximately 3 fold in the absence of *KU70* alone as well as in the *KU70-KU80* double mutant. Surprisingly the loss of *KU80* did not have a statistically significant role on mitochondrial direct repeat-mediated deletions (p=0.6). The absence of the entire MRX complex and NHEJ pathway lead to a

dramatic 75 – 108 fold reduction in the occurrence of mitochondrial direct repeat mediated

deletions per cell division (p<0.001). Refer to Figure 12 below for a graphical representation

of the role of the MRX complex and the NHEJ pathway in mitochondrial direct repeat-

mediated deletions.
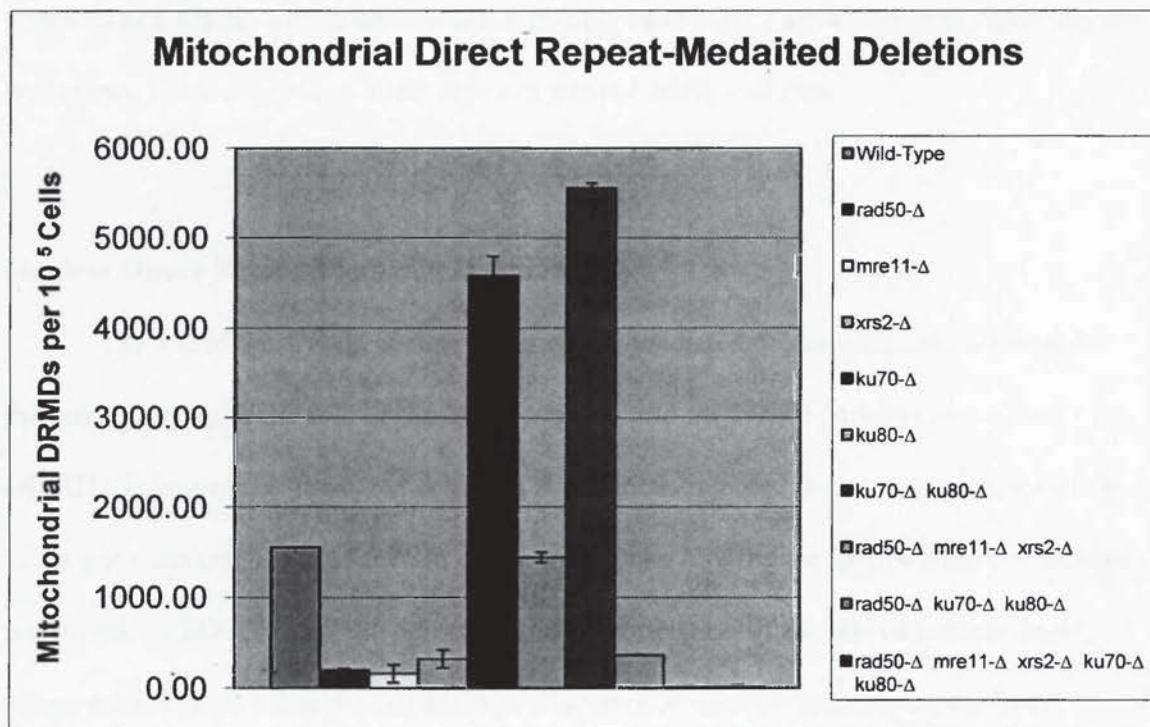
Figure 12. Rates of Mitochondrial Direct Repeat-Mediated Deletions. All strains were plated on YPG, incubated for 3 over nights at 30° C, and then counted. Results shown are the average rates of mitochondrial DRMDs per 10^7 cells for at least 2 independent experiments. Error bars represent positive and negative values of the standard error.

These data suggest that the MRX complex and non-homologous end joining is

involved in the occurrence or regulation of mitochondrial direct repeat-mediated deletions in

Saccharomyces cerevisiae. Mitochondrial direct repeat-mediated deletions are reduced 75 fold

(p<0.001) in the absence of the entire MRX complex and NHEJ pathway. One piece of data

that is particularly interesting is that the absence of *KU80* has no effect on the role of

mitochondrial direct repeat mediated deletions. While in contrast *KU70* has a dramatic effect

on the occurrence of mitochondrial DRMDs. This discrepancy is particularly interesting because the literature states that Ku70p works in unison with Ku80p to repair DNA double strand breaks, while this genetic data suggests that Ku70p may function without Ku80p in the regulation of mitochondrial direct repeat mediated deletion events. When these data are reviewed as a whole, we see that the MRX complex and NHEJ are involved in regulating the occurrence of mitochondrial direct repeat-mediated deletion events.

Nuclear Direct Repeat-Mediated Deletions:

The use of the *URA3* nuclear direct repeat-mediated deletion reporter allowed for the quantification of the role of the MRX complex and the NHEJ pathway in nuclear DRMDs. Direct repeat-mediated deletions at this locus restored the coding sequence of the *TRP1* gene and rescued the function of the tryptophan biosynthetic pathway, which allowed for growth on SD-Trp, and the detection and determination of the rate of nuclear direct repeat-mediated deletions per cell division. The rates of nuclear direct repeat mediated deletions per cell division for all strains in our MRX and NHEJ knock out library are complied in Table 8 listed below.

Yeast Strain	Average rate of nulcear direct repeat-mediated deletions / cell divison	Fold change	P value
wild-type	1.04E-06	1	
rad50-Δ	1.98E-07	-5.27	0.0003
mre11-Δ	2.88E-07	-3.58	0.0103
xrs2-Δ	2.70E-07	-3.83	0.0087
ku70-Δ	5.51E-07	-1.87	0.0257
ku80-Δ	7.19E-07	-1.43	0.0583
ku70-Δ ku80-Δ	1.07E-06	1.03	0.8590
rad50-Δ mre11-Δ xrs2-Δ	1.67E-07	-6.21	0.0009
rad50-Δ ku70-Δ ku80-Δ	1.79E-07	-5.76	0.0011
rad50-Δ mre11-Δ xrs2-Δ ku70-Δ ku80-Δ	2.41E-07	-4.28	0.0018

Table 8. The role of MRX complex and NHEJ members in the occurrence of nuclear direct-repeat mediated deletions. The average rate of nuclear direct repeat mediated deletions was calculated using fluctuation analysis and the method of the median (Lea and Coulson et al., 1949). Fold change compared to the wild-type control is reported as positive unless otherwise noted. P values were determined using a student's two-tailed t-test. Statistical significance was determined by calculating 95% confidence limits for two independent trials.

Upon comparison of the wild-type rate of nuclear direct repeat mediated deletions per cell division to each of the mutants in our MRX complex and NHEJ knockout library, we see that all of the individual genes, with the exception of *KU80* once again (p=0.058), have a statistically significant impact on the rate of nuclear DRMDs per cell division (p=0.003 – 0.025). Nuclear DRMDs were reduced 3 - 5 fold in the absence of *RAD50*, *MRE11*, *XRS2*, as well as the entire MRX complex (as seen in the *RAD50-MRE11-XRS2* triple mutant). Where as the rate of nuclear DRMDs per cell division was only slightly impacted by the loss of *KU70* as seen by the 1.87 fold reduction in the occurrence of spontaneous nuclear DRMDs. Once again it was surprising to discover that the loss of *KU80*

did not have a statistically significant role on the occurrence of nuclear direct repeat-mediated deletions (p=0.058). This trend was further reinforced while reviewing the data for the *KU70-KU80* double mutant. The *KU70-KU80* double mutant showed nearly zero change in the rate of nuclear DRMDs per cell division over that of the wild-type (p=0.85). The absence of the entire MRX complex and NHEJ pathway lead to a dramatic 4 - 5 fold reduction in the occurrence of nuclear direct repeat-mediated deletions per cell division(p=0.001). Refer to Figure 13 below for a graphical representation of the role of the MRX complex and the NHEJ pathway in the occurrence of nuclear direct repeat-mediated deletions.
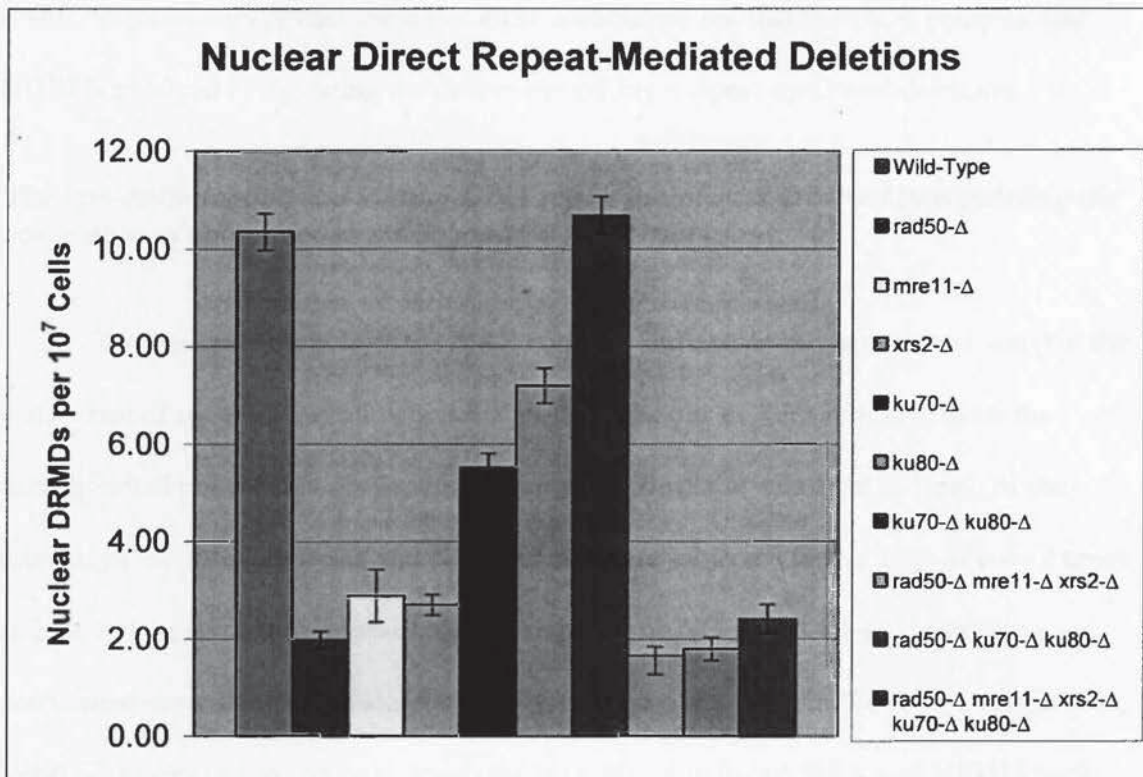
Figure 13. Rates of Nuclear Direct Repeat-Mediated Deletions. All strains were plated on SD-Trp, incubated for 3 over nights at 30° C, and then counted. Results shown are the average rates of nuclear DRMD's per 10^7 cells for at least 2 independent experiments. Error bars represent positive and negative values of the standard error.

These data support the role of the MRX complex and non-homologous end joining in the occurrence of nuclear direct repeat-mediated deletions in *Saccharomyces cerevisiae*. Nuclear direct repeat-mediated deletion events are significantly reduced in the absence of the MRX complex and the non-homologous end joining pathway by 4 – 5 fold (p=0.001). Once again we see that *KU70* and *KU80* may possess unequal roles in regulating the occurrence of spontaneous direct repeat mediated deletions. The loss of *KU70* results in a significant 1.87 fold decrease in the occurrence of DRMDs, while the loss of *KU80* did not (p=0.025 and p=0.058 respectively.) Furthermore, the absence of the entire KU complex showed nearly no impact on the regulation of the occurrence of nuclear direct repeat mediated deletion

events. Yet, when these data are reviewed as a whole, we see that the MRX complex and NHEJ is involved in regulating the occurrence of direct repeat meditated deletions.

The non-homologous end joining DNA repair pathway is involved in regulating the occurrence of spontaneous mitochondrial point mutations.

To determine the role of the MRX complex and non-homologous end joining in the occurrence of spontaneous mitochondrial point mutations in *Saccharomyces cerevisiae* the mitochondrial point mutation assay was performed. Both the wild-type and each of the mutants in our MRX complex and NHEJ library were subjected to this assay at least 2 times, and the rate of erythromycin resistance when plated on YG plus 0.4% erythromycin was determined using fluctuation analysis and the method of the median (Lea and Coulson et al., 1949). The rates of erythromycin resistance for each strain in our MRX and NEHJ knock out library are listed below in Table 9.

Yeast Strain	Average rate of mitochondrial point mutations / cell division	Fold change	P value
wild-type	1.06E-07	1	
rad50-Δ	1.79E-07	1.68	0.2380
mre11-Δ	7.10E-08	-1.48	0.1860
xrs2-Δ	4.77E-08	-2.21	0.0224
ku70-Δ	1.41E-07	1.33	0.2730
ku80-Δ	9.64E-08	1.09	0.8245
ku70-Δ ku80-Δ	1.00E-07	1.05	0.8650
rad50-Δ mre11-Δ xrs2-Δ	7.87E-08	-1.34	0.2905
rad50-Δ ku70-Δ ku80-Δ	9.52E-08	-1.11	0.7536
rad50-Δ mre11-Δ xrs2-Δ ku70-Δ ku80-Δ	7.90E-09	-13.38	0.0126

Table 9. The role of MRX complex and NHEJ members in the occurrence of spontaneous mitochondrial point mutations. The average rate of mitochondrial point mutations was calculated using fluctuation analysis and the method of the median (Lea and Coulson et al., 1949). Fold change compared to the wild-type control is reported as positive unless otherwise noted. P values were determined using a student's two-tailed t-test. Statistical significance was determined by calculating 95% confidence limits for two independent trials.

As we compare the wild-type rate of spontaneous mitochondrial point mutations per cell division to each of the mutants in our MRX complex and NHEJ knockout library, we see that XRS2 is the only gene that directly regulates the occurrence of spontaneous mitochondrial point mutations (p=0.18-0.82). In the absence of XRS2 mitochondrial point mutations were reduced a statistically significant 2.2 fold (0.022). The rate of mitochondrial point mutations per cell division decreased a significant 13.3 fold in the absence of the entire NHEJ DNA repair pathway as seen in the RAD50-MRE11-XRS2-KU70-KU80 mutant (p=0.012). Refer to Figure 14 below for a graphical representation of the role of the MRX

complex and NHEJ members in the occurrence of spontaneous mitochondrial point

mutations.

Average Rate of Erythromycin Resistance
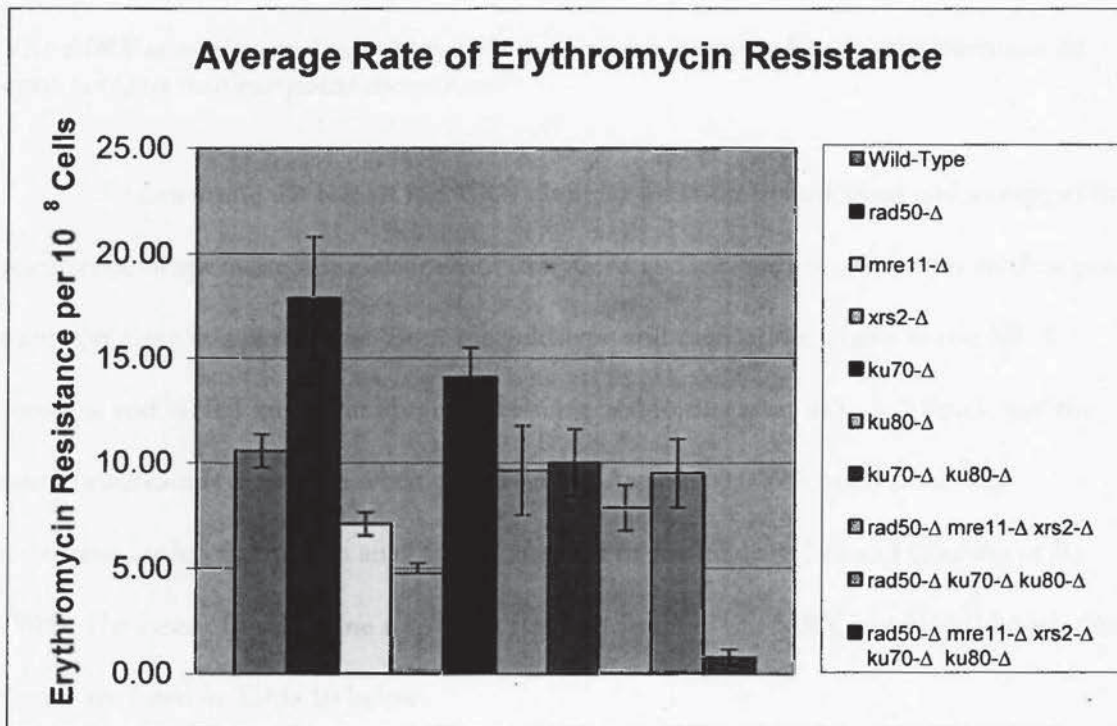
Figure 14. Rates of Erythromycin Resistance. All strains were plated on YG plus 0.4% Erythromycin, incubated for 7 over nights at 30° C, and then counted. Results shown are the average rates of erythromycin resistance per 10^8 cells for at least 2 independent experiments. Error bars represent positive and negative values of the standard error.

These data suggests that the only member of the NHEJ DNA repair pathway that

plays a role in regulating the occurrence of spontaneous mitochondrial point mutations in

Saccharomyces cerevisiae is *XRS2*. When *XRS2* is disrupted the rate of erythromycin resistance

decreases 2.2 fold over the wild-type. When the entire NHEJ pathway was disrupted (as seen

in the *RAD50- MRE11-XRS2 KU70-KU80* mutant) the rate of erythromycin resistance

decreased 13.4 fold compared to the wild-type control. These data suggest that non-

homologous end joining DNA repair pathway is involved in the regulation of mitochondrial

point mutations, and supports our hypothesis that this pathway is intricately involved in the regulation of mitochondrial genome integrity.

The MRX complex and non-homologous end joining regulates the occurrence of spontaneous nuclear point mutations.

To determine the role of the MRX complex and non-homologous end joining in the occurrence of spontaneous nuclear point mutations in *Saccharomyces cerevisiae* the nuclear point mutation assay was performed. Both the wild-type and each of the strains in our MRX complex and NHEJ knockout library were subjected to this assay at least 2 times, and the rate of canavanine resistance when plated on SD-Arg plus 0.006% canavanine was determined using fluctuation analysis and method of the median (Lea and Coulson et al., 1949). The rates of canavanine resistance for each strain in our MRX and NEHJ knock out library are listed in Table 10 below.

Yeast Strain	Average rate of nuclear point mutations / cell division	Fold change	P value
wild-type	2.22E-07	1	
rad50-Δ	9.90E-08	-2.42	0.0010
mre11-Δ	3.18E-07	1.43	0.0585
xrs2-Δ	4.26E-07	1.92	0.0001
ku70-Δ	2.19E-07	1.01	0.894
ku80-Δ	2.12E-07	1.04	0.657
ku70-Δ ku80-Δ	2.31E-07	1.04	0.785
rad50-Δ mre11-Δ xrs2-Δ	5.38E-07	2.45	0.0037
rad50-Δ ku70-Δ ku80-Δ	1.93E-06	8.69	0.0001
rad50-Δ mre11-Δ xrs2-Δ ku70-Δ ku80-Δ	4.98E-07	2.24	0.0006

Table 10. The role of MRX complex and NHEJ members in the occurrence of spontaneous nuclear point mutations. The average rate of nuclear point mutations was calculated using fluctuation analysis and the method of the median (Lea and Coulson et al., 1949). Fold change compared to the wild-type control is reported as positive unless otherwise noted. P values were determined using a student's two-tailed t-test. Statistical significance was determined by calculating 95% confidence limits for two independent trials.

Upon the review of Table 10 we see that the wild-type rate of spontaneous nuclear point mutations per cell division for each of the mutants in our MRX and NHEJ knockout library, we see that *XRS2* and *RAD50* directly regulate the occurrence of spontaneous nuclear point mutations. In the absence of *XRS2* nuclear point mutations increase a statistically significant 1.92 fold (p=0.0001). While in contrast, when *RAD50* is disrupted the rate of spontaneous nuclear point mutations decreases a significant 2.42 fold (p=0.001). Furthermore the absence of *MRE11*, *KU70*, *KU80*, and both *KU70* and *KU80* did not have a significant impact on the rate of canavanine resistance in this study (p=0.058 – 0.89). In the absence of a functional MRX complex the rate of spontaneous nuclear point mutations

increases a significant 2.4 fold (p=0.003), and when members of both the MRX and KU

complexes are disrupted (as seen in the *RAD50-KU70-KU80* triple mutant) the rate of

spontaneous nuclear point mutations increases a significant 8.6 fold (p=0.0001). Interestingly

when all 5 members of the pathway are disrupted the rate of spontaneous nuclear point

mutations increases only 2.24 fold (p=0.0006). Refer to Figure 15 below for a graphical

representation of the role of the MRX complex and NHEJ members in the occurrence of

spontaneous nuclear point mutations.
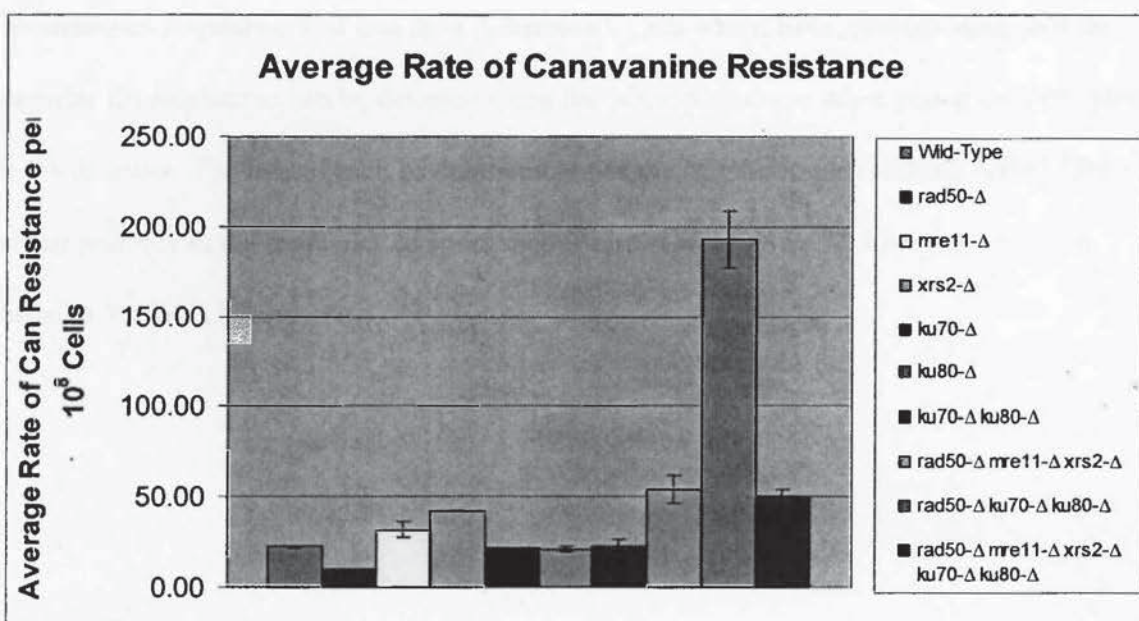
Figure 15. Rates of Canavanine Resistance. All strains were plated on SD-TRP+0.006% canavanine, incubated for 7 over nights at 30° C, and then counted. Results shown are the average rates of canavanine resistance per 10^8 cells for at least 2 independent experiments. Error bars represent positive and negative values of the standard error.

These data suggests that the MRX complex and the non-homologous end joining

DNA repair pathway are involved in the regulation or processing of spontaneous nuclear

point mutations in *Saccharomyces cerevisiae*. Taken together, these data support the highly

established role of the MRX complex and non-homologous end joining in maintaining

genomic stability and repair.

The MRX complex and the non-homologous end joining pathway are required for maintaining the capacity for cellular respiratory in Saccharomyces cerevisiae.

In order to document the role of the MRX complex and the non-homologous end joining pathway in maintaining cellular respiration in *Saccharomyces cerevisiae* the spontaneous respiration loss assay was performed on each of the strains in our MRX and NHEJ knock out library. Each strain was subjected to this assay at least 3 times and the frequency of spontaneous respiration loss was then determined. Cells which have spontaneously lost the capacity for respiration can be detected using the petite phenotype when plated on YPG plus 0.2% dextrose. The role of each of the members of the MRX complex and the NHEJ DNA repair pathway in the frequency of spontaneous respiration loss in *Saccharomyces cerevisiae* is listed in Table 11 below.

Yeast Strain	Frequency of average median percent respiration loss	Fold change	P value
wild-type	2.25	1	
rad50-Δ	2.48	1.10	0.6124
mre11-Δ	2.98	1.33	0.3477
xrs2-Δ	2.86	1.27	0.5333
ku70-Δ	1.80	-1.25	0.4662
ku80-Δ	2.01	-1.12	0.6605
ku70-Δ ku80-Δ	1.83	-1.23	0.5028
rad50-Δ mre11-Δ xrs2-Δ	5.38	2.39	0.0003
rad50-Δ ku70-Δ ku80-Δ	7.85	3.49	0.00001
rad50-Δ mre11-Δ xrs2-Δ ku70-Δ ku80-Δ	7.97	3.54	0.0026

Table 11. The role of MRX complex and NHEJ members in the occurrence of spontaneous respiration loss. The frequency of average median percent respiration loss was calculated by scoring yeast colonies as either grande or petite and then dividing the number of petite colonies by the total number of colonies. The median for each independent trial was then taken and an average rate of median percent respiration loss was then determined for at least 4 independent trials. Fold change compared to the wild-type control is reported as positive unless otherwise noted. P values were determined using a student's two-tailed t-test. Statistical significance was determined by calculating 95% confidence limits for two independent trials.

After carefully reviewing Table 11 we see that none of the individual genes in the MRX complex and the non-homologous end joining DNA repair pathway are involved in regulating spontaneous respiration loss in *Saccharomyces cerevisiae* (p=0.34-0.66). The absence of the entire KU complex (*KU70* and *KU80*) once again did not have a significant effect on the occurrence of spontaneous respiration loss over that of wild-type control (p=0.50). Yet when the entire MRX complex was compromised the frequency of spontaneous respiration loss increased a significant 2.39 fold (p=0.0003). In the absence of *RAD50*, *KU70*, and *KU80* the observed frequency of spontaneous respiration loss increased a significant 3.49

fold compared to that of the wild-type control (p=5.1E-6). The frequency of spontaneous

respiration loss increased 3.54 fold in the absence of all 5 members of the NHEJ pathway

over the wild-type control (p=0.002). Refer to Figure 16 below for a graphic representation

of the role of the MRX complex and the NHEJ pathway in the occurrence of spontaneous
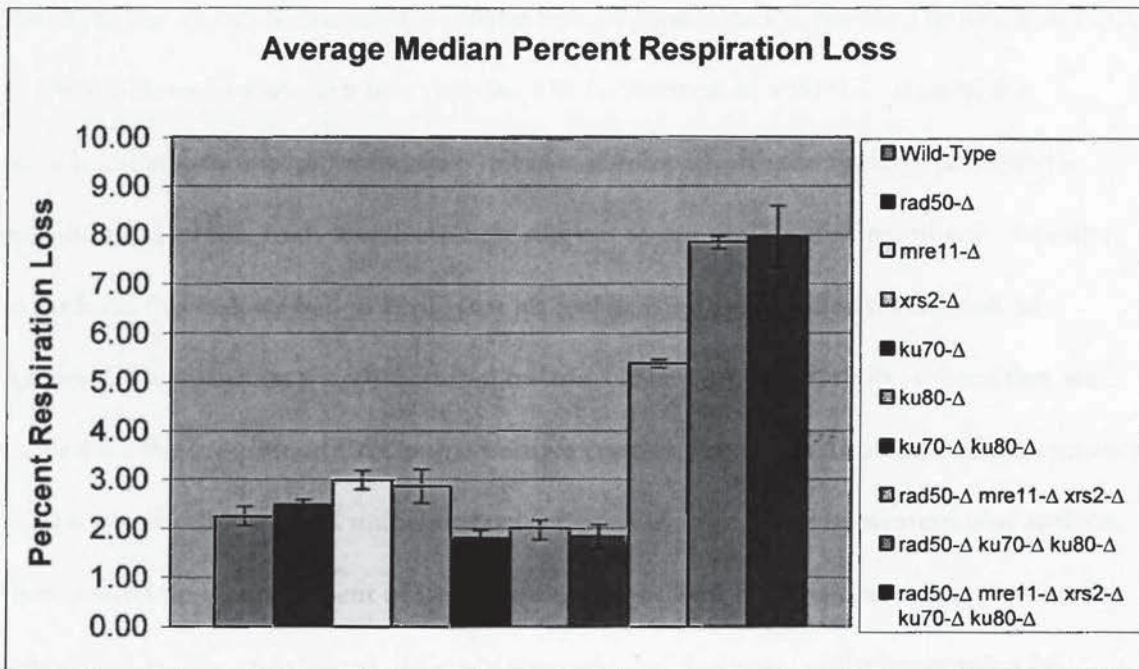
respiration loss.

Figure 16. Frequencies of Spontaneous Respiration Loss. All strains were plated on YPG plus 0.2% dextrose, incubated for 3 over nights at 30° C, and then scored and counted. Results shown are the average median percent respiration loss of at least 4 independent experiments. Error bars represent positive and negative values of the standard error.

These data suggests that individual members of the non-homologous end joining

DNA repair pathway do not appear to directly impact the rate of spontaneous respiration

loss in *Saccharomyces cerevisiae*. However, the absence of the MRX complex and the entire non-

homologous end joining pathway does lead to a significant increase in the observed

frequency of spontaneous respiration loss. These data taken together support our hypotheses

73

that the MRX complex and non-homologous end joining regulate cellular respiration, and mitochondrial genome integrity.

Specific Aim II:

The second goal of this study was to localize non-homologous end joining factor Ku70p to the mitochondria using a cellular fractionation protocol (devised by Glick and Pon in 1995) followed by western blot analysis. The localization of a NHEJ factor to the mitochondrial genome of *Saccharomyces cerevisiae*, combined with the findings presented in specific aim I of this study would strongly support to our preliminary hypothesis. In order to perform this task we had to verify that we had isolated and purified mitochondrial fractions. To determine if mitochondrial fractions have been successfully isolated they were probed for the presence of Cox2p as a positive control. When equal volumes of total protein from a whole cell lysate and mitochondrial fractions were analyzed by western blot analysis, there should be an enrichment of Cox2p within the cellular fraction containing mitochondria. The enrichment of Cox2p supports the purification of mitochondria by verifying an increased concentration of mitochondrial proteins per unit weight of total protein. An enrichment in the presence of Cox2p within mitochondrial fractions among equal amount of total protein from a whole cell lysate were verified by an increase in Cox2p associated signal using western blot analysis.

After we had determined that Cox2p was enriched within the cellular fractions corresponding to mitochondria, it became necessary to verify that these fractions did not possess any nuclear material which may skew these NHEJ localization results. In order to document mitochondria that these mitochondrial fractions had been purified of all nuclear

material, they were probed for the presence of nuclear protein Histone H4. The absence of Histone H4p in mitochondrial fractions can confirm the absence of nuclear proteins within these fractions, and confirm the successful purification of mitochondria.

In order to localize the NHEJ factor Ku70p to the mitochondria a *KU70:HA* epitope strain was generated by our collaborators at the University of Rochester and provided for our use in this study. This strain allowed for detection of Ku70p using an anti-HA antibody. The anti-HA probe was used to monitor for the presence of Ku70:HAp in a whole cell lysate positive control, and in the 3 – 4 bands present in the discontinuous Nycodenz gradients following ultracentrifugation which corresponded to purified mitochondrial fractions. A negative whole cell lysate control was used in this localization experiment to verify the specificity of the HA antibody. Once we verified that Ku70:HAp can be localized to purified mitochondrial fractions, proteinase K treatment was performed upon these fractions to determine at what stage Ku70:HAp was susceptible to degradation. The proteinase K treatment is designed to sequentially remove the outer and inner mitochondrial membranes, and aide in the determination of the precise location of Ku70:HAp within the mitochondria. The samples which resulted from the proteinase K treatment were probed for the presence of Ku70:HAp to identify the precise location of this protein within the mitochondria of *Saccharomyces cerevisiae*.

Mitochondria can be isolated from cellular fractions in *Saccharomyces cerevisiae*.

Saccharomyces cerevisiae cultures were harvested, lysed, and fractionated according to the methods devised by Glick and Pon in 1995. To determine if cellular fractions isolated by the previously described method were purified mitochondria, they probed for the presence of Cox2p in an attempt to verify an enrichment of mitochondria and mitochondrial proteins

per unit weight of total protein over the whole cell lysate control. A whole cell lysate was

generated for use in determining the banding pattern associated with the presence of Cox2p,

and for use in the relative quantification of the levels of Cox2p in the whole cell lysate and

the mitochondrial fractions. Total protein content was determined using the Bio-Rad protein

assay system, and 100 µg of total protein from the whole cell lysate and the mitochondrial

fractions were loaded on a 10% acrylamide gel, and probed for Cox2p. The results are

displayed in Figure 17 below.
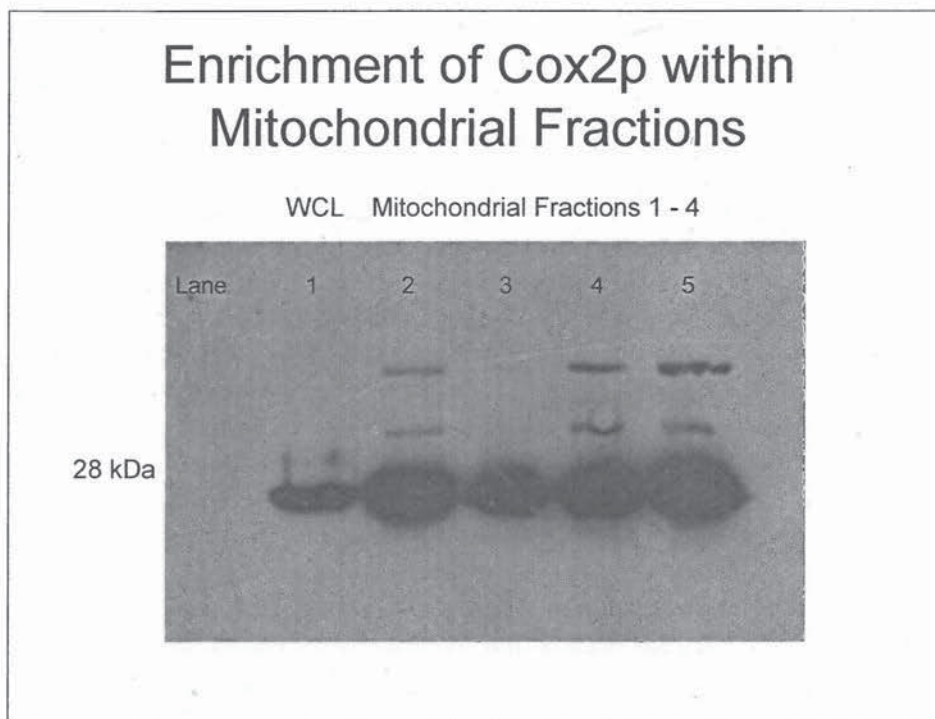
**Figure 17. Enrichment of Cox2p in mitochondrial fractions. 100 µg of total protein
was loaded for both the whole cell lysate control in lane 1, and for mitochondrial
fractions 1 – 4 in lanes 2 – 5 respectively. Samples were loaded on a 10% acrylamide
gel and probed for the presence of Cox2p at 1:1000 dilution.**

From Figure 17 it becomes evident that Cox2p is enriched in mitochondrial fractions

1 - 4. Enrichment can be verified due to the knowledge that equal amounts (100 µg) of total

protein were loaded for all samples. From this figure we see 5 robust bands at 28 kDa which

is consistent with the size of Cox2p in *Saccharomyces cerevisiae* (SGD). 100 μg of total protein from the whole cell lysate control was loaded in lane 1, and from mitochondrial fractions 1 – 4 were loaded in lanes 2 – 5. Lanes 2 - 5 of Figure 17 show a significantly increased signal associated with the presence of Cox2p over the whole cell lysate control. With the verification of the enrichment of Cox2p within mitochondrial fractions over the whole cell lysate control, we can infer that we have successful isolated mitochondria for *Saccharomyces cerevisiae.*

Histone H4 protein is absent in mitochondrial fractions.

After the confirmation of the successful isolation of mitochondrial from yeast cells using the methods devised by Glick and Pon in 1995, it became necessary to verify that these isolated mitochondrial fractions were free of nuclear containments. To perform this task mitochondrial fractions were probed for nuclear protein Histone H4 to confirm that these fractions were free of nuclear proteins. As previously described total protein content of the whole cell lysate control and mitochondrial fractions were determined using the Bio-Rad Protein Assay system, and as described in methods devised by Glick and Pon in 1995. 100 μg of total protein were loaded for all samples, which were then run 10% acrylamide gel, and probed for Histone H4. These results are displayed in Figure 18 below.
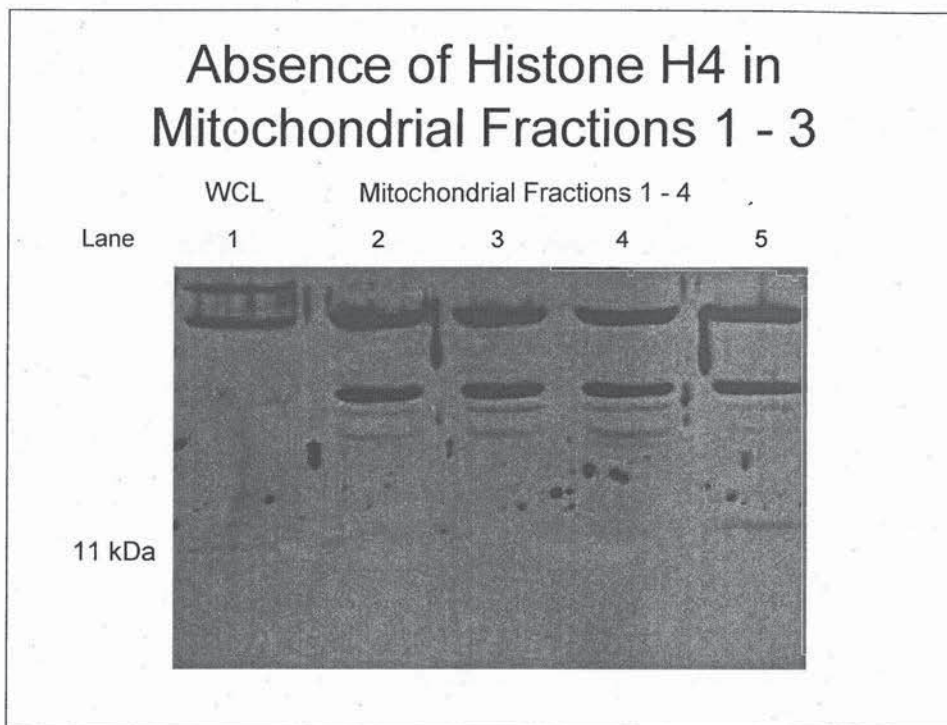
Figure 18. Absence of nuclear protein Histone H4 in purified mitochondrial fractions. 100 μg of total protein was loaded for the WCL in lane 1 and mitochondrial fractions 1 – 4 in lanes 2 – 5. Samples were loaded on a 10% acrylamide gel and probed for Histone H4 protein at 1:500 dilution.

Figure 18 demonstrates that mitochondrial fractions 1 - 3 loaded in lanes 2 – 5 are devoid of nuclear protein Histone H4, and thus verify the successful purification of mitochondria from *Saccharomyces cerevisiae*. In Figure 18 we see a faint band at 11 kDa in lane 1 and lane 5, which is consistent with the size of Histone H4 protein in *Saccharomyces cerevisiae* (SGD). Knowing that equal amounts of total protein were loaded for both the whole cell lysate control and purified mitochondrial fractions 1 - 4, we can be sure that the signal associated with Histone H4 protein in lanes 1 and 5 (at 11 kDa) is absent in lanes 2, 3, and 4. This lack of signal in lanes 2, 3, and 4 verify the absence of Histone H4 in mitochondrial fractions 1, 2, and 3, but not 4. Figure 18 verifies that mitochondrial fractions 1 – 3 have been successfully purified of nuclear protein Histone H4, and we can infer that these

mitochondrial fractions have been successfully purified according to the methods devised by Glick and Pon in 1995.

Non-homologous end joining factor Ku70:HA protein can be localized to purified mitochondria in Saccharomyces cerevisiae.

Now that mitochondrial fractions which were isolated from *Saccharomyces cerevisiae* according to the methods devised by Glick and Pon have been verified as purified mitochondria, we then set out to verify that the NHEJ factor Ku70p can be localized to the mitochondria. In order to perform this task purified mitochondrial fractions were probed for Ku70:HAp using the anti-HA antibody. A whole cell lysate positive control derived from the *KU70:HA* strain and a whole cell lysate negative control derived from a wild-type strain which possessed a wild-type Ku70p were used to demonstrate the specificity of the anti-HA antibody, and to determine the banding pattern associated with the presence of Ku70:HAp. The negative control ensures that all of signal detected is due to the presence of HA epitope fused to the NHEJ factor Ku70p. As before equal amounts of total protein were loaded for both of the whole cell lysate controls and purified mitochondrial fractions 1 – 3. 50 μg of total protein were loaded for all samples on a 10% acrylamide gel, and then probed for the HA epitope fused to NHEJ factor Ku70p at a 1:500 dilution. The results are displayed in Figure 19 below.

Figure 19. Presence of NHEJ factor Ku70:HAp in purified mitochondrial fractions. 50 µg of total protein were loaded for the positive WCL control in lane 1, the negative WCL control in lane 2, and mitochondrial fractions 1 – 3 in lanes 3 - 5. Samples were loaded on a 10% acrylamide gel and probed for HA epitope at 1:500 dilution.

Figure 19 demonstrates that the non-homologous end joining factor Ku70p can be localized to the mitochondria in *Saccharomyces cerevisiae*. In this figure we see bands at 95 kDA in lanes 1 and 5 which is consistent to size of the Ku70:HA fusion protein. An absence of signal at 95 kDa in lane 2 confirms the specificity of the anti-HA antibody, and verifies that all of the detected signal is due to the presence of Ku70:HAp. The presence of Ku70:HAp signal in lane 5 verifies that Ku70p can be localized to mitochondrial fractions, and the mitochondria in *Saccharomyces cerevisiae*.

Non-homologous end joining factor Ku70:HA protein appears to be localized to the outer mitochondrial membrane in Saccharomyces cerevisiae.

To further determine the location of NHEJ factor Ku70:HAp within the mitochondria, proteinase K treatment was performed to sequentially remove each of the mitochondrial membranes according to the protocol adapted by Heather Fuimera at Cornell University. Samples taken from mitochondrial fraction 3 which had been verified to contain Ku70:HAp (see Figure 19), were subjected to the previously described proteinase K treatment protocol. 50 µg of total protein were loaded for all samples on to a 10% acrylamide gel, and probed for the presence of Ku70:HAp using the anti-HA antibody at a 1:500 dilution. These results are displayed in Figure 20 below.

Ku70:HAp is localized to
the outer mitochondrial membrane

Samples 1 – 5 resulting from protease treatment

WCL (+) WCL (-) "1"   "2"   "3"   "4"   "5"

Lane   1   2   3   4   5   6   7

95 kDA
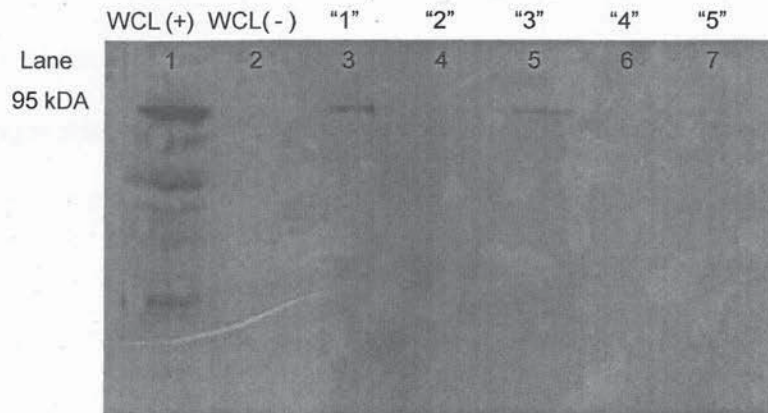
Figure 20. Ku70:HAp is present within the outer mitochondrial membrane. 50 μg of total protein was loaded in all lanes on a 10% acrylamide gel and probed for Ku70:HAp at 1:500 dilution. Lane 1 contains a KU70:HA WCL, Lane 2 contains a wild-type WCL, lane 3 contains untreated purified mitochondria known as "sample 1", lane 4 contains purified mitochondria treated with 20 μl of 5 mg/ml proteinase K known as "sample 2", lane 5 contains mitoplasts (mitochondria lacking the outer membrane) known as "sample 3", lane 6 contains mitoplasts plus 20 μl of 5 mg/ml proteinase K known as "sample 4", and lane 7 contains ruptured mitoplasts plus 20 μl of 5 mg/ml proteinase K known as "sample 5".

Figure 20 demonstrates that NHEJ member Ku70:HAp can be localized to the outer mitochondrial membrane in *Saccharomyces cerevisiae*. Lane 1 contains 50 μg of total protein from a whole cell lysate positive control derived from the KU70:HA epitope tagged strain. Lane 2 contains 50 μg of total protein from a whole cell lysate negative control derived from the wild-type strain. Lane 3 contains 50 μg of total protein from sample 1 which was treated with the sorbitol buffer, 100mg/ml BSA, and 200 mM PMSF. Sample 1 contains purified intact mitochondria, as well as NHEJ factor Ku70:HAp. Lane 4 contains 50 μg of total protein from sample 2 which was treated with the sorbitol buffer, 100mg/ml BSA, and with

5 mg/ml proteinase K. Ku70:HAp does not appear to be present in lane 4. Lane 5 contains 50 μg of total protein from sample 3 which was treated with the 20 mM HEPES, 100mg/ml BSA, and 200 mM PMSF. The resulting product in sample 3 are mitoplasts (mitochondria which have had the outer membrane removed), appears to possess Ku70:HAp. Although the resulting products from sample 5 are mitoplasts, the outer mitochondrial membrane still remains fragmented in solution. Lane 6 contains 50 μg of total protein from sample 4 which was treated with the 20 mM HEPES, 100mg/ml BSA, and 5 mg/ml proteinase K. Ku70:HAp does not appear to be present in sample 4. Lane 7 contains 50 μg of total protein from sample 5 which was treated with the 20 mM HEPES plus 1%octo glucopryanoside, and 5 mg/ml proteinase K. The resulting product in sample 5 is ruptured mitoplasts which have been treated with proteinase K. Ku70:HAp is not present in sample 5. From figure 20 we can see that NHEJ factor Ku70:HAp is present in purified mitochondria, and appears to be localized to the outer mitochondrial membrane of *Saccharomyces cerevisiae*.

Discussion:

Mitochondrial genome maintenance is required for eukaryotic cell viability. As previously described, the mitochondrial genome encodes for several proteins necessary for oxidative phosphorylation and the ribosomal and transfer RNAs which are required for their synthesis. Similar to the nuclear genome, the mitochondrial genome is constantly under insult from exogenous and endogenous factors such as ionizing radiation and reactive oxygen species which have been shown to reduce its integrity in aging individuals. Replication errors by the mitochondrial DNA polymerase, the inefficient repair of ROS induced mtDNA damage, the acquisition of spontaneous mtDNA point mutations, and spontaneous mitochondrial direct repeat-mediated deletions have all been known to occur

within the mitochondrial genome in both yeast and human. Diabetes, deafness, sudden death, CPEO, Pearsons disease, hepatocellular carcinoma, and Kearns-Sayers disease are all known to occur as a result of mitochondrial DNA mutations (refer to Table 2). Since the mitochondrial genome is constantly under mutagenic threats, it relies upon the efficient targeting of nuclear encoded DNA repair proteins to the site of mtDNA damage. In a review of mtDNA repair pathways it has been suggested that the primary mechanisms for mtDNA repair are mismatch repair (MMR), base excision repair (BER), direct reversal (DR), and recombinational repair (RER) (Larsen et al, 1995). Refer to Figure 4 for a complete comparison of the nuclear and mitochondrial DNA repair pathways.

We performed this study because we had a preliminary hypotheses that the MRX complex and the NHEJ pathway function with in the mitochondria to regulate mitochondrial stability and repair. Furthermore we hypothesize that the absence of the MRX complex and non-homologous end joining will alter the overall stability of the mitochondrial genome. To perform this task we set two Specific Aims. Aim I was to determine the role of the MRX complex and non-homologous end joining in the occurrence of mitochondrial and nuclear direct repeat-mediated deletions, the occurrence of mitochondrial and nuclear point mutations, as well as the occurrence of spontaneous respiration loss within the model organism, *Saccharomyces cerevisiae*. Aim II was to localize the non-homologous end joining factor Ku70p to the mitochondria using cellular fractionation and Western blot analysis. The results of this study will be discussed in subsections with regard to Specific Aim 1 and 2.

Specific Aim I

The MRX complex and the non-homologous end joining DNA repair pathway are directly involved in the regulation of mitochondrial direct repeat-mediated deletions.

To determine the role of the MRX complex and the NHEJ pathway in the occurrence of spontaneous direct repeat mediated deletions the direct repeat-mediated deletions assay was performed upon all of the strains in our NHEJ knock out library. Refer to Table 7 and Figure 12 for the role of MRX complex and NHEJ members in the occurrence of spontaneous mitochondrial DRMDs.

From Table 7 we see that the loss of *RAD50*, *MRE11*, and *XRS2* all lead to a significant 4 - 10 fold decrease in the rate of mitochondrial direct repeat-mediated deletions ($p<0.006$). While in contrast, in the absence of *KU70* the rate of mitochondrial DRMDs increases 2.9 fold ($p=0.0001$). This same trend is observed in the absence of both *KU70* and *KU80*, but not in the absence of *KU80* alone as the absence of *KU80* had no effect on the occurrence of mitochondrial DRMDs ($p=0.62$). Due to the fact that the loss of *KU80* had little effect on the rate of mitochondrial DRMDs, the increase in mitochondrial DRMDs observed in the *KU70-KU80* double mutant over the *KU70* single mutant may be due to the loss of *KU70* alone. While in contrast, in the absence of *RAD50*, *KU70*, and *KU80* as well as the entire NHEJ DNA repair pathway there is a 70-100 fold decrease in the occurrence of spontaneous DSB induced mitochondrial direct repeat-mediated deletions ($p<0.0003$).

The results obtained from our mitochondrial direct repeat-mediated deletion assay lead me to hypothesize that the KU complex may posses a regulatory role in determining which DNA double strand break repair pathway is initiated upon the discovery of a mtDNA DSB with in the cell. Therefore I would like to present three hypotheses regarding the

mitochondrial DRMD data. First, mitochondrial and nuclear DRMDs occur as a result of single strand annealing SSA. Second, the KU complex acts to inhibit the occurrence of mitochondrial single strand annealing which thereby alters the rate of mitochondrial direct repeat-mediated deletions. Third, Rad50p, Mre11p, and Xrs2p are involved in the occurrence of SSA, therefore the absence of these factors reduces the occurrence of SSA, and thus reduces the rate of mitochondrial direct repeat-mediated deletions observed in this study.

Single strand annealing (SSA) is thought to be the leading mechanism for the occurrence of nuclear direct repeat-mediated deletions, and appears to also be directly involved in the occurrence of mitochondrial direct repeat-mediated deletions. Single strand annealing is occurs following a DNA DSB within two directly repeating DNA sequences. The 3' ends of one strand on each side of the DNA DSB is processed by an exonuclease exposing the homologous repeating sequences. These repeating sequences on opposite strands are complementary and can thus anneal to one another leaving non-homologous flaps. These non-homologous flaps can then be processed and the remaining gaps can be filled. SSA results in the deletion of one of the directly repeating sequences as well as DNA between these directly sequences (Phadnis et al, 2005). A diagram for the generation of a direct repeat mediated deletion event due to single strand annealing is presented in Figure 21 below.
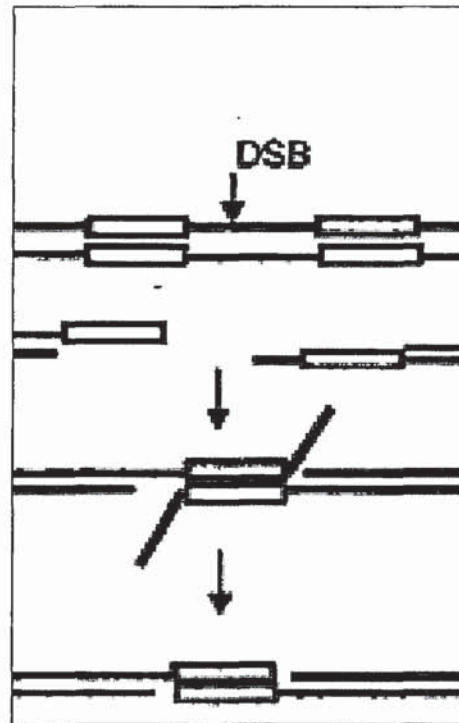
Figure 21. The mechanism for the generation of direct repeat-mediated deletion events due to single strand annealing. Figure created by Phadnis et al, 2005. Published by Phadnis et al, 2005. *Genetics* 171: 1549-1559.

Based upon the previously described hypothesis, the absence of the Ku complex (and specifically Ku70) would account for the increase in the observed rate of mitochondrial direct repeat-mediated deletions compared to the wild-type control. In the event that my hypothesis is correct in that mitochondrial SSA annealing is a source for the occurrence of mitochondrial direct repeat-mediated deletions, a reduction in the functional activity of SSA would lead to a reduction in the occurrence of mitochondrial direct repeat-mediated deletions.

In order for the site specific direct repeat-mediated deletion event to occur at our mitochondrial reporter, a DNA double strand break must occur downstream of the ATG start codon. After the double strand break has occurred it may be repaired through 3 highly

compeitive DNA repair mechanisms; single strand annealing (SSA), gene conversion (GS), and recombinational repair.

The *Sacchromyces* genome database (SGD) states that direct repeat mediated deletions occur as a result of single strand annealing (SSA), while others have suggest that SSA generates DRMDs only 80% of the time (Ivanov et al, 1996). Ivanov et al. induced HO-endonuclease double strand breaks between directly duplicated *E. coli LacZ* genes to investigate the occurrence of direct repeat-mediated deletions in *Sacchromyces cerevisiae*. Using this reporter construct they determined that direct repeat-mediated deletions occurred as the result of single strand annealing 80% of the time, while these double strand breaks were repaired using gene conversion (or Holiday junction formation) the remaining 20% of the time. Although single strand annealing has been well documented, all of the genes involved in regulating the occurrence of SSA have yet to be discovered. Ivanov et al stated that *RAD52* is required for SSA, while *RAD50* and *XRS2* are involved in the occurrence of SSA. In this study *RAD50* and *XRS2* mutants possessed only 40-50% of the wild-type single strand annealing capacity.

The role of *RAD50* and the MRX complex in the occurrence of single strand annealing following a DNA DSB has been further supported by findings published by Clerici et al. in 2005. In this study Clerici et al. in 2005 demonstrated that HO-endonuclease induced DNA DSB residing between two directly repeating DNA sequences showed impaired single strand annealing in the presence of a mutant RAD50 allele. Therefore, from the work published by Ivanov et al., and Clerici et al., MRX complex members are directly involved in the occurrence of single strand annealing following a DNA DSB between two direct repeats.

In a recent study it was discovered that there is a hierarchy which regulates the occurrence of the single strand annealing, gene conversion, and non-homologous end joining. In this article (published by Mansour et al, 2008) it was determined using GFP SSA, GFP GC, and GFP NHEJ reporter constructs, that each of these DNA repair pathways is competitively regulated at the occurrence of induced DNA double strand breaks. These authors discovered that the KU complex (*KU70* and *KU80*) as well as *RAD51* possessed the ability to inhibit the occurrence of single strand annealing and gene conversion (Mansour et al, 2008). Therefore it is logical that the absence of Ku mediated SSA inhibition would lead to an increase in the occurrence of single strand annealing. Furthermore, if my hypothesis is correct in that mitochondrial DRMDs occur as a result of SSA, the absence of KU mediated SSA inhibition would account for the increase in the observed rate of mitochondrial direct repeat-mediated deletions in the absence of *KU70* and *KU70* and *KU80*.

While the findings of Mansour et al, and the mitochondrial DRMD data presented in this study, it appears that the KU complex may act to inhibit SSA within the mitochondria in a manner similar to nuclear KU mediated SSA inhibition. Therefore my hypothesis may be correct in that the increase in the observed rate of mitochondrial DRMDs associated with the loss of *KU70*, as well as *KU70* and *KU80*, may be due to removal of KU mediated SSA inhibition. Furthermore, if mitochondrial DRMDs occur due to SSA (as their nuclear counterparts have been shown to do), this would account for the increase in mitochondrial DRMDs associated with the loss of the KU complex.

The findings of Ivanov et al., Clerici et al., and the mitochondrial DRMD data presented in this study appear to support the hypothesis that the absence of Rad50p, Mre11p, and Xrs2p leads to a 4 – 7 fold reduction in the occurrence of mitochondrial DRMDs ($p < 0.006$) by decreasing the activity of mitochondrial SSA. Therefore it appears

that the decrease in mitochondrial DRMDs associated with the loss of the MRX complex and the entire NHEJ pathway is due to the impairment of single strand annealing following a mitochondrial DNA double strand break.

In conclusion we have demonstrated that the MRX complex and the non-homologous end joining DNA repair pathway are directly involved in regulating the occurrence of mitochondrial direct repeat-mediated deletions, and that the impairment of this pathway greatly effects the stability of the mitochondrial genome in the budding yeast, *Saccharomyces cerevisiae*.

The MRX complex and the non-homologous end joining DNA repair pathway are directly involved in the regulation of nuclear direct repeat-mediated deletions.

To determine the role of the MRX complex and the NHEJ pathway in the occurrence of spontaneous nuclear direct repeat mediated deletions the direct repeat-mediated deletions assay was performed upon all of the strains in our NHEJ knock out library. Refer to Table 8 and Figure 13 for the role of MRX complex and NHEJ members in the occurrence of spontaneous nuclear direct repeat-mediated deletions.

While reviewing the data from our nuclear DRMD assay in Table 8, we see that the loss of any of the individual members of the MRX complex as well as the entire NHEJ pathway resulted in an approximate 4 fold reduction in the occurrence of nuclear DRMDs ($p<0.002$). When all 3 members of the MRX complex are disrupted there is a 6 fold decrease in the occurrence of the nuclear DRMDs ($p<0.001$). The observed decrease in nuclear DRMDs seen when *RAD50, MRE11,* and *XRS2* are all disrupted compared to any single member of the MRX complex appears to be additive in that the rate of nuclear DRMDs decreases 6 fold in the triple mutant, and approximately 4 fold in any of this single

mutants. In contrast, when the entire KU complex is disrupted we see near wild-type levels of nuclear DRMDs

After reviewing the observations regarding the role of the MRX complex and the NHEJ DNA repair pathway in the occurrence of nuclear DRMDs it is my hypothesis that the reduction in nuclear DRMDs associated with the loss of *RAD50, MRE11, XRS2*, the MRX complex, as well as the entire NHEJ pathway is due to the impairment of the single strand annealing pathway.

As described in the previous section of this discussion, the *Saccharomyces* genome database, the findings published by Ivanov et al. in 1996, and Phadnis et al. in 2005, suggest that direct repeat mediated-deletions may occur as a result of single strand annealing following a DNA double strand break between two directly repeating DNA sequences. Furthermore the work published by Ivanov et al. in 1996, and Clerici et al. in 2005, suggests that MRX complex members are directly involved in the occurrence of single strand annealing following a DNA DSB. Therefore, in the event that single strand annealing is a mechanism for the occurrence of direct repeat-mediated deletions, and MRX complex members are involved in the occurrence of SSA, my hypothesis may be correct. Specifically, a reduction in nuclear DRMDs associated with the loss of *RAD50, MRE11, XRS2*, the MRX complex, and the entire NHEJ pathway may be due to the impairment of SSA at the site of our nuclear DRMD reporter.

In conclusion, the nuclear DRMD data presented in this study support our preliminary hypothesis, and support the well established role of the MRX complex and the NHEJ pathway in the maintenance of genomic stability within the cell.

The MRX complex and non-homologous end joining play an important role in regulating the occurrence of spontaneous mitochondrial point mutations.

To determine the role of the MRX complex and non-homologous end joining in the occurrence of spontaneous mitochondrial point mutations we subjected each of the mutants in our knock out library to the mitochondrial point mutation assay. Yeast cells which possess mutations in the 21S ribosomal RNA gene encoded within the mitochondrial genome may possess resistance to the pharmacological agent erythromycin. The rates of erythromycin resistance for each strain in our MRX and NHEJ knockout library is listed in Table 9, and graphed in Figure 14.

As we review Table 9 and Figure 14, we see that only the gene in our MRX complex and NHEJ knockout library that directly impacts the rate of spontaneous mitochondrial point mutations in *Saccharomyces cerevisiae* is *XRS2*. In the absence of *XRS2* the rate of spontaneous mitochondrial point mutations decreases a significant 2.21 fold (p=0.023). While *XRS2* is the only single gene who loss lead to a significant change in the rate of erythromycin resistance, the loss of *RAD50, MRE11, XRS2, KU70*, and *KU80* lead to a significant 13 fold reduction in the rate of erythromycin resistance(p<0.013).

From these observations it is my hypothesis that the decrease in erythromycin resistance associated with the loss of the non-homologous end joining pathway is due to a reduction in the occurrence of spontaneous point mutations associated with the potentially error prone DNA repair activity of the NHEJ pathway.

Rad50p, Mre11p, Xrs2p, Ku70p, and Ku80p are known to function in numerous potentially mutagenic DNA repair pathways such as single strand annealing, microhomology mediated end joining, as well as non-homologous end joining, (SGD). Rad50p, Mre11p, and Xrs2p have all been shown to be involved in the occurrence of spontaneous deletions within

dicentric plasmids (Tsukamoto et al, 1997), and direct repeat mediated deletions via single strand annealing (Ivanov et al, 1995). While reviewing the non-homologous end joining DNA repair pathway (described in Figure 7) we see that an the event that a DNA DSB occurs with incompatible ends the exonuclease function of Mre11p processes these ends generating compatible ends which can then be ligated by Dnl4p. In the event that a DNA DSB occurs with incompatible ends, the exonucleolitic processing can therefore be considered mutagenic. (Krough and Symington, 2004). Depending upon the type of DNA DSB that occurs (compatible vs. incompatible), NHEJ can thus be error free, or error prone.

It has also recently been suggested that the KU complex may be involved in micro-homology end joining, MMEJ (Yukitaka et al. 2007). MMEJ occurs when several base pairs of homology are used to align and repair a DNA DSB prior to processing. MMEJ has been suggested to always generate a small deletion of within one of the homologous sequences and can therefore be considered mutagenic (Liang et al, 2005).

In order for erythromycin resistance to occur within yeast cells a point mutation must occur within the 21S ribosomal RNA gene at loci Er 221, and Er 514 (refer to appendix 2 for complete map of 21S rRNA gene). In order yeast cells to possess resistance to erythromycin a single base pair substitution, or single base insertion or deletion must occur at these loci. If NHEJ factors were involved in the regulating the occurrence of point mutations at Er 221, and Er 514, and that NHEJ factors are known to potential be mutagenic due to the production of insertions and deletions, it is possible that the absence of NHEJ factors (and the NHEJ pathway) may reduce point mutations at these loci within the 21S rRNA gene, thereby leading to a reduction in a cells resistance to erythromycin.

Another possible explanation for the reduction in erythromycin associated with the loss of the NHEJ pathway could be an up regulation in the expression of homologous

recombination in the absence of the NHEJ pathway, which reduces the frequency of point mutations occurring within the mitochondrial 21S rRNA gene. Homologous recombination is commonly thought of as an error-free DNA DSB repair mechanism because it employs sequence homology on neighboring DNA strands to replace the damaged DNA strand. Homologous recombination seems like an excellent choice for the repair of damaged mtDNA because of the fact that there are numerous copies of the mitochondrial genome wrapped in close proximity to one another with a mtDNA nucleoid.

Therefore it appears future work is needed to determine the exact mechanism for the increase in erythromycin sensitivity associated with the loss of the NHEJ before my hypothesis can be deemed correct. In conclusion we have provided data that strongly supports our preliminary hypothesis that the MRX complex and the non-homologous end joining pathway are involved in maintaining the stability of the mitochondrial genome in *Saccharomyces cerevisiae*.

The MRX complex and non-homologous end joining regulate the occurrence of spontaneous nuclear point mutations.

To determine the role of the MRX complex and non-homologous end joining in the occurrence of spontaneous nuclear point mutations we subjected each of the mutants in our knock out library to nuclear point mutation assay. Yeast cells which possessed mutations in the *CAN1* gene will possess resistance to the pharmacological agent canavanine. The rates of canavanine resistance for each strain in our MRX and NHEJ knockout library is listed in Table 10, and graphed in Figure 15 above.

As we review Table 10 and Figure 15, we see that the absence of *RAD50* and *XRS2* have a significant impact on the rate of spontaneous nuclear point mutations in *Saccharomyces cerevisiae*. In the absence of *RAD50* the rate of canavanine resistance is a reduced a significant 2.4 fold (p=0.001), while the absence of *XRS2* causes a significant 1.9 fold increase in the rate of canavanine resistance (p=0.0001). From Table 10 we see that the loss of *MRE11*, *XRS2*, and *RAD50* leads to a significant 2.4 fold increase in the rate of canavanine resistance (p=0.0037). The loss of *MRE11* lead to a 1.4 fold increase in canavanine resistance, but this increase can not be deemed significant (p=0.0585). While the increase in canavanine resistance associated with the loss of *MRE11* alone can not be considered significant, it is probable that the increase in the rate of canavanine resistance in the MRX triple mutant may be additive due to the loss of both Mre11p and Xrs2p. In the absence of *RAD50*, *KU70*, and *KU80* there is significant 8.69 fold increase in the rate spontaneous nuclear point mutations (p=0.0001). These results are of specific interest due to the fact that the loss of *RAD50*, *MRE11*, *XRS2*, *KU70*, and *KU80* only generated a 2.24 fold increase in the rate of canavanine resistance (p=0.0006).

From these observations I have two specific hypotheses regarding the findings presented in this study for the role of the MRX complex and the NHEJ pathway in the occurrence of nuclear point mutations. First, non-homologous end joining is involved in maintaining the stability of the nuclear genome of *Saccharomyces cerevisiae*, and in the absence of the NHEJ pathway leads to an increase in the rate of nuclear point. Second, there is an epistatic interaction occurring between Mre11p or Xrs2p, and Ku70 and Ku80p which accounts for difference in canavanine resistance associated with the loss of RAD50, KU70, and KU80 compared to loss of all five members of the NHEJ pathway.

Although the absence of NHEJ factors is not lethal to *Saccharomyces cerevisiae*, the absence of NHEJ factors greatly affect their overall stability on their nuclear genome. In the absence of *KU70* and *KU80*, *Saccharomyces cerevisiae* has been shown to possess a reduction in the length of telomeres, and transcriptional silencing in regions neighboring the telomeres (SGD). The absence of *MRE11* in *Saccharomyces cerevisiae* has been shown to decrease resistance to radiation, decrease resistance to the DNA damaging agent MMS and hydroxyurea, increased transposable element transposition, decrease telomere length, and decreased chromosomal maintenance (SGD). The absence of *RAD50* and *XRS2* leads to increased sensitivity to gamma and x-rays, increases sensitivity to MMS and hydroxyurea, increases transposable element transposition, and decreased chromosomal maintenance (SGD).

The information provided by the *Saccharomyces* genome database regarding the phenotypes present in yeast cells with mutations in the genes required for NHEJ function directly support my hypothesis that the NHEJ pathway is required for maintaining the stability of the nuclear genome in *Saccharomyces cerevisiae*. The statistically significant 2.4 increase in the rate of spontaneous nuclear point mutations associated with the loss of the NHEJ pathway presented in this study further supports this hypothesis.

Upon the careful review reviewing of the data presented in Table 11, and Figure 15, it appears that either *MRE11* or *XRS2* function upstream of *KU70* and *KU80* and therefore the absence of *MRE11* or *XRS2* affects the activity of *KU70* and *KU80*. The epistatic interaction between *MRE11* or *XRS2* and *KU70* and *KU80* is supported by the observation that the absence of RAD50, KU70, and KU80 generated a 8.6 fold (p=0.0037) increase in spontaneous nuclear point mutations compared to the wild-type control, where as in the

absence of all five members of the NHEJ pathway the rate of spontaneous nuclear point mutations 2.2 fold (p=0.0006).

When one compares the functions of Mre11p and Xrs2p it is logical for one to infer that the source of the epistatic trend seen above may be due to Xrs2p. Although the exonuclease role of Mre11p may be required for the processing of DNA DSB with incompatible ends, it may be more probable that the DNA damage sensing role of Xrs2p has a greater relevance to the health of the cell especially in the context of previously described hierarchy of DNA damage repair pathways. It may be more probable that a protein involved in sensing DNA damage (Xrs2p) may alter the function of Ku70p and Ku80p which have been shown to regulate a hierarchy of multiple DNA repair pathways, versus an exonucleolytic protein which functions exclusively within just one of these repair pathways. The probability that Xrs2p possesses this epistatic role over Mre11p is further supported by our observation that the loss of *XRS2* lead to an extremely significant (p=0.0001) increase in the rate of canavanine resistance, while the loss of *MRE11* did not (p=0.0585).

After extensive research, this epistatic interaction does appear to be documented within the scientific community, and thus future work should be done to further clarify this interaction. It is my recommendation that colleagues at the University of Rochester should generate a *RAD50-MRE11* double mutant, a *RAD50-XRS2* double mutant, a *MRE11-KU70-KU80* triple mutant, and a *XRS2-KU70-KU80* triple mutant, and then subjecting these strains to this assay. The information generated from this future experiment will provide evidence that may further support my hypothesis regarding the epistatic interaction between these non-homologous end joining factors.

In conclusion the data resulting from the spontaneous nuclear point mutation assay strongly supports our initial hypothesis that that the MRX complex and non-homologous end joining is directly involved in maintaining genomic integrity of *Saccharomyces cerevisiae*.

The MRX complex and the non-homologous end joining pathway are required for maintaining the capacity for respiration in Saccharomyces cerevisiae.

As previously described *Saccharomyces cerevisiae* is a facultative anaerobic organism that is able to produce ATP through fermentation or cellular respiration. The facultative anaerobic nature of this organism is an ideal model system for determining the role of gene or pathway in regulating the ability of yeast cells to undergo cellular respiration, as well as mitochondrial genome maintenance. To determine the role of the MRX complex and non-homologous end joining in the occurrence of spontaneous respiration loss we subjected each of the mutants in our knock out library to the spontaneous respiration loss assay.

The spontaneous respiration loss assay relies upon the formation of a petite phenotype when yeast cells are plated on media containing a non-fermentable carbon source such as glycerol that is enriched with a 0.2% of a fermentable carbon source such as dextrose. Yeast cells which possess mitochondrial function and are respiration proficient will consume the dextrose in the media using fermentation, and then switch its metabolic pathway to cellular respiration to utilize the remaining non-fermentable carbon source. Yeast cells which are respiration proficient will continue to grow after they have exhausted the fermentable carbon source and are scored as grande, while cells that are respiration deficient will arrest when they have exhausted the supply of the fermentable carbon source and are

therefore referred to as petite. Refer to Figure 11 for further explanation on scoring the respiration capacity of yeast cells.

While reviewing the results of from our spontaneous respiration loss assay described in Table 11, we see that the loss of *MRE11*, *XRS2*, and *RAD50* leads to a significant 2.39 fold increase in the frequency of spontaneous respiration loss ($p<0.0001$). While the loss of *RAD50*, *KU70*, and *KU80* as well as *RAD50*, *MRE11*, *XRS2*, *KU70*, and *KU80* lead to an approximate 3.5 fold increase in spontaneous respiration loss ($p<0.003$). This significant increase in occurrence of spontaneous respiration loss over the wild-type frequency therefore suggests that the MRX complex and NHEJ pathway are directly involved in regulating mitochondrial genome stability and repair.

It has been demonstrated that spontaneous respiration loss can occur in *Saccharomyces cerevisiae* through direct repeat mediated deletions within mtDNA (Dujon et al, 1981). While these authors have show that spontaneous respiration loss can be due to mtDNA DRMDs, the increase in spontaneous respiration loss associated with the disruption of the NHEJ pathway observed in this study does not appear to be due to mtDNA DRMDs. In Figure 12 and Figure 13, we have demonstrated that mitochondrial and nuclear DRMDs are reduced in the absence of the MRX complex and NHEJ pathway. From Figure 12 and 13 we can infer that the mechanism for the occurrence of spontaneous respiration loss observed due to the absence of the MRX complex and the NHEJ pathway is not due to an increase in the rate of DRMDs. Therefore, there must be several potential mechanisms leading to spontaneous respiration loss in *Saccharomyces cerevisiae*.

Another potential mechanism that could lead to an increase in spontaneous respiration loss would be an increase in the occurrence of spontaneous point mutations within genes required for cellular respiration. In the event that the rate of spontaneous

mitochondrial point mutations (or nuclear DNA point mutations in essential mitochondrial genes) increased significantly in the absence of the MRX complex and the NHEJ pathway it could lead to an increase in spontaneous respiration loss. Table 9 and Figure 14 demonstrate that mitochondrial point mutations are reduced dramatically in the absence of the NHEJ pathway, and therefore the increase in spontaneous respiration loss associated with the disruption of the NHEJ pathway is not due to an increase in the rate of mitochondrial point mutations.

In 1990 Alexander Tzagoloff and Carol Dieckmann compiled a list of all of the genes known to date which when mutated may lead to the petite phenotype. These authors defined *PET* genes (or genes that when mutated generate the petite phenotype) as a nuclear gene having at least one mutant allele that will confer a respiratory deficient phenotype (Tzagoloff and Dieckmann, 1990). These authors also suggested that this phenotype could result from a cytoplasmic mutation in mtDNA. The compiled list of *PET* genes that these authors generated in their 1990 publication is located in the Appendix following the conclusion of this study. These authors were investigating only nuclear genes which acted in regulating mitochondrial function, where as it is obvious that any single gene encoded within the mitochondrial genome that when mutated in a large proportion of the mitochondrial genomes within a cell may lead to respiration deficiency.

From the list of *PET* genes compiled by Tzagoloff and Dieckmann as well as the genes encoded within the mitochondrial genome seen in Table 1, it becomes logical that a mutation in any gene required for the transcription, translation, localization, or assembly of any gene which function in the mitochondria, may lead to the petite phenotype and spontaneous respiration loss. Therefore, it is plausible that a significant increase in the rate of

spontaneous nuclear point mutations associated with the loss of the MRX complex and the NHEJ pathway may lead to an increase in the rate of spontaneous respiration loss.

In Figure 15 we see the absence of the MRX complex and the entire NHEJ pathway leads to a 2 fold increase in the occurrence of spontaneous nuclear point mutations ($p<0.004$). Table 10 also demonstrates this, but from Table 10 we see that the actual rate of spontaneous nuclear point mutations increases from 2.2 E-07 mutations/cell division to 5.38 E-07 mutations/cell division due to the absence of the MRX complex and the NHEJ pathway ($p<0.004$). Table 11 demonstrates that the rate of spontaneous respiration loss increases from 2.25% to 7.9% in the absence of the entire NHEJ pathway ($p<0.003$). From this information it appears that although the rate of nuclear point mutations does increase in the absence of the NHEJ pathway, it only increase to 0.0000005 mutations/cell division. Re-writing this data shows us spontaneous nuclear point mutations occur 0.00002% of the time in wild-type cells, and in the absence of the NHEJ pathway they occur 0.00005% of time. Thus, although the rate of nuclear point mutations does increase in the absence of the NHEJ pathway, it is most likely not significant enough to lead to spontaneous respiration loss in 7.9% of yeast cells subject to this assay.

Due to the fact that the increase in spontaneous respiration loss associated with the disruption of the NHEJ pathway does not appear to be due to an increase in the rate of direct repeat-mediated deletions, or an increase in the rate of spontaneous point mutations, it is my hypothesis that the MRX complex and the NHEJ pathway are involved in replication induced DNA repair within *Saccharomyces cerevisiae*. Specifically, it my hypothesis that the MRX complex and NHEJ players are involved in replication induced repair (RIR), and that the absence of these players reduces the efficiency of RIR, leading to an increase in the frequency of spontaneous respiration loss.

In 2002 Shelley Lusetti and Michael Cox published an article about recombinational repair of DNA at stalled replication forks in the *Annular Review of Biochemistry*. These authors stated that replication forks are halted at the site of DNA damage, and unless repaired it can lead to cell death. These authors went on to state that the rate of replication fork collapse or the stalling of replication forks is not know in higher eukaryotes, but replication fork stalling and replication fork collapse is known to occur in nearly every cell cycle in prokaryotes under normal oxidative conditions (Lusetti and Cox, 2002). These authors then went on to state that primary repair mechanism in prokaryotes for replication induced repair is homologous recombination (HR). Their model for replication induced repair of blocked or collapsed replication forks by HR is described in Figure 22 below.
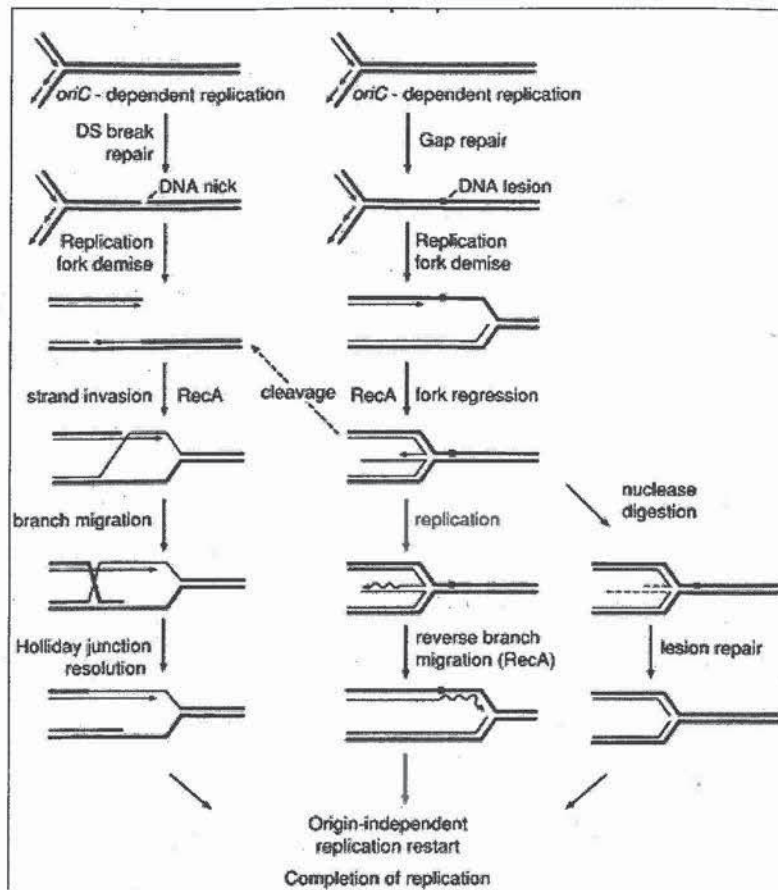
Figure 22. Replication induced repair of replication forks by homologous recombination. Figure published by Shelley Lusetti and Michael Cox. (2002). The Bacterial RecA protein and the Recombination DNA Repair of Stalled Replication Forks. *Annual Review of Biochemistry,* **71: 71-100.**

The homologous recombination pathway is similar between prokaryotes such as

Escherichia coli and *Saccharomyces cerevisiae.* The eukaryotic homolog to the Rec Ap in bacteria is

Rad51p. Rad51p and Rec Ap are required for strand invasion in homologous recombination,

and Holliday junction formation. In order for replication induced repair to occur via

homologous recombination a 3' DNA end needs to be generated by the MRX complex prior

to strand invasion (Krough and Symington, 2004). Therefore, it becomes apparent that the

MRX complex and NHEJ members are required for replication induced repair.

103

In a recent study published by Lundin et al. in 2002, it was determined that non-homologous end joining plays a crucial role in DNA double strand break repair during S-phase. In this study these authors exposed cells to hydroxyurea to arrest DNA replication. In this study Lundin et al. discovered that NHEJ is up regulated in the presence of hydroxyurea, and that NHEJ protects the cell from a potentially cytotoxic event such as replication fork block. The role of the NHEJ pathway in the protection of a cell from replication fork block is strongly supported by the fact that *MRE11*, *XRS2*, and *RAD50* mutants possess significantly decreased resistance to hydroxyurea, and a decrease in replication induced repair (SGD).

From the information provided by Alexander Tzagoloff and Carol Dieckmann in 1990, we see that there are approximately 100 genes known to be involved in cellular respiration that when mutagenized lead to the petite phenotype, and limit the respiratory capacity of *Saccharomyces cerevisiae*. When this information is taken together with the role of *MRE11*, *XRS2*, and *RAD50* in replication induced DNA repair (as suggested by Lundin et al. 2002; Lusetti and Cox, 2002; and the *Saccharomyces* genome database), and the significant 2.4 fold increase in the frequency of spontaneous respiration loss ($p < 0.003$) associated with the disruption of the MRX complex observed in this study, it appears that my hypothesis may be correct. These findings appear to support my hypothesis the MRX complex and NHEJ players are involved in replication induced repair (RIR), and that the absence of these players reduces the efficiency of RIR, leading to an increase in the frequency of spontaneous respiration loss. Furthermore, in the event that my hypothesis is correct, then the facultative anaerobic nature of *Saccharomyces cerevisiae* may make it an excellent model organism in the investigation of the role of replication induced repair within genes required for mitochondrial function.

In conclusion, although the NHEJ DNA repair pathway is not the most prominent DNA DSB repair pathway in yeast, it is highly conserved throughout evolution, and is required for the repair of DNA DSBs in higher eukaryotes. We have provided a wealth of genetic data in Specific Aim 1 that directly supports our preliminary hypothesis, in that the MRX complex and the non-homologous end joining DNA repair pathway are involved in regulating the stability and repair of the mitochondrial genome of the budding yeast, *Saccharomyces cerevisiae*.

Specific Aim II:

The second aim of this study was to localize non-homologous end joining factor Ku70p to the mitochondria using cellular fractionation and western blot analysis. Using a modified differential centrifugation protocol devised by Glick and Pon in 1995 we were able to isolate and purify mitochondria from the budding yeast, *Saccharomyces cerevisiae*. This protocol relies upon the use of the varying sedimentation coefficients, or sedimentation rates of all of the components of a cell to isolate mitochondria. Once mitochondria had been crudely purified using this method, they were suspended on to top of Nycodenz gradients and spun at 40,000 rpm for 30 minutes in an ultracentrifuge. 3 – 4 bands were removed (which depended upon the degree of zymolase treatment, and the successful completion of the differential centrifugation protocol), and their total protein concentration was determined as described by Glick and Pon in 1995. According to these methods the first band which can be isolated at the 5% - 10% Nycodenz interface was composed of mitochondrial fragments. The second band was isolated within the 10% Nycodenz fraction and was composed of mitoplasts. The third band was isolated within the 15% Nycodenz

fraction and represented purified and active mitochondria. The final band was isolated from the 15% - 20% Nycodenz interface, and was composed of cell debris.

Once the mitochondrial purification protocol had been completed equal volumes of total protein were analyzed using SDS-PAGE for both a whole cell lysate (WCL) positive control and from each of the 4 purified fractions, and the resulting blot was probed for the presence of Cox2p. From Figure 17 we see that there is an enrichment of mitochondrial protein Cox2p within purified mitochondrial fractions 1 – 4 over the whole cell lysate positive control. The enrichment of Cox2p within these fractions supports that we have successfully isolated mitochondria as there is an increase in mitochondrial proteins per unit weight of total protein over the WCL control.

We then set out to verify that our mitochondrial fractions were free from nuclear debris by probing for the nuclear localized protein Histone H4. From Figure 18 we see that in lanes 1 and 5 there are faint bands at 11 kDA which is consistent with the size of the Histone H4 protein in *Saccharomyces cerevisiae*. Although the bands 1 and 5 are faint at 11 kDA this author chose to incorporate the whole gel as is, instead of cropping the gel to enhance the presence of these bands. The absence of Histone H4 associated signal at 11 kDA in lanes 2, 3, and 4 confirm that mitochondrial fractions 1, 2, and 3, are free of Histone H4, and are purified mitochondria. The presence of Histone H4 in lane 5, which corresponds to mitochondrial fraction 4 is not surprising as the protocol for gradient purification used in this study suggests that band 4 may contain cell debris. Thus from Figure 18 we see that mitochondrial fractions 1 – 3 do not possess Histone H4 proteins, and we can infer that we have successfully purified mitochondria from *Saccharomyces cerevisiae*.

Once we had verified that our mitochondrial fractions were pure, we then set out to localize non-homologous end joining factor Ku70p to the mitochondria. Equal amounts of

total protein were loaded for a positive WCL control derived from the KU70:HA strain, a negative WCL control derived from a wild-type strain lacking the HA epitope, and purified mitochondrial fractions 1 – 3 on 10% acrylamide gel and analyzed using SDS-PAGE. The resulting blot was probed for the presence of NHEJ factor Ku70:HAp using an antibody against the HA epitope. While reviewing the results in Figure 19 we see that we there are bands in lanes 1 and 5. The lack of signal in lane 2 (the negative WCL control) ensures the specificity of our anti-HA antibody, and confirms that the band at 95 kDA is due to the presence of NHEJ factor Ku70:HAp in our WCL positive control. Wild-type Ku70p in *Saccharomyces cerevisiae* is 70 kDA (SGD), while our HA tagged Ku70p is approximately 95 kDA due the addition of a citrine-HA tag. While the presence of Ku70:HAp in lane 5 confirms that Ku70p can be localized to the mitochondria, the lack of signal in lane 4 is surprising because it was loaded with a sample taken from band 2 in our gradient purification protocol which suggested that it was composed of mitoplasts. Although this finding is interesting, it will be discussed in detail within the next section of this discussion with reference to Figure 20. From Figure 19 we can confirm that NHEJ factor Ku70:HAp can be localized to the mitochondria, but it does not appear to be localized to the mitoplasts.

We next attempted to precisely determine the location of NHEJ factor Ku70:HAp within the mitochondrial compartment. To perform this task aliquots of purified mitochondria from fraction 3 that had previously been shown to possess NHEJ factor Ku70:HAp were subjected to the protease protection protocol previously described. This protocol employs the use of 5 reactions that sequentially removes the outer and inner mitochondrial membranes and allows for the remaining products to be probed for the

NHEJ factor Ku70:HAp using western blot analysis. Please refer to Table 6 for a complete description of the protease reactions.

In Figure 20 we see that there are bands at 95 kDA associated with the presence of NHEJ factor Ku70:HAp in lanes 1 (the positive WCL control), lane 3 (untreated mitochondria), and lane 5 (the mitoplast). Once again we see that our anti-HA antibody is specific for the anti-HA epitope on Ku70:HAp due to the lack of signal in the negative WCL control loaded in lane 2 when compared to the positive WCL control loaded in lane 1. In lane 3 we see the Ku70:HAp is present in product from the protease reaction number 1. In reaction number 1 sorbitol buffer was added to osmoticly buffer the outer mitochondrial membrane, and PMSF was added to protect against naturally occurring yeast proteases and to hault the enzymatic activity of proteinase K after its desired effect had been accomplished. Thus reaction number 1 is an internal second control containing purified intact mitochondria. In lane 4 there is no signal associated with the presence of Ku70:HAp in the product following protease reaction number 2. Protease reaction number 2 contained the sorbitol buffer and proteinase k. The product from protease reaction number 2 is a mitoplast generated from proteinase K treatment. In lane 5 there is signal associated with the presence of Ku70:HAp in the product following protease reaction number 3. Protease reaction number 3 contained a non-osmoticly controlled buffer and PMSF once again. The resulting product from protease reaction number 3 is a mitoplast generated by the lysing of the outer membrane due to the absence of the sorbitol buffer. Lanes 6 and 7 did not possess a signal associated with the presence of Ku70:HAp following protease reaction 4 and 5 respectively. Protease reaction 4 and 5 contained mitoplasts treated with the proteinase K, and ruptured mitoplasts treated with proteinase K.

After reviewing the effects of protease reactions 1 – 5 it appears that Ku70:HAp can be localized to the mitochondria, but that it does not appear to make it through the inner membrane into the mitoplast. Although Ku70:HAp signal can be detected in lane 5 following protease reaction 3, Ku70:HAp can not be localized within the inner mitochondrial membrane due the lack of signal in lane 4 which results from the product of protease treatment number 2. The most plausible explanation for the presence of Ku70:HAp in lane 3, but not lane 2 is that while protease reaction number 2 removed and degraded the outer mitochondrial membrane (and Ku70:HAp) using enzymatic digestion, protease reaction number 3 simply lysed the outer mitochondrial membrane and left Ku70:HAp undisturbed in solution. While the absence of the sorbitol buffer in protease reaction number 3 is sufficient to generate a mitoplast, it does not have the ability to prove that Ku70:HAp is present within the mitoplast. Therefore we see from the absence of Ku70:HAp signal in lane 4 of Figure 19 and lane 4 of Figure 20, that Ku70:HAp is localized to the outer mitochondrial membrane, but not the mitoplast.

It is my hypothesis that the inability of Ku70:KAp to be localized within the inner membrane of the mitochondria is due to the presence of C-terminal citrine-HA tag. In this study we used an anti-HA antibody to localize the Ku70:HA fusion protein to the mitochondria. Although the total size of the fusion protein is only 95 kDA, it appears that the citrine-HA tag may be preventing its complete passage through the TOM complex within the outer mitochondrial membrane. Typically the mitochondrial heat shock protein (mtHSP70) and mitochondrial import stimulation factor (MSF) facilitates the passage of proteins being targeted to the matrix of the mitochondria through the TOM complex on the outer mitochondrial membrane and the TIM complex on the inner mitochondrial membrane as seen in Figure 23 below published by Nikolaus Pfanner and Michiel Meijer in 1997.
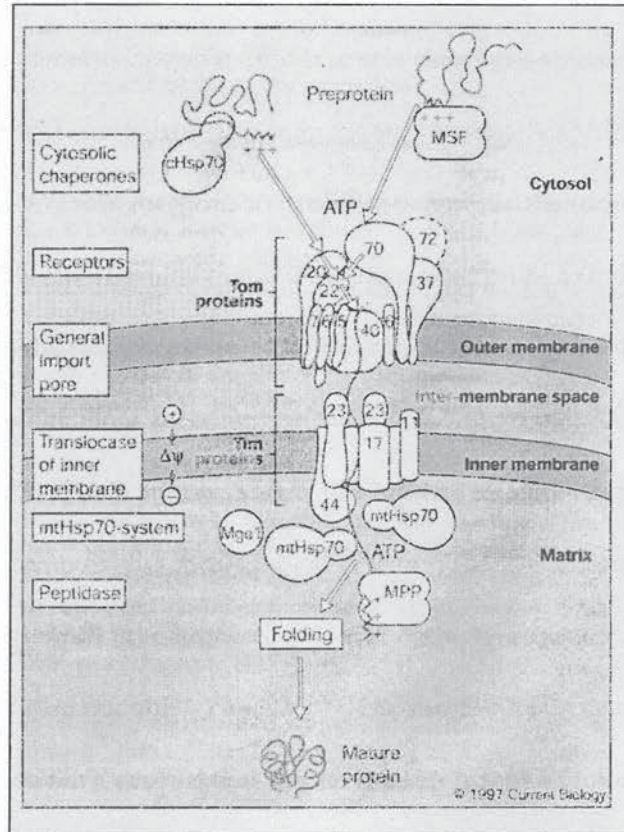
Figure 23. TOM and TIM mitochondrial complexes. Figure created by Nikolaus Pfanner and Michiel Meijer. Published by Nikolaus Pfanner and Michiel Meijer, 1997. Mitochondrial Biogenesis: The TOM and TIM machine. *Current Biology*, **R100-103.**

From Figure 23 we that the TOM and TIM complexes are both composed of multi protein complexes that may not recognize a foreign epitope such as the citrine-HA epitope. The HA epitope tag fused to NHEJ member Ku70p used in this study is a 10 amino acid peptide tag from the *hemophilis influenza* virus (Santa Cruz Biotechnologies), and thus may not recognized by *Saccharomyces cerevisiae*. It is logical then that even though the KU70:HA fusion gene is transcribed and translated within this model organism, the resulting protein product does not have the ability to completely pass through the TOM complex as seen in Figure 23 above. If Ku70:HAp was prevented from completely moving through the TOM complex by the c-terminus HA tag, it would account for the results observed in this study. In a recent

study published by Naina Phadnis and Elaine Sia the FLAG epitiope was fused to *SED1* and over expressed in *Saccharomyces cerevisiae*. In this article they were able to localize Sed1:FLAGp within the mitochondrial compartment using western blot analysis. Although these authors did not use the same protease reactions to precisely determine the location of this fusion protein, they were able to determine that it was resistant to proteinase K treatment and thus was contained within the mitochondria. According to SGD Sed1p is 34 kDA and is thus one half of the size of Ku70p. Since these authors were able to localize this protein within the mitochondria using the FLAG epitope and in unison with an over expression construct, it may be beneficial to try to further localize Ku70p within the mitochondria using these methods.

Although we were not able to localize NHEJ factor Ku70p to the mitochondrial matrix in this study, we have verified that the NHEJ DNA repair factor Ku70p can be localized to the outer mitochondrial membrane. The ability of the NHEJ factor Ku70p to be localized within the mitochondrial membrane proves that Ku70p is targeted to this organelle where we can infer it performs its cytological duty as a DNA repair protein. Thus in conclusion the genetic data presented in specific aim I, and the localization data presented in specific aim II of this study supports our hypothesis that the MRX complex and the non-homologous end joining DNA repair pathway are involved in maintaining the integrity of the mitochondrial genome in *Saccharomyces cerevisiae*.

Conclusion

DNA double strand breaks can be toxic to the cell. This toxic nature of DNA double strand breaks has lead to development of highly efficient DNA double strand break repair pathways which are conserved throughout evolution. The non-homologous end joining DNA repair pathway is present in some form in nearly every biological domain. While this pathway has been investigated thoroughly in its role in maintaining the integrity of nuclear genome, there has been little work done to elucidate its role in mitochondrial genome maintenance. In this study we provided a wealth of data supporting the role of the MRX complex and the non-homologous end joining DNA repair pathway in promoting mitochondrial genome stability and repair in the model organism, *Saccharomyces cerevisiae*. It is our hope that the insights that we have made into mitochondrial DNA repair in our model organism will enhance the scientific communities understanding of mitochondrial genome maintenance, and allow for the translation of this understanding into a form which can better our quality of life.

References:

Alexeyev, Mikhail F.; LeDoux, Susan P.; Wilson, Glenn L. (2004). Mitochondrial DNA and Aging. *Clinical Science* 107, 355 – 364.

G Baldacci, B Chérif-Zahar, and G Bernardi. (1984).The initiation of DNA replication in the mitochondrial genome of yeast. *EMBO J.* 9, 2115 – 2120.

Barr, Neiman, Taylor.(2005). Inheritance and recombination of mitochondrial genomes in plants, fungi, and animals. *New Phytologist.* 168, 39 - 50.

Becker, Kleinsmith, and Hardin. (2006). The World Of The Cell. Benjamin Cummins Press, San Franscisco, 248-255, 420, 540-541, 660-661.

Burgart, L.J., J. Zheng, Q. Shu, J. G. Strickler and D. Shibata. (1995). Somatic mitochondrial mutation in gastric cancer. *Am. J Pathol.* 147, 1105-1111.

Chen, X. J. and Butow, R. A. (2005). The organization and inheritance of the mitochondrial genome. *Nat. Rev. Genet.* 6, 815 -825.

Chomyn, A., and Attardi, G. (2003). mtDNA mutations in aging and apoptosis. *Biochem. Biophys. Res. Comm.* 304, 519–529.

Clerici, M., Mantiero, D., Lucchini, G., and Longhese, M. (2005). The Saccharomyces cerevisiae Sae2 Protein Promotes Resection and Bridging of Double Strand Break Ends. *J. Biol. Chem.*, Vol. 280, Issue 46, 38631-38638.

Cortopassi,G., Arnheim N. (1990) Detection of a specific mitochondrial DNA deletion in tissues of older humans. *Nucleic Acids Res.* 23, 6927 – 33.

Dujon, B. (1981). Mitochondrial genetics and function. *Molecular Biology of the Yeast Saccharomyces cerevisiae: Life Cycle and Inheritance.* Cold Spring Harbor Laboratory Press, Cold Spring Harbor, NY. 505–635.

Ehrenhofer-Murray. (2004). Chromatin dynamics at DNA replication, transcription and repair. *Eur. J. Biochem.* 271, 2335 - 2349.

Fantes, P., and Creanor, J. (1984). Canavanine Resistance and the Mechanism of Arginine Uptake in the Fission Yeast *Schizosaccharomyces pombe. Journal of General Microbiology* 130, 3265 – 3273.

Foury, F. and Vanderstraeten, S. (1992) Yeast mitochdrial DNA mutations with deficient proofreading exonucleolytic activity. *Embo. J.* 11, 2717 - 2726.

Feldmann, H.,Winnacker, E.(1993). A putative homologue of the human autoantigen Ku from *Saccharomyces cerevisiae. J. Biol. Chem.* 268, 12895–900.

Game JC, Mortimer RK. (1974). A genetic study of X-ray sensitive mutants in yeast. *Mutat. Res.* 24, 281–92.

Glick and Pon. (1995). *Methods in Enzymology* V260 Chp14, 213 - 223.

Goffeau, Barrell, Bussey, Davis, Dujon, Feldmann, Galibert, Hoheisel, Jacq, Johnston, Louis, Mewes, Murakami, Philippsen, Tettelin, Oliver. (1996). Life with 6000 Genes. *Science* 274, 546 – 567.

Griffiths, Gelbart, Lewontin, and Miller. (2002). Modern Genetic Analysis: Integrating Genes and Genomes. W.H. Freeman and Company, New York, NY 10010.

Grimes, Mahler, et al. (1974). Nuclear gene dosage effects on mitochondrial mass and DNA. *J. Cell Biol.* 61, 565 - 74.

Giaever, G., Chu, A., Ni, L., Connelly, C., Riles, L., Véronneau, S., Dow, S, Lucau-Danila, S., Anderson, K., André, B., Arkin, A., Astromoff, A., Bakkoury, M., Bangham, R., Benito, R., Brachat, S., Campanaro, S., Curtiss, M., Davis, K., Deutschbauer, A., Entian, K., Flaherty, P., Four, F., Garfinkel, D., Gerstein, M., Gotte, D., Güldener, U., Hegemann, J., Hempel, S., Herman, Z., Jaramillo, D., Kelly, D., Kelly, S., Kötter, P., LaBonte, D., Lamb, D., Lan, N. Liang, H., Liao, H., Liu, L., Luo, C., Lussier, M., Mao, R., Menard, P., Ooi, S., Revuelta, J., Roberts, C., Rose, M. Macdonald, P., Scherens, B., Schimmack, G., Shafer, B., Shoemaker, D., Sookhai-Mahadeo, S., Storms, R., Strathern, J., Valle, G., Voet, M., Volckaert, G., Wang, C., Ward, T., Wilhelmy, J., Winzeler, E., Yang, Y., Yen, G., Youngman, E., Yu, K., Bussey, H., Boeke, J., Snyder, M., Philippsen, P., Davis R., & Johnston, M. (2002). Functional profiling of the *Saccharomyces cerevisiae* genome. *Nature* 418, 387 - 391.

JE Haber. (1998). Mating-type gene switching in *Saccharomyces cerevisiae*. *Annual Review of Genetics* 32, 51 - 99.

Haslbrunner, E., Tuppy, H., and Shatzm, G.(1964). Deoxyribonucleic Acid Associated with Yeast Mitochondria. *Biochem. Biophys. Res. Commun.* 15, 127 - 132.

Herrmann G, Lindahl T, Schar P. (1998). *Saccharomyces cerevisiae* LIF1: a function involved in DNA double-strand break repair related to mammalian XRCC4. *EMBO J.* 17, 4188 – 98.

Human / Yeast mitochondrial genome map:
http://www.clinsci.org/cs/107/0355/cs1070355f01.gif

Ivanov, Sugawara, Fishmann-Lobell, and Haber. (1996). Genetic requirements for the Single-Strand Annealing Pathway of Double-Strand Break Repair in *Sacchromyces cerevisiae*. *Genetics* 142, 693 – 704.

Jeggo PA. (1998). Identification of genes involved in repair of DNA double-strand breaks in mammalian cells. *Radiat. Res.*150, S80–91.

Katsura, Sasaki, Sato, Yamaoka, Suzukawa, Nagasawa, Yokoto, and Kohno. (200). Involment of Ku80 in microhomology-mediated end joining for DNA double-strand breaks in vivo. *DNA Repair* 6, 639-648.

Kim J Krishnan, Amy K Reeve, David C Samuels, Patrick F Chinnery, John K Blackwood, Robert W Taylor, Sjoerd Wanrooij, Johannes N Spelbrink, Robert N Lightowlers & Doug M Turnbull.(2008). What causes mitochondrial DNA deletions in human cells? *Nature Genetics* 40, 275 – 279.

Nicolai Balle Larsen, Merete Rasmussen and Lene Juel Rasmussen (2005). Nuclear and mitochondrial DNA repair: similar pathways? *Mitochondrion* 5, 89 - 108.

Larimer, F., Ramey, D., Lijinsky, W., and Epler, J. (1978). Mutagenicity of methylated N-nitrosopiperidines in *Saccharomyces cerevisiae*. *Mutation Research* 57 – 161.

Liang, L., Deng, L., Chen, Y., Li, G., Shao, C., Tischfield, J. (2005). Modulation of DNA End Joining by Nuclear Proteins. *The Journal of Biological Chemistry* 280, 31442 - 31449.

Lundin, C., Erixon, K., Arnaudeau, C., Schultz, N., Jenssen, D., Meuth, M., and Helleday, T. (2002). Different Roles for Nonhomologous End Joining and Homologous Recombination following Replication Arrest in Mammalian Cells. *Molecular and Cellular Biology* 22, 5869 - 5872

Lusetti S., and Cox, M. (2002). The Bacterial Rec A Protein And The Recombination DNA Repair Of Stalled Replication Forks. *Annual Review of Biochemistry* 71, 71-100.

MacAlpine, D., Perlman P., et al. (1998). The high mobility group protein ABf2 influences the level of yeast mitochondrial DNA recombination intermediates in vivo. *PNAS.* 95, 6739 - 43.

Mitochondrial point mutation assay figure adapted from http://fig.cox.miami.edu/~cmallery/150/cells/ribosome.jpg

Mansour, Schumacher, Rosskopt, Rhein, Schmidt-Peterson, Gatzemeier, Haag, Bormann, Willers, and Dahm-Daphi. (2008). Hierarchy of nonhomologous end joining, single-strand annealing and gene conversion at site-directed DNA double-strand breaks. *Nucleic Acids Research 1 – 11.*

Nass S., and Nass, M. (1963). Intramitochondrial Fibers with DNA characteristics. *Journal of Biological Chemistry* 19, 593 – 629.

O'Rourke, T. W., Doudican, N. A., Mackereth, M. D., Doetsch, P. W. and Shadel, G. S. (2002). Mitochondrial dysfunction due to oxidative mitochondrial DNA damage is reduced through cooperative actions of diverse proteins. *Mol. Cell. Biol.* 22, 4086 – 4093.

Nikolaus Pfanner and Michiel Meijer. (1997). Mitochondrial Biogenesis: The TOM and TIM machine. *Current Biology* R 100 - 103.

Naina Phadnis, Rey A. Sia, and Elaine A. Sia. (2005) Analysis of Repeat-Mediated Deletions in the Mitochondrial Genome of *Saccharomyces cerevisiae*. *Genetics* 171, 1549 - 1559.

Reyes, A., Yang, M., Bowmaker, M., Holt, I. (2005).Bidirectional replication initiates at sites throughout the mitochondrial genome of birds. *J. Biol.* Chem. 5, 3242 - 3250.

Schar, P., Herrmann, G., Daly, G., Lindahl, T. (1997). A newly identified DNA ligase of *Saccharomyces cerevisiae* involved in *RAD52*-independent repair of DNA double-strand breaks. *Genes Dev.* 11, 1912 – 24.

Schoffner, J., Lott, M., Voljavec, A., Soueidan S., Costigan, D., and Wallace, D. (1989). Spontaneous Kearns-Sayre/chronic external ophthalmoplegia plus syndrome associated with a mitochondrial DNA deletion: A slip-replication model and metabolic therapy. *PNAS.* USA 86, 7952 – 7956.

Solano, A., Playán A, López-Pérez MJ, Montoya J. (2001). Enfermedades genéticas del ADN mitocondrial humano.*Salud Publica Mex* 43, 151 - 161.

Frédéric Sor and Hiroshi Fukuhara. (1982). Identification of two erythromycin resistance mutations in the mitochondrial gene coding for the large ribosomal RNA in yeast. *Nucleic Acids Research* 10, 6571 - 6577.

Fredrick Sor and Hiroshi Fukuhara. (1983). Complete DNA sequence for the large ribosomal RNA of yeast mitochondria. *Nucleic Acids Research* 11, 339 - 348.

Sutovsky, P., Ramalho-Santos, J., Dominko, T., Simerly, C., Schatten, G. (1999). Ubiquitin tag for sperm mitochondria. *Nature* 402, 371 - 372.

Tong Wu. (2005). Cyclooxygenase-2 in hepatocellular carcinoma. *Cancer Treatment Reviews* 32, 28 – 44

Tsukamoto, Y., Kato, J., Ikeda, H. (1997). Budding Yeast Rad50, Mre11, Xrs2, and Hdf1, but not Rad52 are involved in the formation of deletions on a dicentric plasmid. *Mol Gen Genet.* 5, 543– 7.

Alexander Tzagoloff, and Carol Dieckmann.(1990). PET Genes of Saccharomyces cerevisiae. *Microbiological Reviews.* 54, 211 - 225.

Valencia, M., Bentele, M., Vaze, M., Herrmann, G., Kraus, E., et al.(2001). *NEJ1* controls non-homologous end joining in *Saccharomyces cerevisiae*. *Nature* 414, 666 – 69.

Huichen Wang, Ange Perrault, Yoshihiko Takeda, Wei Qin, Hongyan Wang, and George Iliakis. (2003). Biochemical evidence for Ku-independent backup pathways of NHEJ. *Nucleic Acids Res.* 31, 5377 – 5388.

De Zamaroczy, M., and Bernardi, G. (1986). The GC clusters of the mitochondrial genome of yeast and there evolutionary origin. *GEN.* 41, 1 - 22.

Zeviani, M., Servidei, C., Gekkera, E., Bertini, S., and DiMauro et el. (1989) An autosomal dominant disorder with multiple deletions of mitochondrial DNA starting at the D-loop region. *Nature* 339: 309-311.

Appendix:

Appendix 1. *PET* Genes in Sacchromyces Cerevisiae. Published by Alexander Tzagoloff amd Carol Dieckman, 1990. Micorbiological review, vol 54 211-225.

TABLE 2. *PET* complementation groups

Group	Mu-tant[a]	Total no. of mutants[b]	Clone[c]	Gene name	Gene product or phenotype	Sequence obtained[d]	Deposited[e]	Reference(s)[f]
G1	C103	46	+	ATP2	β subunit of F_1 ATPase	C		151, 173, 179
G2	C146	62	+		Coenzyme QH_2-cytochrome c reductase deficient	P		A
G3	C296	32	+	COQ1	Hexaprenyl pyrophosphate synthetase	C		B
G4	C4	72	+		Cytochrome oxidase deficient	C		D
G5	C5	3	+	FUM1	Mitochondrial and cytoplasmic fumarase	C	ATCC, YC	200
G6	C6	26	+	LIP1	Lipoic acid deficient	C		E
G7	C153	22	+	COR1	45-kDa subunit of coenzyme QH_2-cytochrome c reductase	C	ATCC, YC	183
G8	C8	2	+		Cytochrome oxidase deficient	C		F
G9	C9	10	−		Coenzyme Q deficient			
G10	C33	26	−	COQ2	Hexaprenyl pyrophosphate transferase			B
G11	C145	7	+	MSK1	Mitochondrial lysyl-tRNA synthetase	C		G
G12	C13	25	+	RIP1	Rieske protein of coenzyme QH_2-cytochrome c reductase	C		5
G13	C15	14	+	ATP11	Assembly of F_1 ATPase	C		H
G14	C17	2	−		Cytochrome oxidase deficient			
G15	C18	13	−		Pleiotropic[g]			
G16	C19	8	+		Cytochrome oxidase deficient			
G17	C83	20	+	COQ5	Coenzyme Q deficient			
G18	C141	7	−		Pleiotropic			
G19	C28	37	+	COX10	Cytochrome oxidase deficient (homolog of ORF1 in *Paracoccus denitrificans* cytochrome oxidase operon)	C		I
G20	C23	3	−		Heme deficient			
G21	C100	13	−		Normal[g]			
G22	C25	5	+		Cytochrome oxidase deficient			
G23	C26	18	+	PET494	COXIII mRNA translation factor	C		24, 43, 116
G24	C27	4	−		Pleiotropic			
G25	C30	17	−		Normal			
G26	C31	1	+	MSY1	Mitochondrial tyrosyl-tRNA synthetase	C		J
G27	C34	5	−		ATPase deficient			
G28	C35	10	+	CBP3	Coenzyme QH_2-cytochrome c assembly factor	C	ATCC, YC	201
G29	C279	7	+		Pleiotropic	C		F
G30	E125	8	+		Pleiotropic	C		K
G31	C39	41	−	COQ3	3,4-Dihydroxy-5-hexaprenylbenzoic acid methylase			59, 166
G32	C41	5	+	HEM2	δ-Aminolevulinate dehydratase	C	ATCC, YC	62, 117
G33	C43	1	−		Normal			
G34	C46	14	+		Cytochrome oxidase deficient			
G35	C47	3	−		Cytochrome oxidase deficient			
G36	·89	27	+	CBP2	Intron bI5 splicing factor	C	ATCC, YC	56, 108
G37	C155	3	+	MEF1	Mitochondrial elongation factor (homolog of procaryotic elongation factor G)	C		L
G38	C50	8	+		Pleiotropic			
G39	C51	2	−		Pleiotropic			
G40	C52	2	−		Pleiotropic			
G41	C171	8	+	SCO1	Cytochrome oxidase deficient	C		153
G42	C54	22	−		Heme deficient			
G43	C55	41	+	OP1	ATP-ADP exchange carrier	C		1, 4, 84, 126
G44	C59	1	−		Normal			
G45	C139	22	+	CYT2	Cytochrome c_1 heme lyase			M
G46	C106	18	+	COX5a	Subunit Va of cytochrome oxidase	C		32, 79, 158
G47	C62	3	+		Cytochrome oxidase deficient			
G48	C251	6	−		Pleiotropic			
G49	C249	9	−	LIP3	Lipoic acid deficient			
G50	C198	43	+	ATP1	α subunit of F_1 ATPase	C		172
G51	C69	13	−		Normal			
G52	C70	5	−		Pleiotropic			
G53	C164	14	+	COX11	Cytochrome oxidase deficient (homolog of ORF3 in *P. denitrificans* cytochrome oxidase operon)	C		N
G54	C75	2	+	MRP4	Mitochondrial ribosomal protein (homolog of *Escherichia coli* S2)	C		P
G55	C76	2	+	SDH1	Succinate dehydrogenase deficient			
G56	C79	1	−		Pleiotropic			
G57	C264	16	+	ATP12	F_1 assembly factor	C		Bowman[h]
G58	C119	41	−		Cytochrome oxidase deficient			
G59	C151	17	+	MSL1, NAM2	Mitochondrial leucyl-tRNA synthetase	C	ATCC, YC	71, 88, 178

118

TABLE 2—Continued

Group	Mu-tant[a]	Total no. of mutants[b]	Clone[c]	Gene name	Gene product or phenotype	Sequence obtained[d]	Deposited[e]	Reference(s)[f]
G60	C116	29	+	CBP1	5' end processing factor for cytochrome b pre-mRNA	C	ATCC, YC	36, 37
G61	C92	7	–		Normal			
G62	C94	7	–		Pleiotropic			
G63	C96	18	–	COQ6	Coenzyme Q deficient			
G64	C97	28	–	COQ7	Coenzyme Q deficient			
G65	C101	3	–		Normal			
G66	C102	4	+	COX4	Subunit IV of cytochrome oxidase	C		80, 99
G67	C105	5	+	COR4	14-kDa subunit of coenzyme QH$_2$-cytochrome c reductase	C		30, 33, 189
G68	C108	3	–		Normal			
G69	C110	10	+	MST1	Mitochondrial threonyl-tRNA synthetase	C	ATCC, YC	128
G70	C225	6	+	KGD1	α-Ketoglutarate dehydrogenase	C	ATCC, YC	143
G71	C121	20	+	COX6	Subunit VI of cytochrome oxidase	C		80, 199
G72	C134	8	+	MSM1	Mitochondrial methionyl-tRNA synthetase	C	ATCC, YC	182
G73	C125	8	+		Cytochrome oxidase deficient			
G74	C129	1	–		Cytochrome oxidase deficient			
G75	C130	40	–	COQ8	Coenzyme Q deficient			
G76	C246	2	–		Normal			
G77	C212	22	+	PET111	COXII mRNA translation factor	C		43, 140, 169
G78	C142	8	+		Pleiotropic			
G79	C143	12	+	MSS116	COXI pre-mRNA processing factor	C		156, 157
G80	C154	14	–		Cytochrome oxidase deficient			
G81	E135	4	–		Normal			
G82	C149	3	+		Pleiotropic	C		O
G83	C156	13	+	PET54	COXIII mRNA translation factor	C		25, 26, 187
G84	E206	2	–		Normal			
G85	C158	4	–		Pleiotropic			
G86	C312	11	+	LIP2	Lipoic acid deficient	P		E
G87	C161	2	–		Normal			
G88	C162	1	–	HEM4	Coproporphyrinogen decarboxylase			62
G89	C167	1	+	MRP2	Mitochondrial ribosomal protein (homolog of E. coli S14)	C		118
G90	P11	1	–		Normal			
G91	C173	2	+		Cytochrome oxidase deficient	C		F
G92	C176	11	+		Cytochrome oxidase deficient	C		F
G93	C179	4	+		Cytochrome oxidase deficient	C		Q
G94	E234	2	+	MSD1	Mitochondrial aspartyl-tRNA synthetase	C	ATCC, YC	57
G95	N230	7	+		ATPase deficient	P		H
G96	C199	22	+	MSS51	COXI pre-mRNA splicing factor	C		50
G97	C202	5	+		Cytochrome oxidase deficient			
G98	C204	3	+		Normal			
G99	C208	9	+		Pleiotropic	C		F
G100	E220	2	+		Pleiotropic	C		M
G101	C210	12	+	CYT1	Cytochrome c$_1$	C		30, 90, 150
G102	N174	11	+	CBP4	Coenzyme QH$_2$-cytochrome c reductase assembly factor	C		M
G103	C220	5	+	MSE1	Glutamyl-tRNA synthetase	C		F
G104	E250	3	+	KGD2	Dihydrolipoyl transsuccinylase	C	ATCC, YC	E
G105	C229	1	–		Normal			
G106	N1	3	+		Pleiotropic	C		F
G107	C235	6	–	LIP4	Lipoic acid deficient			
G108	E290	3			Normal			
G109	P16	1	–		Normal			
G110	N160	2	+	PET56	Pleiotropic	P		F, 170
G111	C260	5	+		Cytochrome oxidase deficient			
G112	C261	23	+	CYC3	Cytochrome c heme lyase	C		42, 148, 162
G113	N205	3	+		ATPase deficient	C		H
G114	E177	9	–		Normal			
G115	C287	2	–		COXI mRNA deficient			
G116	C297	6	–		Pleiotropic			
G117	N241	1	+		Pleiotropic	C		F
G118	N266	2	+		Cytochrome oxidase deficient			
G119	C295	4	+		Normal			
G120	C303	5	+	MSF1	α subunit of mitochondrial phenylalanyl-tRNA synthetase	C	ATCC, YC	81
G121	N328	4	+		Normal			

Continued on following page

119

TABLE 2—*Continued*

Group	Mutant[a]	Total no. of mutants[b]	Clone[c]	Gene name	Gene product or phenotype	Sequence obtained[d]	Deposited[e]	Reference(s)[f]
G122	E221	6	−		Pleiotropic			
G123	N356	2	+	CBS1	Cytochrome *b* pre-mRNA and mRNA translation factor	C		82, 135, 145
G124	C317	1	+		Normal			
G125	C318	3	−		Normal			
G126	N363	2	−		Normal			
G127	N380	2	+	MRP3	Mitochondrial ribosomal protein (S19 homolog?)	C		O
G128	N393	8	−		Normal			
G129	N413	1	−		Pleiotropic			
G130	N415	1	+	TUFm	Mitochondrial elongation factor (homolog of procaryotic factor EFTu)	C		121
G131	N420	2	+		Normal			
G132	N472	2	−		Normal			
G133	N518	1	+		Pleiotropic	C		O
G134	N520	4	+		Cytochrome oxidase deficient			
G135	E282	3	−		Normal			
G136	P37	1	−		Normal			
G137	E384	4	+	FBP	Fructose-1,6-bisphosphatase	C		146, 155
G138	P39	1	−		Normal			
G139	E204	2	+		Pleiotropic			
G140	E205	2	+		COXI mRNA deficient			
G141	P48	1	−		Pleiotropic			
G142	E252	4	+	MTF2	Mitochondrial initiation factor (homolog of procaryotic factor IF2)	C		F
G143	E307	3	+	HAP3	Nuclear transcription factor	C		68
G144	E354	4	+	COR2	40-kDa subunit of coenzyme QH₂-cytochrome *c* reductase	C		30, 127, 190
G145	E359	1	−		Cytochrome *c* deficient			
G146	E203	1	−		Normal			
G147	E214	1	+		COXI mRNA deficient			
G148	E241	4	−		Pleiotropic			
G149	E275	4	+	PET122	COXIII mRNA translation factor	C		78, 106, 107, 125
G150	E411	7	−		Pleiotropic			
G151	P65	1	−		Normal			
G152	E123	1	−		Normal			
G153	E145	2	+	COR5	11-kDa subunit of coenzyme QH₂-cytochrome *c* reductase	C		30, 98, 189
G154	E158	1	+	CBP6	Cytochrome *b* mRNA translation factor	C		38
G155	E264	6	−		Normal			
G156	P68	1	−		Normal			
G157	E8	7	−		Cytochrome *c* deficient			
G158	E39	2	−		Normal			
G159	E59	5	−		Normal			
G160	E57	1	−		Pleiotropic			
G161	E64	1	−		Cytochrome oxidase deficient			
G162	E67	5	+	CBP7 CBS2	Cytochrome *b* pre-mRNA and mRNA translation factor	C		135, 145, Muroff[f]
G163	E96	5	−		Normal			
G164	E280	1	−		Pleiotropic			
G165	E103	3	+	ATP10	ATPase deficient	C	ATCC, YC	H
G166	E128	1	−		Normal			
G167	E130	8	−		Normal			
G168	E153	1	−		Pleiotropic			
G169	E358	1	−		Pleiotropic			
G170	E362	1	−		Normal			
G171	E322	1	−		Pleiotropic			
G172	E330	4	−		COXI mRNA deficient			
G173	E343	1	−		Normal			
G174	E372	2	+	MRF1	Mitochondrial release factor	C		S
G175	E374	2	−		Pleiotropic			
G176	P77	1	−		Normal			
G177	E392	1	+		Pleiotropic			
G178	P96	1	−		Normal			
G179	E553	7	−		Normal			
G180	E567	1	−		Pleiotropic			
G181	E569	2	+	MSW1	Mitochondrial tryptophanyl-tRNA synthetase	C	ATCC, YC	120

120

TABLE 2—Continued

Group	Mutant[a]	Total no. of mutants[b]	Clone[c]	Gene name	Gene product or phenotype	Sequence obtained[d]	Deposited[e]	Reference(s)[f]
G182	P104	1	–		Normal			
G183	E602	2	–		Pleiotropic			
G184	E530	2	–		Normal			
G185	E649	1	–		Cytochrome c deficient			
G186	P115	1	–		Normal			
G187	E688	1	–		Pleiotropic			
G188	E708	2	–		Cytochrome oxidase deficient			
G189	E730	1	+		Pleiotropic			
G190	E742	1	–		Normal			
G191	E428	3	–		Cytochrome oxidase deficient			
G192	E749	2	–		Pleiotropic			
G193	E779	1	–		Pleiotropic			
G194	E783	1	–		Normal			
G195	E795	1	+	MRP1	Mitochondrial ribosomal protein	C		118
G196	E827	2	–		Cytochrome oxidase deficient			
G197	E838	1	–		Pleiotropic			
G198	E847	2	+	ATP4	Subunit 4 of ATPase	C		132, 191
G199	E880	1	–		Cytochrome oxidase deficient			
G200	E884	1	–		Normal			
G201	E885	2	–	KGD3	Deficient in α-ketoglutarate dehydrogenase			
G202	E887	2	–	PDH1	Pyruvate dehydrogenase deficient			
G203	E889	2	–		Normal			
G204	E899	1	–		Pleiotropic			
G205	P217	1	–		Pleiotropic			
G206	E199	1	–		Pleiotropic			
G207	E81	4	+	PET123	Mitochondrial ribosomal protein(?)	C		R
G208	P235	1	–		Normal			
G209	P272	1	–		Normal			
G210	P274	1	–		Pleiotropic			
G211	P287	1	–		Pleiotropic			
G212	P302	1	–		Normal			
G213	P311	1	–		Normal			
G214	P317	1	–		Normal			
G215	P403	1	–		Normal			

Appendix 2. Restriction map of yeast mitochondrial 21s rRNA gene. Published by Fredrick Sor and Hiroshi Fukuhara. 1983. Complete DNA sequence for the large ribosomal RNA of yeast mitochondria. Nucleic Acids Research. Vol 11, 339-348.

Figure 1 : (A) Restriction map of the sequenced region. The top line shows the mature 21S rRNA. Thick lines indicate the localization of the rho⁻ mtDNAs used for the rRNA gene sequencing. Lengths of fragments are in base-pairs. The wavy line indicates the intron. gc means a GC cluster with the indicated orientation (see text). E^R_{514}, E^R_{221}, C^R_{323} and C^R_{321} are drug resistance genetic markers. ω is the intron.
(B) Sequencing scheme. Each arrow indicates the position of labelling (5' or 3') and the length of sequence read.